DEPARTMENT OF COMMERCE
SINCLAIR WEEKS, Secretary

WEATHER BUREAU
F. W. REICHELDERFER, Chief

MONTHLY WEATHER REVIEW

JAMES E. CASKEY, JR., Editor

Volume 85
Number 7

JULY 1957

Closed September 15, 1957
Issued October 15, 1957

PREDICTIVE CONSEQUENCES OF CERTAIN PHYSICAL INCONSISTENCIES IN THE GEOSTROPHIC BAROTROPIC MODEL

FREDERICK G. SHUMAN, U. S. Weather Bureau

Joint Numerical Weather Prediction Unit, Suitland, Md.

[Manuscript received June 7, 1957; revised July 22, 1957]

ABSTRACT

The physical inconsistency of geostrophic flow and small surface pressure tendencies is discussed. The frequently disastrous consequences in conventional geostrophic barotropic predictions are numerically identified by comparisons with experimental "semi-geostrophic" barotropic predictions from which the inconsistency has been removed. Effects of the inconsistency of the geostrophic wind field with the equations of motion are also quantitatively isolated by comparisons of semi-geostrophic predictions with predictions made with wind fields which satisfy the balance equation. It is concluded that the principal fault of the conventional geostrophic approximation lies in the violation of the continuity equation. Its lack of the dynamic effects expressed in the equations of motion seems also significant, but is less important.

1. INTRODUCTION

Conventional geostrophic barotropic 72-hour predictions were inaugurated on a daily basis by the Joint Numerical Weather Prediction (JNWP) Unit on September 29, 1955. The classic model of Charney [1] was the basis for the computations. Although not always present, the most consistent and characteristic error in these predictions was spurious anticyclogenesis, usually associated with flow around the western side of large subtropical Highs. Its maximum frequencies were over the southeastern coast of the United States, and in the central Pacific Ocean. Figure 3 is taken from a typical case when spurious anticyclogenesis was present over the former area.

2. THE IMPORTANCE OF THE LAW OF CONSERVATION OF MASS

The error is related to the divergence of the geostrophic wind, and can be traced to a particular physical inconsistency in the geostrophic barotropic model. For ease of reference the derivation of the model will be briefly reviewed here. A model equivalent barotropic atmosphere is first created in which

$$u=A(p)u'(x,y)$$
$$v=A(p)v'(x,y) \tag{1}$$

where u and v are the two horizontal components of velocity.[1]

The two horizontal equations of motion are integrated with respect to pressure, p, with the vertical convection terms neglected. The result in isobaric coordinates is

$$\overline{u}_t+K\overline{u}\overline{u}_x+K\overline{v}\overline{u}_y-f\overline{v}+g\overline{z}_x=0$$
$$\overline{v}_t+K\overline{u}\overline{v}_x+K\overline{v}\overline{v}_y+f\overline{u}+g\overline{z}_y=0 \tag{2}$$

where f is the Coriolis parameter and g the acceleration of

[1] In order to avoid confusion in the following pages, it should be understood that equations (1), which represent the basic departure of the equivalent barotropic equations from the primitive meteorological equations are not, as they stand, inconsistent with the primitive equations. They are merely a statement of an instantaneous condition concerning the 3-dimensional distribution of wind velocities. An integration in time in which it is assumed that this condition is maintained is, of course, inconsistent with the primitive equations. This article will not deal with this physical inconsistency of the equivalent barotropic model when used as a predictive tool, nor will it deal with the validity of the concept of an equivalent barotropic level in the real atmosphere (Charney [1, 2]). In the calculations to be discussed, the equivalent barotropic level was taken to be at 500 mb., and the value of K, defined in equation (3), was set to unity.

gravity. The functions $\overline{u}$ and $\overline{v}$ are the values of u and v at the level $\overline{p}$ where $A(p)$ is equal to its vertical pressure average; i. e.,

$$\overline{u}=A(\overline{p})u'$$

$$\overline{v}=A(\overline{p})v'$$

$$A(\overline{p})=-p_0^{-1}\int_{p_0}^{0}A(p)dp$$

The function, p_0, is the pressure at the lower boundary. It is assumed to be constant, which is nearly true in the real atmosphere. The function, $\overline{z}$, is the vertical pressure average of the height, z, of isobaric surfaces; i. e.,

$$\overline{z}=-p_0^{-1}\int_{p_0}^{0}zdp$$

The constant, K, is related to the shape of the vertical windspeed profile, and is defined as follows.

$$K=\frac{-p_0^{-1}\int_{p_0}^{0}A^2dp}{\left(-p_0^{-1}\int_{p_0}^{0}Adp\right)^2} \tag{3}$$

The vorticity equation for the equivalent barotropic atmosphere is then derived from equations (2) by cross differentiation.

$$\overline{\zeta}_t+\overline{u}(K\overline{\zeta}_x+f_x)+\overline{v}(K\overline{\zeta}_y+f_y)+(K\overline{\zeta}+f)(\overline{u}_x+\overline{v}_y)=0 \tag{4}$$

where $\overline{\zeta}$ is the relative vorticity,

$$\overline{\zeta}=\overline{v}_x-\overline{u}_y$$

The importance of physical consistency in the introduction of the geostrophic approximation to the wind may be seen at this point in the derivation. The divergence of the geostrophic wind is

$$(\overline{u}_x+\overline{v}_y)_g=-f^{-1}(\overline{u}_gf_x+\overline{v}_gf_y)$$

Thus, if one were to substitute from the geostrophic approximation into the vorticity equation (4), the Rossby term, $\overline{u}f_x+\overline{v}f_y$, would cancel, and the model could not properly account for the propagation of long westerly waves.

Proceeding with the derivation, we next introduce the equivalent barotropic continuity equation in the form of Margules' tendency equation.

$$\omega_0=-p_0(\overline{u}_x+\overline{v}_y) \tag{5}$$

Where ω_0 is the substantial time derivative of pressure at the lower boundary. The vorticity equation (4) may then be written

$$\overline{\zeta}_t+\overline{u}(K\overline{\zeta}_x+f_x)+\overline{v}(K\overline{\zeta}_y+f_y)-(K\overline{\zeta}+f)p_0^{-1}\omega_0=0 \tag{6}$$

The next step has been to turn to the real atmosphere for two empirical facts. It has been noted that ω_0 is small, and that the wind is nearly geostrophic. These facts have been applied in the model by an omission of the last term in equation (6), and by a direct substitution into equation (6) from the geostrophic approximation,

$$-f\overline{v}_g+g\overline{z}_x=0$$

$$+f\overline{u}_g+g\overline{z}_y=0$$

Vanishing surface pressure tendencies and geostrophic winds, however, are physically inconsistent, for geostrophic flow would lead to large pressure tendencies at the lower boundary which could not be ignored. This can be made clear by a direct substitution from the geostrophic approximation into Margules' tendency equation (5). A light southerly mean wind of 10 knots would yield a value of ω_0 of 3 mb. hr.$^{-1}$ even at middle latitudes. The situation is worse at low latitudes, for with a given southerly wind component, geostrophic divergence varies as the cotangent of the latitude angle. Perspicacious neglect of the last term in equation (6) largely compensates for the direct substitution from the geostrophic approximation, otherwise the conventional geostrophic barotropic model would not predict as well as it does. Certain effects are not compensated, however.

In particular, the implied sink of vorticity in the convergence field of southerly geostrophic winds explains qualitatively the spurious anticyclogenesis exhibited in figure 3. If equation (4) is integrated over a region,

$$\iint\overline{\zeta}_tdxdy+\oint\overline{v}_n(K\overline{\zeta}+f)ds=0$$

where $\overline{v}_n$ is the wind component outward and normal to the boundary, and s is distance measured counter-clockwise along the boundary. Thus equation (4) implies that an increase of vorticity within a region equals the net transport of vorticity into the region across the boundary. The vorticity equation (4) is a statement of conservation in that sense.

Equation (6), on the other hand, if the last term is neglected, and if the geostrophic approximation to the wind is substituted, leads to

$$\iint\overline{\zeta}_tdxdy+\oint\overline{v}_n(K\overline{\zeta}+f)=-\iint(K\overline{\zeta}+f)f^{-1}(\overline{u}f_x+\overline{v}f_y)dxdy$$

The conventional geostrophic barotropic vorticity equation thus implies a vorticity sink in regions of southerly flow, and a vorticity source in regions of northerly flow. The strength of the source is related to the right-hand side of the preceding equation. Although initially (fig. 1) no pronounced southerly flow was evident over southern United States, any tendency toward development of southerly flow in the prediction would lead to creation of a sink of vorticity. It is not difficult to conceive of such

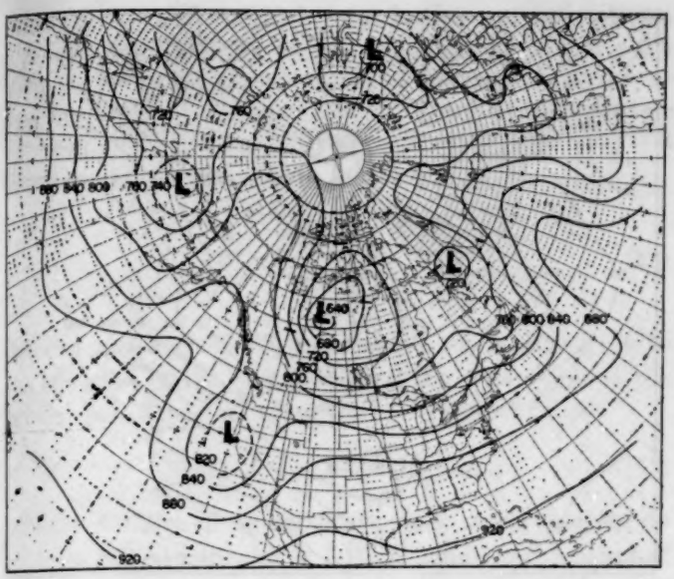

FIGURE 1.—Initial 500-mb. heights, 0300 GMT April 26, 1956. Contours are labeled in tens of feet.

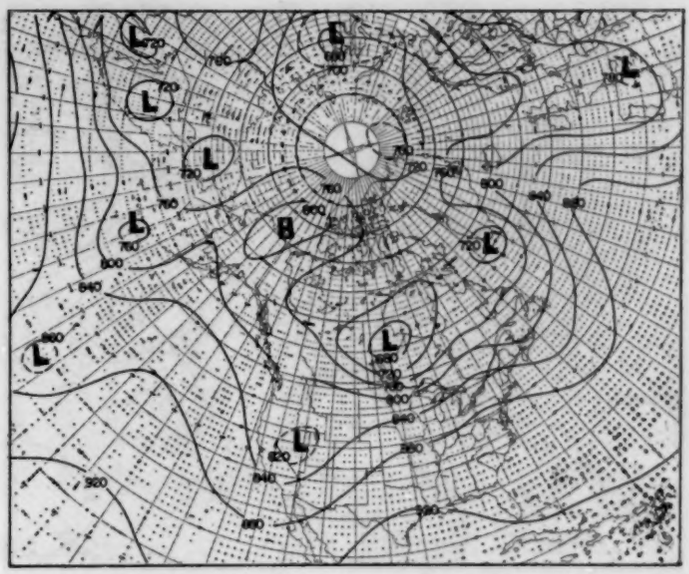

FIGURE 2.—Verifying 500-mb. heights for 36-hour forecasts, 1500 GMT April 27, 1956. Contours are labeled in tens of feet.

a sink "feeding back" to create more southerly flow, which in turn would strengthen the vorticity sink. It is just such a "feedback" mechanism which the author believes is directly responsible for the spurious anticyclone over South Carolina in figure 3.

It is incontrovertible that the conventional geostrophic barotropic model is physically inconsistent in the respect that it does not conserve mass. It is in order, therefore, to inquire into what errors arise from this physical inconsistency of the model, as opposed to other inconsistencies or to the lack of correspondence of the equivalent barotropic atmosphere (1) to the real atmosphere. One may make such an inquiry by devising a barotropic model in which the wind field is defined as very nearly geostrophic, but non-divergent. Such a model, which I shall call "semi-geostrophic barotropic," does not violate the law of mass conservation for the classes of motion in which the surface pressure tendency is small or vanishing.

The geostrophic wind vector field shall be divided into an irrotational divergent part described by a velocity potential, S_1, and a non-divergent rotational part described by a stream function, S_2, in the expectation that the non-divergent part will closely approximate the geostrophic wind vector field, itself.

$$\mathbf{V}_g=-f^{-1}\nabla(gz)\times\mathbf{k}=\nabla S_1-\nabla S_2\times\mathbf{k} \tag{7}$$

where $\mathbf{V}_g$ is the geostrophic wind velocity vector and $\mathbf{k}$ is a unit vertical vector. The velocity potential, S_1, does not appear in the curl of equation (7), while the stream function, S_2, does not appear in the divergence of the equation.

$$\nabla\times\mathbf{V}_g\cdot\mathbf{k}=f^{-1}\nabla^2(gz)+\nabla(gz)\cdot\nabla f^{-1}=\nabla^2S_2 \tag{8}$$

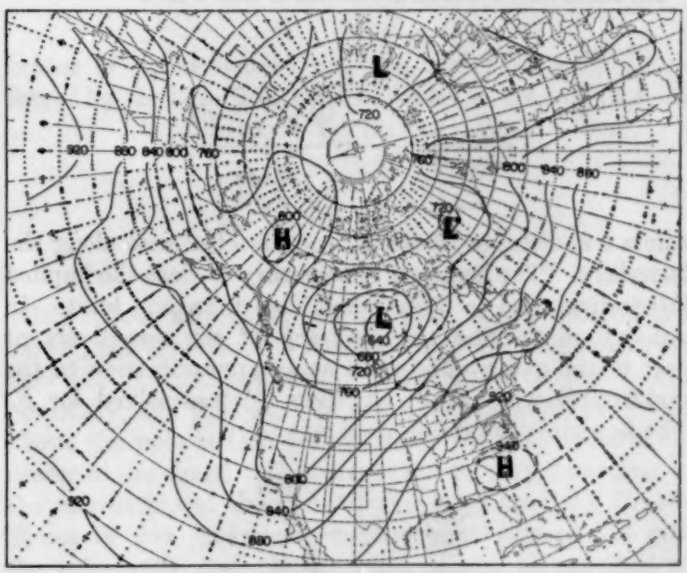

FIGURE 3.—A conventional geostrophic barotropic 36-hour prediction computed from initial conditions at 500 mb. at 0300 GMT April 26, 1956. Contours are labeled in tens of feet.

$$\nabla\cdot\mathbf{V}_g=J_{x,y}(gz,f^{-1})=\nabla^2S_1 \tag{9}$$

where $J_{x,y}$ is the Jacobian with respect to coordinates x, y. Since equations (8) and (9) are linear in the variables $\mathbf{V}_g$, S_1, S_2, and z, the only variables appearing which depend on pressure, p, vertical pressure averages of the equations may be directly indicated by barring those variables. With the field of $\bar{z}$ given as in figure 1, equation (8) was solved for S_2. With the intention of making the non-divergent part of the wind component at and normal to the boundary nearly geostrophic, the boundary condition used was

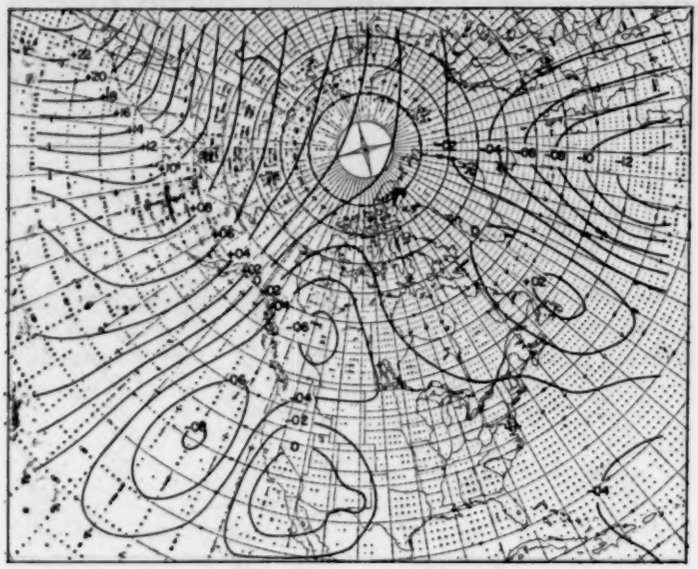

FIGURE 4.—The initial field of $\bar{f}g^{-1}S_1$ at 500 mb. at 0300 GMT April 26, 1956. The irrotational divergent part of the geostrophic velocity vector is equal to the gradient of S_1, both in magnitude and direction. Contours are labeled in tens of feet.

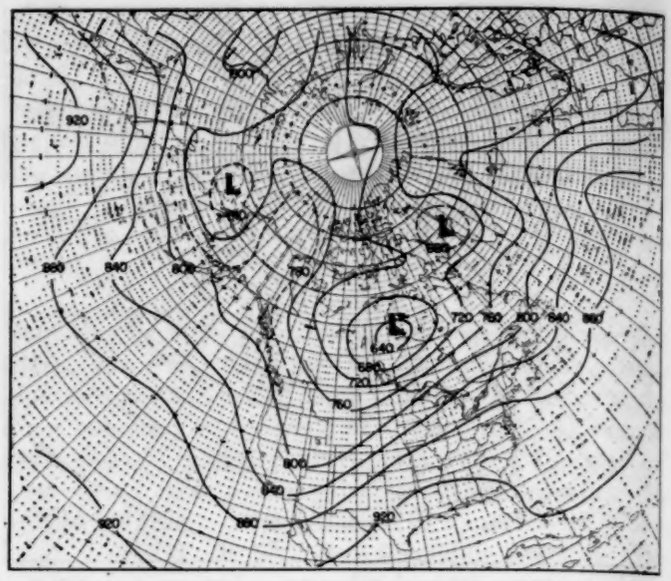

FIGURE 5.—A semi-geostrophic barotropic 36-hour prediction computed from initial conditions at 500 mb. at 0300 GMT April 26, 1956. For prediction purposes the wind field was defined by means of the gradient of S_2, according to equation (10). Contours are labeled in tens of feet.

$$\frac{\partial \bar{S}_2}{\partial s}=\frac{1}{\bar{f}}\frac{\partial(g\bar{z})}{\partial s}-\frac{\oint \frac{1}{\bar{f}}\frac{\partial(g\bar{z})}{\partial s}\,ds}{\oint ds}$$

where s is distance measured counter-clockwise along the boundary. The last term is necessary to close the implied integration, and is quite small, less than one knot. In order to determine the accuracy of the non-divergent part of the geostrophic wind as an approximation to the geostrophic wind itself, equation (9) was solved for $\bar{S}_1$. The boundary condition used was

$$\frac{\partial \bar{S}_1}{\partial n}=-\frac{\oint \frac{1}{\bar{f}}\frac{\partial(g\bar{z})}{\partial s}\,ds}{\oint ds}$$

where n is distance measured outward and normal to the boundary. Figure 4 shows the field of $\bar{f}g^{-1}\,\bar{S}_1$, where $\bar{f}$ is the value of the Coriolis parameter at 45° latitude. The largest irrotational wind velocity measured on figure 4 is less than 6 knots. The non-divergent part of the geostrophic wind as given by the stream function, $\bar{S}_2$, is therefore nearly the same as the geostrophic wind itself; and equation (8) shows that $\nabla^2\bar{S}_2$ is a complete accounting of the geostrophic vorticity.[2]

[2] In geostrophic barotropic predictions, vorticity is conventionally evaluated without the term $\nabla(gz)\cdot\nabla f^{-1}$. That is, the approximation, $v_g-u_g=f^{-1}\nabla^2(gz)$, is made. To eliminate experimentally this approximation as a possible source of spurious anticyclogenesis, a prediction was made in which S_2 was computed from the equation $\nabla^2 S_2=f^{-1}\nabla^2(gz)$. The case was again 0300 GMT April 26, 1956. The result at 36 hours showed even less anticyclogenesis over the southeastern coast of the United States than the S_2 forecast in figure 5 does. The important point of this article is that any *non-divergent* estimate of the wind field, within reason, will result in the virtual elimination of the spurious anticyclogenesis of geostrophic predictions.

Without violating the continuity equation (5), while making use of the empirical facts of near-vanishing pressure tendency at the lower boundary and the quasi-geostrophic nature of atmospheric flow, we may approximate the wind field by means of the stream function $\bar{S}_2$.

$$\bar{\mathbf{V}}=-\nabla\bar{S}_2\times\mathbf{k} \tag{10}$$

A substitution from equation (10) into equation (4); or equivalently, a substitution from equation (10) first into equation (5) and then into equation (6) yields for the barotropic mechanism

$$\frac{\partial}{\partial t}\nabla^2\bar{S}_2+J_{x,y}[\bar{S}_2,(K\nabla^2\bar{S}_2+f)]=0 \tag{11}$$

Figure 5 shows a 36-hour prediction of z, according to the system (11). The spurious anticyclogenesis over the southeastern coast of the United States has indeed been markedly suppressed. Numerical experiments with other cases have verified that the use of $\bar{S}_2$ to define the flow invariably leads to marked suppression of spurious anticyclogenesis. The conclusion seems inescapable. Spurious anticyclogenesis in conventional geostrophic barotropic forecasts arises, in the main, from the violation of the law of conservation of mass implicit in the conventional geostrophic barotropic equations.

3. THE BALANCE EQUATION AND THE BAROTROPIC MODEL

Having derived the equivalent barotropic equations of motion (2) and the equation of continuity (5), and specifying a vanishing pressure change at the lower boundary, in

principle one need not make any further approximations. The three equations (2) and (5) in that circumstance are a complete set in the three unknowns $\bar{u}$, $\bar{v}$, and $\bar{z}$. For convenience we shall replace equation (5) in the set with two equivalent equations relating the velocity components to a fourth unknown, the stream function, $\bar{\psi}$.

$$\bar{u}=-\bar{\psi}_y \qquad \bar{v}=+\bar{\psi}_x \tag{12}$$

One can now reduce the four equations (2) and (12) to one equation in the one unknown, $\bar{\psi}$. The result is the familiar barotropic equation for non-divergent flow.

$$\nabla^2\bar{\psi}_t+J_{x,y}[\bar{\psi},(K\nabla^2\bar{\psi}+f)]=0 \tag{13}$$

In the practice of numerical weather prediction, we do not have observations of $\bar{\psi}$. Both winds and heights of pressure surfaces are observed, but the observed winds are used only as diagnostic information in the analysis of fields of z. Having a field of $\bar{z}$ for initial time, one may treat the four equations (2) and (12) to obtain a single equation relating $\bar{z}$ and $\bar{\psi}$. The result is the balance equation (Petterssen [3], Charney [4], Bolin [5,6], Shuman [7]).

$$f(\bar{\psi}_{xx}+\bar{\psi}_{yy})-2K(\bar{\psi}_{xy}^2-\bar{\psi}_{xx}\bar{\psi}_{yy})+\bar{\psi}_x f_x+\bar{\psi}_y f_y-g(\bar{z}_{xx}+\bar{z}_{yy})=0 \tag{14}$$

Equation (14) differs from previous derivations of the balance equation in the appearance of K, which is a part of the equivalent barotropic equations of motion, but which has been set equal to unity in all of our computations. The geostrophic approximation may thus be entirely avoided, except perhaps in lateral boundary conditions for the solution of equation (14), and then only in integrations over limited areas of the earth.

Upon integrating the balance equation (14), one finds that the validity of the geostrophic wind as an approximation is upheld. Figure 6 shows the difference between $\bar{f}g^{-1}\bar{S}_2$ and $\bar{f}g^{-1}\bar{\psi}$. In areas of small gradients of $\bar{f}g^{-1}\bar{S}_1$ in figure 4, the quantity displayed in figure 6 may be considered as a scaled stream function of the ageostrophic component of the "balanced" wind. In any case, $\bar{S}_1$ and the difference between $\bar{S}_2$ and $\bar{\psi}$ may be simply combined to determine the ageostrophic component of the "balanced" wind. It is to be noted that the ageostrophic wind from figure 6 is, in its general level, an order of magnitude smaller than the geostrophic wind of figure 1.

In the solution displayed in figure 6, the most pronounced feature is the large-scale circulation about the center of the chart. This is to be expected, because of the cyclostrophic effects of the mean circumpolar flow and other net cyclonic conditions in the atmosphere. However, in an integration over the entire earth, or over a hemisphere, the center of the ageostrophic circulation would undoubtedly be near the pole. The shift of the

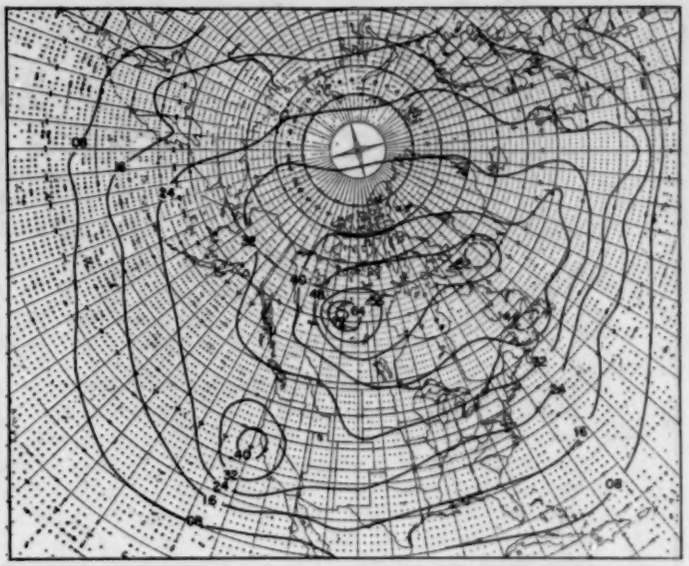

FIGURE 6.—The field of the difference $\bar{f}g^{-1}(\bar{\psi}-\bar{S}_2)$ at 500 mb. at 0300 GMT April 26, 1956. $\bar{\psi}$ was computed from the balance equation (14) using the 500-mb. heights for z. $\bar{S}_2$ was computed from equation (8). Contours are labeled in tens of feet.

center of circulation toward the center of the chart is forced by the boundary condition used in the computation

$$\frac{\partial\bar{\psi}}{\partial s}=\frac{1}{f}\frac{\partial g\bar{z}}{\partial s}-\frac{\oint\frac{1}{f}\frac{\partial g\bar{z}}{\partial s}\,ds}{\oint ds}$$

With inflow arbitrarily set to very nearly geostrophic values, the ageostrophic component of the balanced wind near the boundary is forced to be nearly tangent to the boundary, and the center of any net circulation otherwise about the pole is forced away from the pole toward the center of the chart. This should not be very damaging to the calculation of the ageostrophic wind over the United States in our grid, but on the Asian side of the grid the calculated ageostrophic wind cannot be expected to bear any resemblance to reality. The most obvious remedy for this is a calculation on a hemispheric grid, which is at present being carried out by the JNWP Unit.

With reservations concerning the boundary errors discussed above, differences between predictions made with balanced ($\bar{\psi}$) winds and semi-geostrophic ($\bar{S}_2$) winds must be due to the inconsistencies between the initial $\bar{S}_2$ wind and the initial field of $\bar{z}$, in terms of the equivalent barotropic balance equation (14). Figure 7 shows a prediction made with $\bar{\psi}$ computed initially from equation (14). Comparing figures 5 and 7 we find that the residual spurious anticyclogenesis of the prediction made with $\bar{S}_2$ winds has been eliminated by bringing the initial wind field into correspondence with the initial $\bar{z}$ field in an equivalent barotropic sense. Sufficient comparisons of this kind have not yet been made to determine the degree of universality of the improvement of balanced predictions

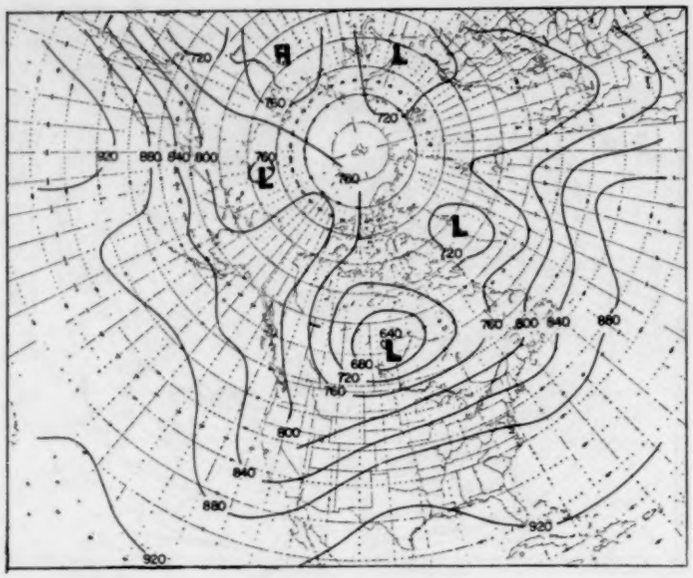

FIGURE 7.—A balanced barotropic 36-hour prediction computed from initial conditions at 500 mb. at 0300 GMT April 26, 1956. For prediction purposes the wind field was defined by means of the stream function, ψ, computed from the balance equation (14). Contours are labeled in tens of feet.

over semi-geostrophic ($\overline{S}_2$) predictions. Such comparisons, in any event, will not be conclusive until they are carried out on a hemispheric grid.

4. CONCLUDING REMARKS

Since April 20, 1956, the Joint Numerical Weather Prediction Unit has been computing balanced barotropic 72-hour predictions on a daily basis over the area shown in the figures illustrating this article. Equations (13) and (14) are the basis of the daily operational barotropic computations. In comparisons which have been made with conventional geostrophic barotropic predictions, it has been found that in some cases the two systems yield predictions of comparable accuracy, but in many cases the spurious anticyclogenesis of the geostrophic predictions is disastrous. Such errors are characteristically associated with weather regimes, so that they may appear day after day for a week or more, rendering numerical predictions useless for a like period.

The results of this study in hand may be summarized by saying that the use of a slightly modified geostrophic wind, which is strictly non-divergent, leads to a dramatic improvement over conventional geostrophic predictions. Use of winds calculated from the balance equation, on the other hand, yields a much less marked improvement over predictions made with semi-geostrophic non-divergent wind fields. It can be logically induced that the primary benefit of balanced winds, as opposed to geostrophic winds, is not, as has been suggested in the literature, due to dynamic effects inherent in the balance equation, but is due to the fact that they satisfy the law of conservation of mass.

Ramifications of the predictive consequences discussed here extend beyond the barotropic model. Proposed baroclinic models until very recently have generally made free use of the geostrophic approximation, while assuming vanishing surface pressure tendencies at the lower boundary. There is no theoretical reason to believe, and indeed there is abundant empirical evidence (Cressman and Hubert [8]) to deny, the thesis that baroclinic models are less sensitive to the violation of the law of mass conservation implied in the direct use of the geostrophic wind.

ACKNOWLEDGMENTS

Full acknowledgments would read like a personnel roster of the Joint Numerical Weather Prediction Unit. Only within such an organization could this study have been completed, depending as it does on inspiration and ideas from associates, professional skills of both meteorologists and mathematicians, long series of cases to inspect, and routine work of drafting and typing. I would especially single out for expressions of gratitude Dr. George P. Cressman, who very early understood the importance of the problem treated, and who lent directional assistance during the search for the underlying causes and solution.

REFERENCES

1. J. Charney, "On the Physical Basis for Numerical Prediction of Large-Scale Motions in the Atmosphere," *Journal of Meteorology*, vol. 6, No. 6, Dec. 1949, pp. 371–385.
2. J. Charney, "The Dynamics of Long Waves in a Baroclinic Westerly Current," *Journal of Meteorology*, vol. 4, No. 5, Oct. 1947, pp. 135–162.
3. S. Petterssen, "On the Relation between Vorticity, Deformation, and Divergence, and the Configuration of the Pressure Field," *Tellus*, vol. 5, No. 3, Aug. 1953, pp. 231–237.
4. J. Charney, "The Use of the Primitive Equations of Motion in Numerical Prediction," *Tellus*, vol. 7, No. 1, Feb. 1955, pp. 22–26.
5. B. Bolin, "Numerical Forecasting with the Barotropic Model," *Tellus*, vol. 7, No. 1, Feb. 1955, pp. 27–49.
6. B. Bolin, "An Improved Barotropic Model and Some Aspects of Using the Balance Equation for Three-Dimensional Flow," *Tellus*, vol. 8, No. 1, Feb. 1956, pp. 61–75.
7. F. Shuman, "A Method for Solving the Balance Equation," *Technical Memorandum* No. 6, Joint Numerical Weather Prediction Unit, 1955, 12 pp.
8. G. Cressman and W. E. Hubert, "A Study of Numerical Forecasting Errors," *Monthly Weather Review*, vol. 85, No. 7, July 1957, pp. 235–242.

A STUDY OF NUMERICAL FORECASTING ERRORS

G. P. CRESSMAN, Air Weather Service* and LCDR. W. E. HUBERT, United States Navy*

Joint Numerical Weather Prediction Unit, Suitland, Md.

[Manuscript received June 14, 1957; revised July 8, 1957]

ABSTRACT

Studies of numerical forecasting errors have revealed that the principal difficulties encountered in models currently operational at the Joint Numerical Weather Prediction Unit arise from errors in the 500-mb. forecasts. These errors are common to both barotropic and baroclinic models. The errors in the 1000–500-mb. thickness forecasts are considerably smaller. Results show that systematic errors are introduced (1) by the use of the geostrophic approximation and (2) by the approximations used on the boundaries. The cases presented in this paper show that the first type of error is virtually nonexistent in non-geostrophic, barotropic forecasts. Boundary errors are particularly serious in cases where the boundaries are meteorologically active, suggesting the future use of hemispheric forecast grids. The elimination of these two types of errors from all forecasts appears to be essential before the smaller errors, such as truncation errors and errors due to baroclinic development, non-adiabatic effects, etc., can be isolated and studied satisfactorily.

1. INTRODUCTION

In the normal routine of development work of the Joint Numerical Weather Prediction (JNWP) Unit a number of tests are made with a view toward isolating and removing certain types of forecasting errors. Some of the results of the tests are used immediately for model improvement. Other results, while yielding significant information, cannot be incorporated into operational forecasting for various reasons. The purpose of this paper is to record the results of several tests which would not otherwise be available for study elsewhere.

These tests which are being reported on by the authors have been suggested, conducted, and evaluated by a number of members of the JNWP Unit. Dr. Fred Shuman, Lt. Col. P. D. Thompson, USAF, Mr. L. Carstensen, Mr. G. Arnason, Lt. E. Carlstead, USN, Mr. C. Cave, and others have contributed to the work described below.

2. THE APPROXIMATION TO THE INITIAL WIND FIELD

Generally speaking, the most troublesome and significant errors found in numerical prediction arise directly from the difficulties in forecasting the 500-mb. flow. These difficulties are equally prominent in barotropic and multilevel forecasting. The first type of error to be discussed has been eliminated from the JNWP Unit barotropic forecasts, but is described below due to its importance. These errors are attributable to the use of the geostrophic approximation in describing the horizontal winds. They are manifested as (a) too strong deepening of Lows east of a strong current from the north, and (b) a tendency for erroneously large anticyclones to develop to the right of the jet stream (see Bolin [1]). The tendency for an erroneously large anticyclone to form is even further exaggerated if the jet stream is directed toward the north.

Errors introduced by the geostrophic approximation may be classified as arising from the fictitious divergence of the geostrophic wind, from the incorrect calculation of the vorticity when taking $\zeta_g = f^{-1} \nabla^2 \phi$ while neglecting the term $f^{-1} \nabla \phi \cdot \nabla f$, and from the failure to take into account accelerations and divergence in the initial wind field. The symbols have their standard meaning, where f is the Coriolis parameter, ϕ is geopotential, and ζ_g is the geostrophic relative vorticity.

Several series of forecasts have been made with the use of different approximations to the wind. Such a series is presented in figures 1 to 7. The wind has been described by (a) the geostrophic wind, (b) a non-divergent, non-geostrophic wind, represented by the stream function ψ (see Shuman [2]), and (c) a wind which is non-accelerated and non-divergent (one could call this a "non-divergent geostrophic wind"), represented by a stream function S_2 (discussed by Shuman [2]) and defined by

$$\nabla^2 S_2 = f^{-1} (\nabla^2 \phi + \beta u_g)$$

where β is the northward variation of the Coriolis parameter, and u_g is the geostrophic west wind component.

These examples do not give typical, but extreme, results. They are presented to show the magnitude of errors that can be introduced by the geostrophic approximation. The situation presented was characterized by an unusually extensive meridional flow in the Gulf of Alaska and a strong zonal flow across the United States. The initial

*Any opinions expressed by the authors are their own and do not necessarily reflect the views of the Department of Defense.

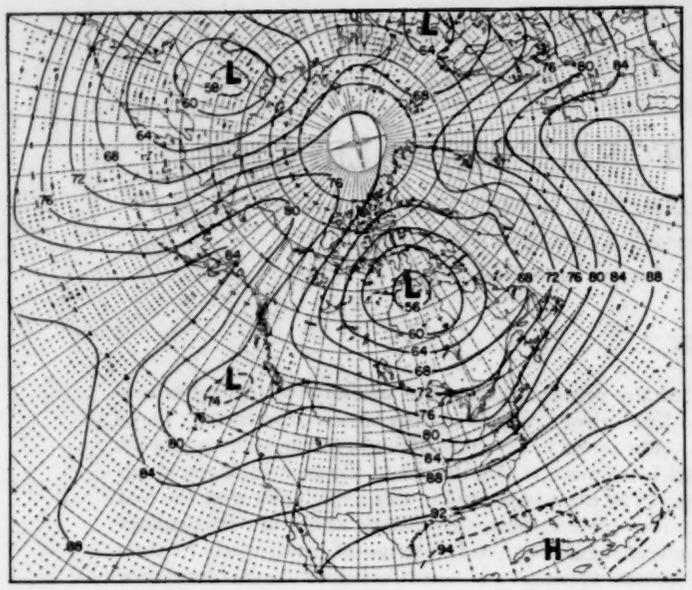

FIGURE 1.—Initial 500-mb. chart, January 10, 1957, 1500 GMT.

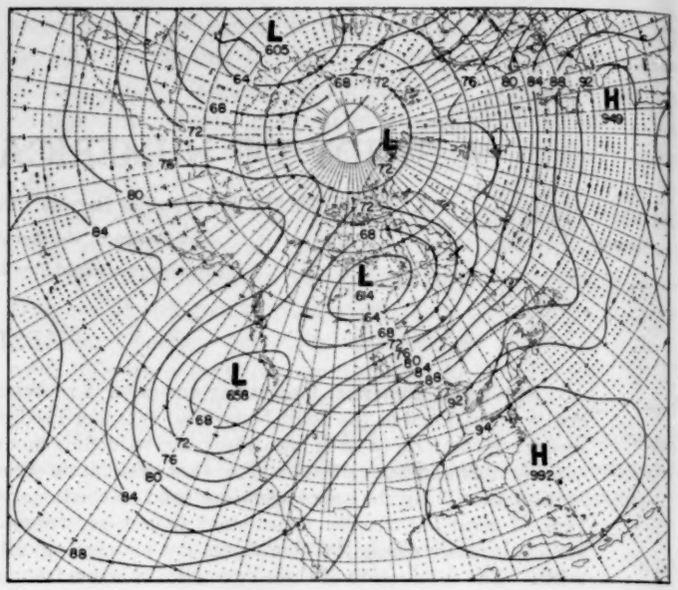

FIGURE 3.—36-hour geostrophic barotropic 500-mb. forecast from January 10, 1957, 1500 GMT.

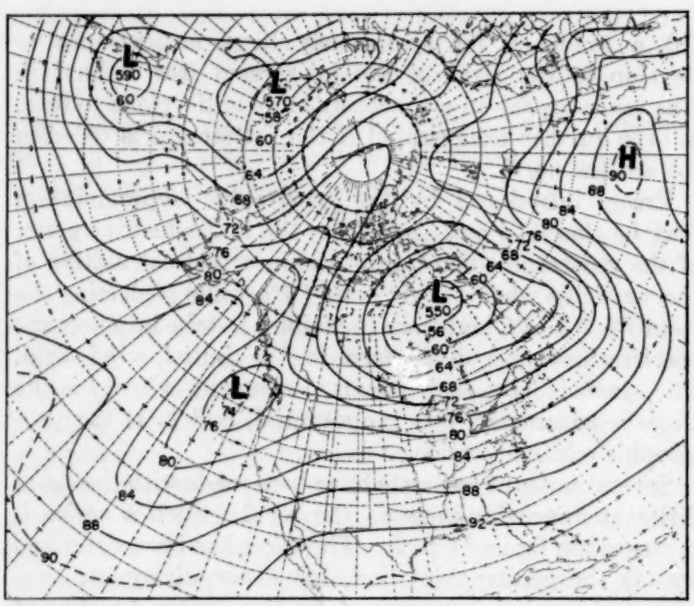

FIGURE 2.—Verifying 500-mb. chart, January 12, 1957, 0300 GMT

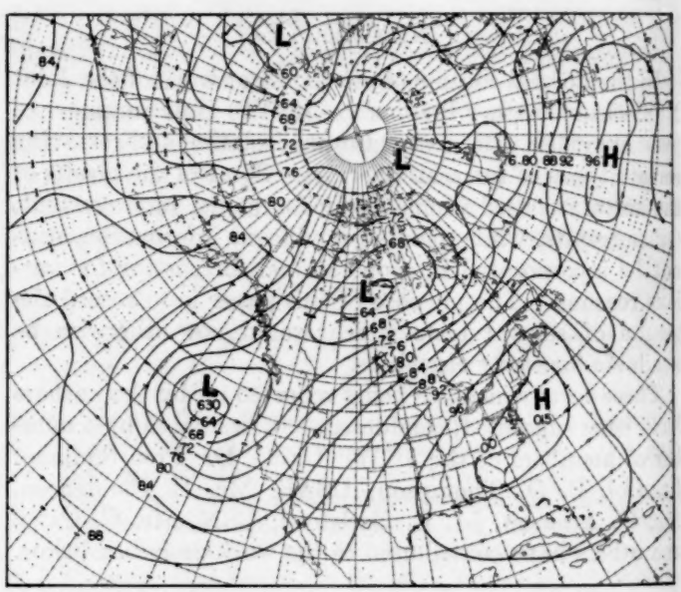

FIGURE 4.—36-hour geostrophic thermotropic 500-mb. forecast from January 10, 1957, 1500 GMT.

and verifying 500-mb. charts are shown in figures 1 and 2. The geostrophic barotropic forecast (with no terrain effects included) is shown in figure 3. In this forecast the excessive development of amplitude across North America has become ruinous. This difficulty is even more pronounced in the geostrophic thermotropic forecast shown in figure 4. For a detailed comparison of these two models see Thompson and Gates [3]. The differences between the two forecasts are that the equation for the thermotropic 500-mb. flow has an added Jacobian of the form $AJ(h,\nabla^2 h)$, h being the 500–1000-mb. thickness; there is also a term including terrain effects. The extra Jacobian has the effect of strengthening the flow in the forecast and has therefore accelerated the growth of the error. The mountain term is unimportant in comparison with the other errors in this case.

Figures 5 and 6 show the barotropic forecasts made with S_2 and ψ, respectively. Each of these is greatly improved over the geostrophic forecasts. Note that the S_2 forecast has an erroneous 19,600-ft. contour in the southeastern States, which does not appear in the ψ forecast. Finally, the thermotropic forecast made with S_2 winds at both the 1000 and 500-mb. levels is shown in figure 7. Further tests (not shown) have been made where the βu_g term was deleted from the S_2 stream function. These indicated that the additional contribution of this term is relatively unimportant, resulting mainly in a slightly stronger belt of westerlies.

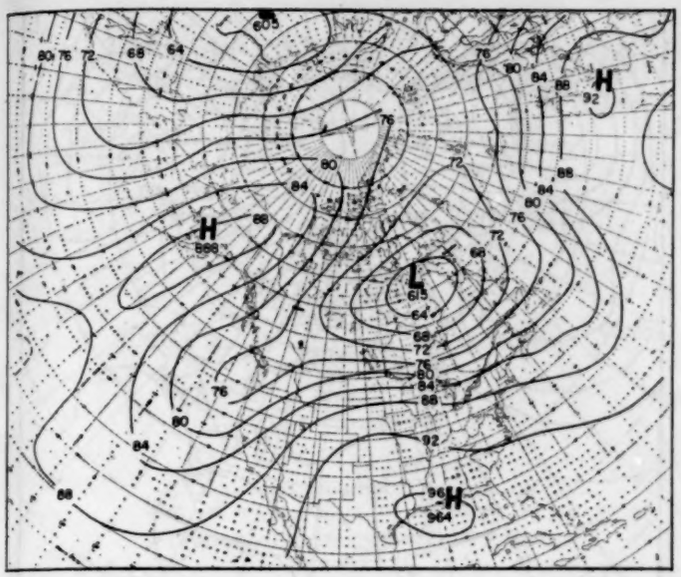

FIGURE 5.—36-hour barotropic 500-mb. forecast made using S_2 stream function from January 10, 1957, 1500 GMT.

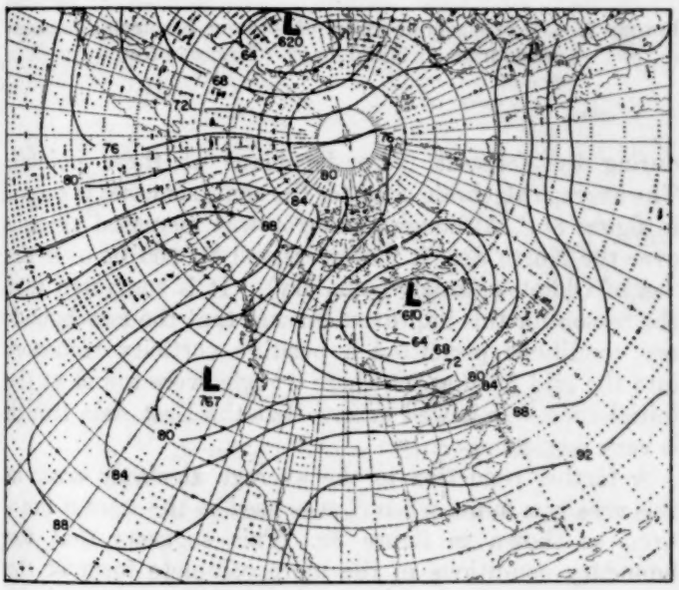

FIGURE 6.—36-hour barotropic 500-mb. forecast made using ψ stream function from January 10, 1957, 1500 GMT.

A comparison of figures 3 and 5 indicates that most of the error found in the geostrophic barotropic forecast was removed by use of the S_2 wind approximation. This leads to the conclusion that the divergence of the geostrophic wind was the largest contributing factor to the large errors of figures 3 and 4, in agreement with Shuman [2]. The further improvement exhibited by the ψ forecast is shown in figure 6. One may conclude that a non-geostrophic wind should be used in numerical prediction, since the errors introduced by the geostrophic approximation can be of such a large magnitude as to obscure all other types of error.

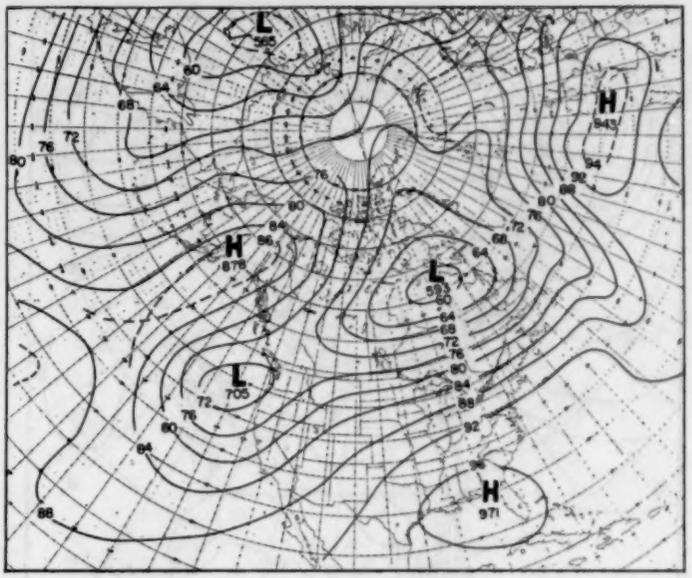

FIGURE 7.—36-hour thermotropic 500-mb. forecast made using S_2 stream function at 500 and 1000 mb. from January 10, 1957, 1500 GMT.

3. BOUNDARY CONDITIONS AND RELATED ERRORS

Another important source of error in numerical prediction is the condition imposed on the lateral boundaries. It should be relatively easy to specify a set of realistic and accurate enough boundary conditions if the boundaries fall in areas which are meteorologically inactive; i. e., with persistent, stagnant circulations. Such an arrangement does not seem to be possible short of using a hemispheric grid. The grid used by the JNWP Unit in 1956 and the first half of 1957 has a Pacific boundary which is meteorologically very active, with variable areas of strong inflow and strong change. It is our experience that the predictions for areas inside boundaries where strong inflow occurs are usually characterized by strong erroneous height rise (the stronger the flow, the greater the rise) particularly if the flow has a southerly component. Smaller erroneous falls are found near outflow boundaries.

A set of six situations from December 1956 and January 1957 has been used for testing remedies for boundary errors. Although the meteorological situations varied among these cases, the large-scale fields of error were relatively similar. The forecasts were made with a stream function ψ given by the balance equation [2] in a barotropic prediction model. Boundary errors are introduced by the boundary conditions in the balance equation, boundary conditions in the forecast model, and boundary problems introduced by smoothing. The boundary conditions used in solutions of the balance equation are essentially that the flow component normal to the boundaries is set equal to the corresponding component of the geostrophic flow.

The boundary conditions previously used in the operational barotropic forecast were (a) constant values of

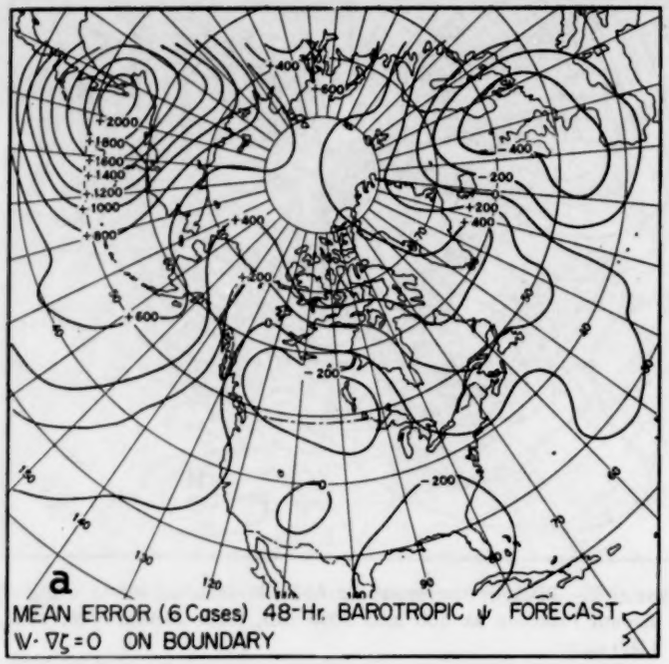

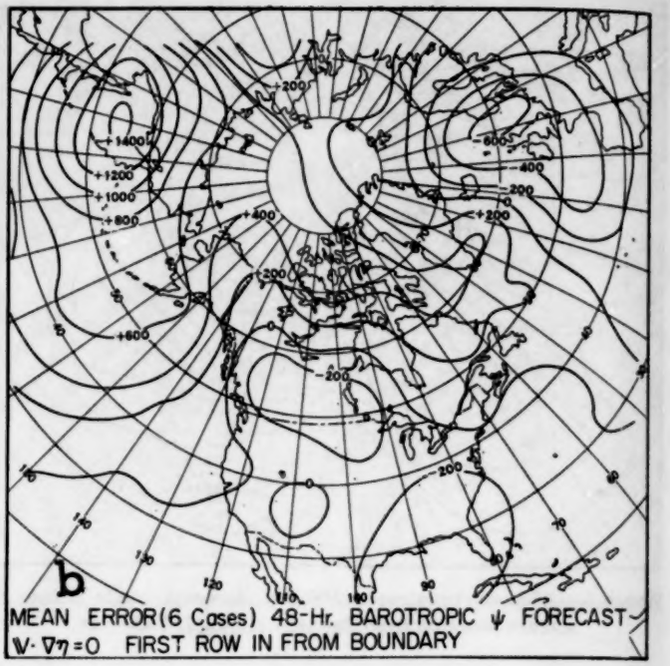

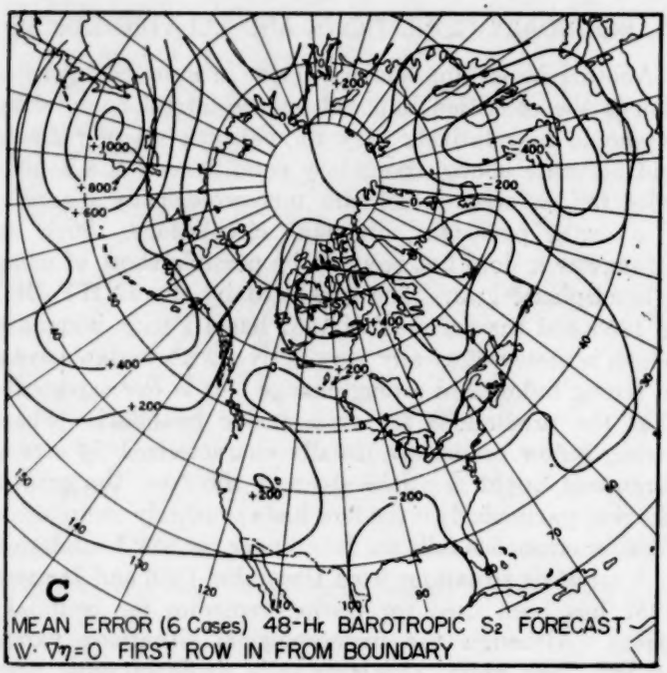

FIGURE 8.—Mean algebraic errors of 48-hour barotropic forecasts made from six initial maps. Errors in feet.

stream function on the boundary points through the forecast period, and (b) zero relative vorticity at the boundaries. The average algebraic errors of the 48-hour forecasts for the six cases mentioned above are shown in figure 8a. Of special interest are the 2000-ft. positive errors over the Sea of Okhotsk and the 400-ft. negative errors over the North Sea.

The forecast program was then changed so that the initial values of vorticity on the rows and columns adjacent to the boundaries were retained with no change during the forecast (zero Jacobians at these points). The average algebraic error for the same six cases is shown in figure 8b. Although the error was increased slightly over the North Sea, it was decreased by 600 ft. over the Sea of Okhotsk (inflow boundary). It is suggested that the reason for this improvement was that the new boundary conditions permitted a positive vorticity transport into the grid from areas where troughs were found at the initial time. It is well known that the East Asia trough is very persistent.

A further reduction in the average algebraic error in this area was found when S_2 was used as the stream function, as shown in figure 8c. This suggests that the boundary conditions in the more complete form of the balance equation may be responsible for some of the difficulty. One should not infer from these results that S_2 is a better stream function for barotropic forecasting than ψ, since only algebraic boundary errors have been discussed here.

Another experiment in the study of boundary errors was performed by making a set of non-geostropic barotropic forecasts with the grid located in two different positions on each map on each of three different days. The first of the two positions, referred to as "normal", is the same as that shown in figure 8. The second grid position, referred to as "rotated", was obtained by rotating the first one 180 degrees about the north pole. The error of each forecast was then averaged along each longitude from 35° N. to 90° N. The errors for each of the

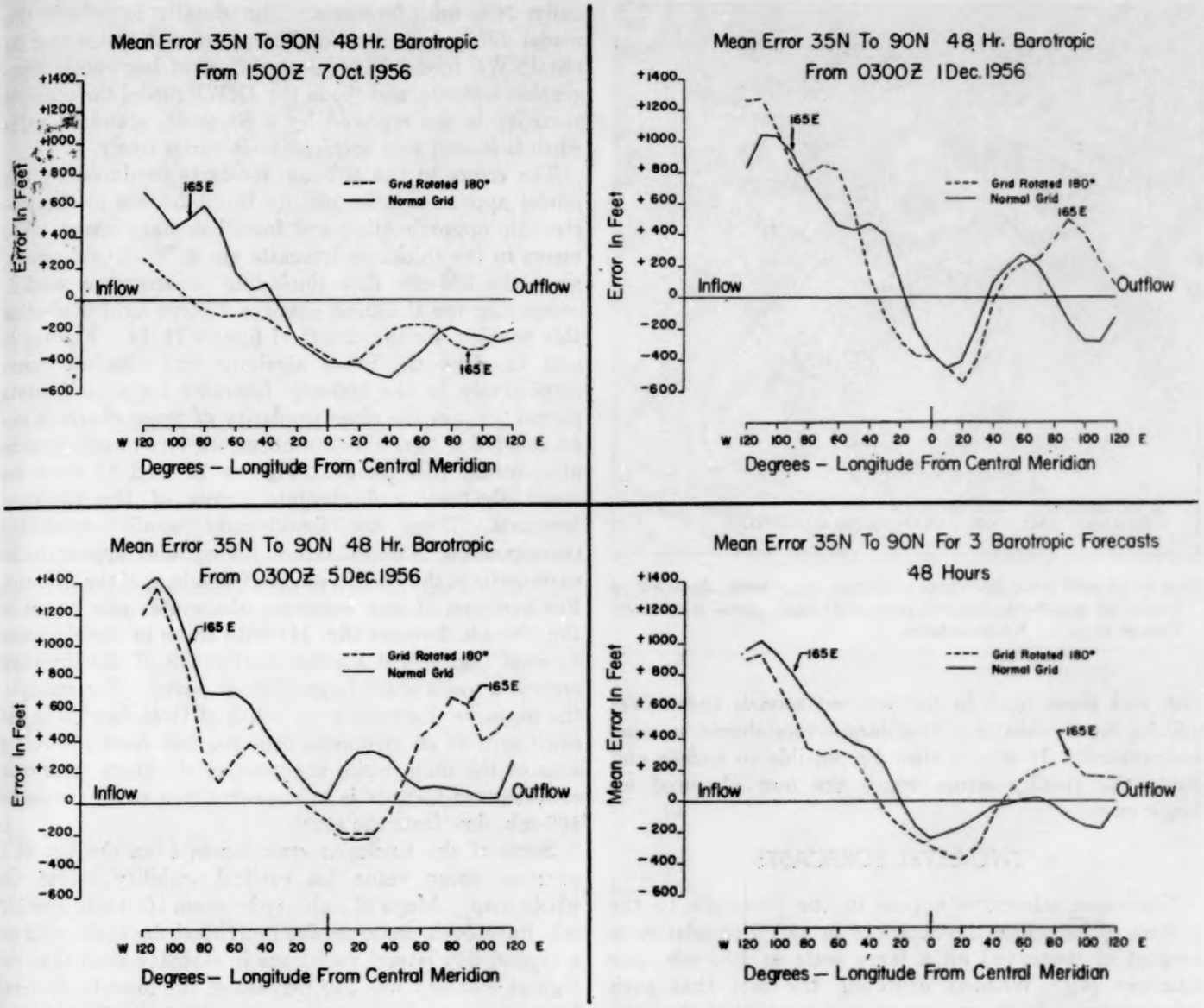

FIGURE 9.—Mean algebraic errors for three sets of non-geostrophic barotropic forecasts as a function of longitude in the grid. Errors in feet.

three days as well as the mean for all three are plotted against longitude in the grid in figure 9. In looking at this figure one gets the distinct impression that the largest forecast errors are a function of position in the grid and move with the grid as it is rotated.

This is not true of all significant errors, however, as can be seen by inspection of the points labeled "165° E." There is a tendency for a significant positive error to occur at or west of this longitude regardless of the grid position. A suggested source for this error is the effect of the divergence induced by the Asian Plateau. This barotropic model ordinarily takes into account the large-scale mountain effect. It was, however, not feasible to do so in this set of eight forecasts. The next barotropic model to be used by the JNWP Unit will be computed on a hemispheric grid, with which it should be possible to include the large-scale effect of the Asian Plateau.

The large-scale errors which are a function of position in the grid can arise from erroneous boundary conditions and truncation errors, the latter resulting from directional properties of the finite-difference Jacobian operators. In a further study of contributing factors to these errors, a fictitious geopotential field yielding 25-knot zonal winds throughout the entire grid was "balanced" to obtain the corresponding ψ field. This field was then used as input data for a 48-hour barotropic forecast. The results of this experiment are shown in figure 10. At least part of the observed error appears to be caused by the boundary conditions used in solving the balance equation. The initially circular ϕ field is distorted slightly, and the resultant long wave (with an amplitude of only 20 feet) in the ψ field grows with time.

When the hemispheric grid is put into operation, the boundary assumptions used in solving the balance equa-

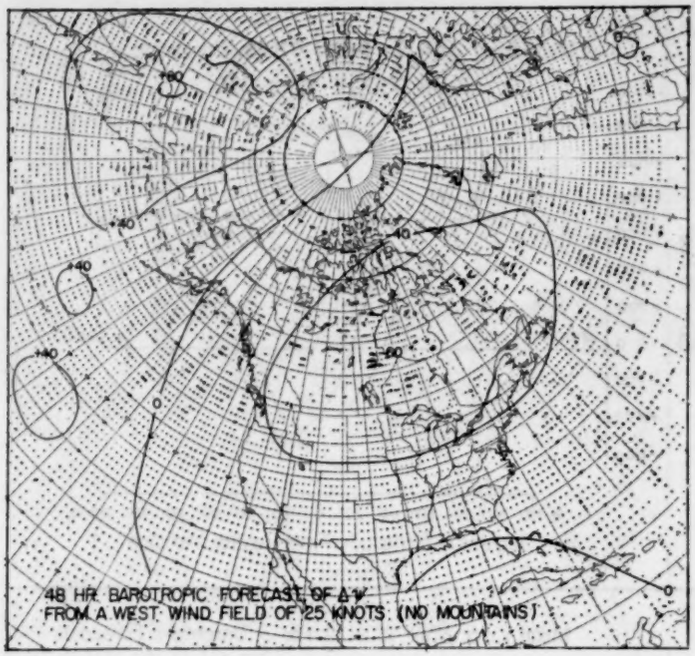

FIGURE 10.—48-hour barotropic change in stream function ψ (scaled as a 500-mb. height) from a 25-knot, zonal wind field. Change in feet. No mountains.

tion and those used in the forecast models themselves will be more realistic. Boundary errors should become insignificant. It should then be possible to isolate and study the smaller errors which are now obscured by larger ones.

4. TWO-LEVEL FORECASTS

Numerous references appear in the literature to the process of baroclinic development in which circulation is created or destroyed on a large scale at 500 mb. (see Charney [4]). Without disputing the fact that such developments do occur, one must remark that they are quite rare. A chronological series of charts of geostrophic absolute vorticity at 500 mb. shows many apparent circulation increases as cyclonic vorticity associated with shear becomes associated with curvature. Most of these apparent increases are erroneously indicated by the geostrophic wind. At the JNWP Unit an extended series of 500-mb. absolute vorticity charts of the non-divergent, non-geostrophic wind has been prepared. These show a remarkable preservation of the size and intensity of the 500-mb. circulation centers from day to day (Vederman and Hubert [5]). In fact, most of the *apparent* circulation changes occur in areas of sparse data. One can conclude that although baroclinic development may at times present a severe local problem in barotropic forecasting, it does not account for a very large fraction of the errors currently encountered in numerical prediction.

A quasi-geostrophic two-parameter model similar to the "thermotropic" model described by Thompson and Gates [3] has been used by the JNWP Unit to obtain daily 1000-mb. forecasts. The details in which this model differs from that of Thompson and Gates are: (a) the JNWP model includes the effect of large-scale topographic features, and (b) in the JNWP model the absolute vorticity is not replaced by a constant, standard value when it is used as a coefficient—it varies freely.

The errors in the 500-mb. forecasts produced by this model appear to arise mainly from the use of the geostrophic approximation and from boundary errors. The errors in the thickness forecasts are difficult to diagnose, since the 500-mb. flow (including its errors) is used in computing the thickness changes. Some light is shed on this problem by the charts of figures 11–14. Figures 11 and 12 show the mean algebraic and absolute errors respectively in the 500-mb. forecasts for a half-month period. From the close similarity of these charts it can be concluded that the 500-mb. errors were mostly systematic during this period. Figures 13 and 14 show the mean algebraic and absolute errors of the thickness forecasts. These are significantly smaller than the corresponding 500-mb. errors. They also appear to be systematic in the Pacific, eastern Canada, and the Atlantic. Furthermore, if one compares the systematic errors in the 500-mb. forecast (fig. 11) with those in the thickness forecast (fig. 13), it appears that much of the thickness error is a result of the larger 500-mb. error. For example, the negative thickness error south of Greenland is in the same area as an erroneous 500-mb. flow from the colder area of the map, while the positive thickness error over southeastern Canada is in the same area as an erroneous 500-mb. flow from the south.

Some of the thickness error arises from the use of a constant mean value for vertical stability across the whole map. Maps of stability between 1000 mb. and 500 mb. have been produced for individual days, showing on a typical day lateral variations in stability such that the highest stability was 240 percent of the lowest. Several forecasts have been made with different (3-level and thermotropic) models using varying values for the static stability. The results can be summarized by saying that the models responded to stability changes in the same way as the atmosphere does; i. e., with high stability the coupling between levels was very loose, and vice versa. One forecast was made in which, by accident, the vertical stability was set at an extremely large value. In this case, the changes in thickness and 500-mb. height were apparently unrelated.

The 1000-mb. forecasts from the thermotropic model are obtained by subtracting the 1000–500-mb. thickness forecast from the 500-mb. forecast. It appears, then, that the most effective way of improving the thickness (and 1000-mb.) forecast is to improve the 500-mb. forecast. It is also concluded that lateral variations of vertical stability must eventually be considered.

Inclusion of the large-scale effect of mountains is important to all forecasts, especially those of the lower levels. These will not be discussed in any detail except

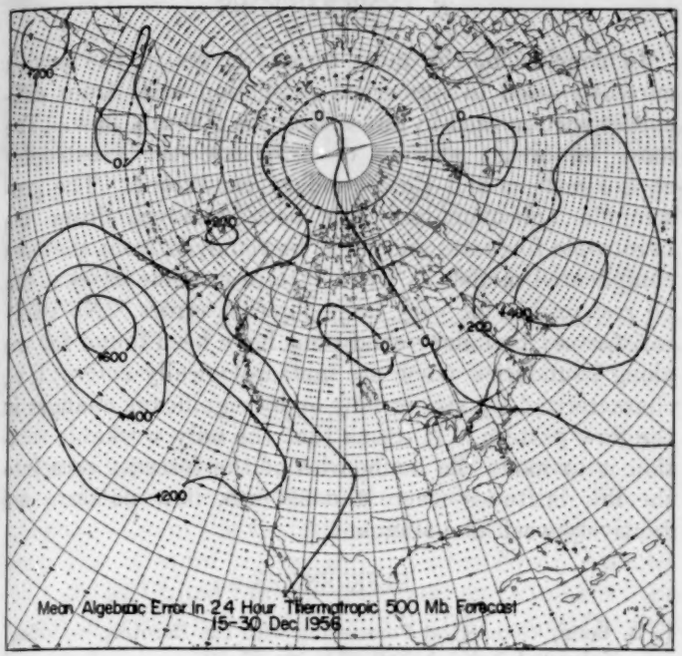

FIGURE 11.—Mean algebraic error of thermotropic 500-mb. forecasts, December 15–30, 1956. Errors in feet.

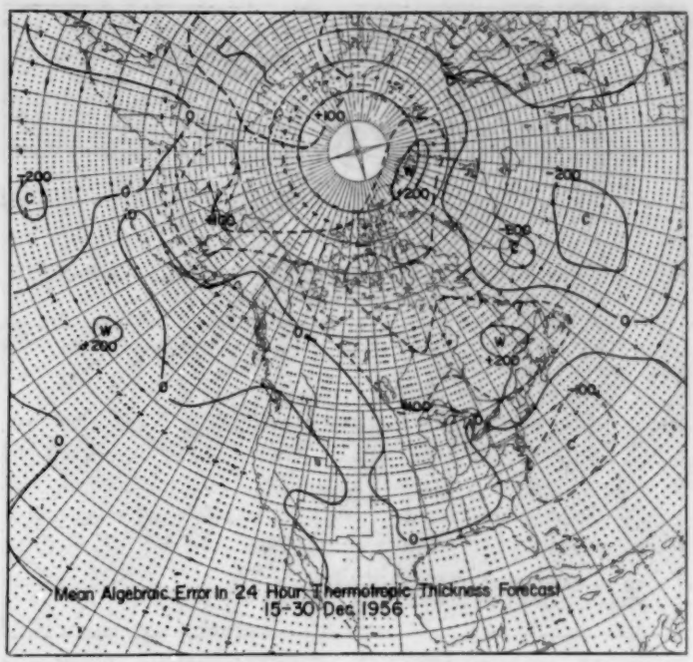

FIGURE 13.—Mean algebraic error of the thickness (500–1000 mb.), December 15–30, 1956. Errors in feet.

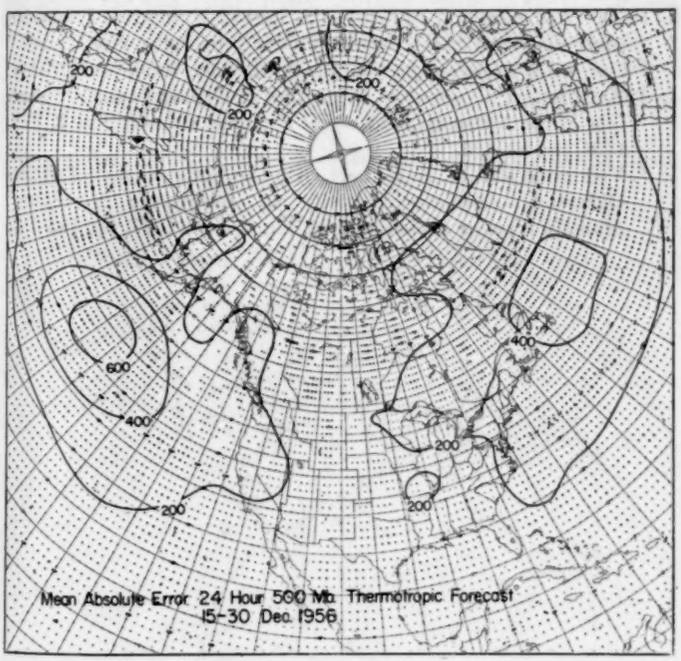

FIGURE 12.—Mean absolute error of thermotropic 500-mb. forecasts, December 15–30, 1956. Errors in feet.

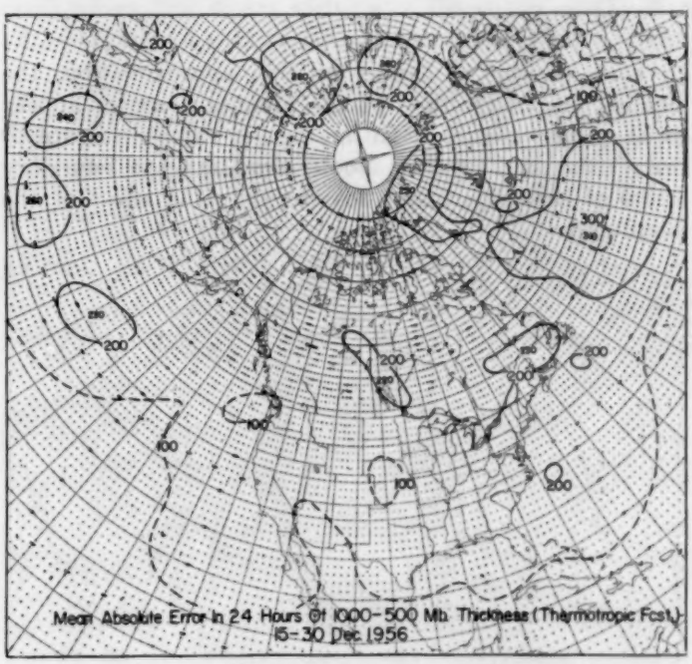

FIGURE 14.—Mean absolute error of the thickness (500–1000 mb.), December 15–30, 1956. Errors in feet.

to say that if f is used instead of $\zeta + f$ for the coefficient of the divergence in the vorticity equation, the computation of mountain effects is not nearly so successful. Smoothing of the terrain does not seem to be especially important unless it is done excessively; e. g., enough to double the apparent lateral extent of Greenland. This leads to undersirable results. Inclusion of mountain effects in the forecasts has a quite spectacular result over Greenland, where it prevents cyclones from crossing the high terrain, steering them around the coasts. Cyclone development on the lee side is clearly encouraged by the mountain effects in the model.

In order to see clearly the results of including a mountain effect in the barotropic model, the experiment with the 25-knot, zonal wind (fig. 10) was repeated with terrain included. The results are shown in figure 15. In the barotropic model, a fixed fraction of the 500-mb. wind is assumed to apply at the surface of the ground.

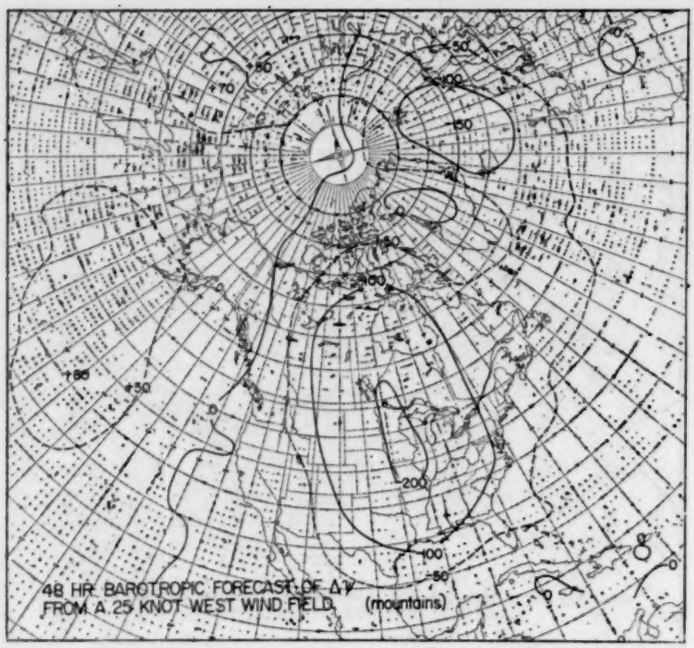

FIGURE 15.—48-hour barotropic change in stream function ψ (scaled as 500-mb. height) from a 25-knot, zonal wind field. Change in feet. Mountains included.

In spite of the crudeness of this approximation, the location and magnitude of the mountain waves appear to be quite realistic. Subtracting the values in figure 10 from those in figure 15 should eliminate the boundary errors of this experiment, leaving only the effect of the mountains.

5. CONCLUSIONS

In conclusion, the most serious errors in the models currently used in numerical prediction arise from difficulties encountered in forecasting the 500-mb. flow. The most important sources of error are the geostrophic approximation and the boundary conditions. The geostrophic approximation has been removed from the barotropic forecasts and must be removed from the more complicated models as well, since in extreme cases it can be responsible for very large forecast errors. No really satisfactory boundary conditions have been found for use along boundaries which are meteorologically active; i. e., characterized by strong flow or by significant changes in the flow pattern. It seems that the only workable solution is to move the boundaries of the forecast area into the low latitudes where the 500-mb. flow patterns are relatively weak and stagnant.

REFERENCES

1. B. Bolin, "Numerical Forecasting with the Barotropic Model," *Tellus*, vol. 7, No. 1, Feb. 1955, pp. 27–49.
2. F. G. Shuman, "Predictive Consequences of Certain Physical Inconsistencies in the Geostrophic Barotropic Model," *Monthly Weather Review*, vol 85, No. 7, July 1957, pp. 229–234.
3. P. D. Thompson and L. Gates, "A Test of Numerical Prediction Methods Based on the Barotropic and Two-Parameter Models," *Journal of Meteorology*, vol. 13, No. 2, Apr. 1956, pp. 127–141.
4. J. S. Charney, "Numerical Prediction of Cyclogenesis," *Proceedings of the National Academy of Sciences*, vol. 40, No. 2, Feb. 1954, pp. 99–110.
5. J. Vederman and W. E. Hubert, "On the Conservation of Finite-Difference Absolute Vorticity in Barotropic Forecasts," *Monthly Weather Review*, vol. 85, No. 6, June 1957, pp. 193–199.

AN ANALYSIS OF THE MOVEMENT OF A HURRICANE OFF THE EAST COAST OF THE UNITED STATES, OCTOBER 12–14, 1947

CONRAD P. MOOK,[1] EUGENE W. HOOVER, AND ROBERT A. HOOVER

U. S. Weather Bureau Forecast Center, Washington National Airport, Washington, D. C.
[Manuscript received February 8, 1957; revised July 27, 1957]

1. INTRODUCTION

During the night of October 11–12, 1947, a tropical hurricane moved northeastward across southern Florida and out to sea in the vicinity of Miami on a course which seemed to offer no further threat to the North Atlantic coast of the United States. However, on October 13 the hurricane turned rather sharply to the left, and on October 15 it moved inland near Savannah, Ga.

The course taken by this hurricane as it made its historic turn has been in doubt due to the scarcity of reports received at the time from ships sailing near the storm center. Several reconnaissance aircraft were in the vicinity of the storm on the 13th, but even their reports did not give a complete enough picture, so that in the annals of meteorology and storms, including the monumental work by Tannehill [1], the path of the storm is shown as being unknown during the period of the turn. The purpose of this report is to show what appears to be the reliable picture of the track of the storm during the period when it made its turn.

[1] Present affiliation: Diamond Ordnance Fuze Laboratories, Ordnance Corps, Department of the Army, Washington 25, D. C.

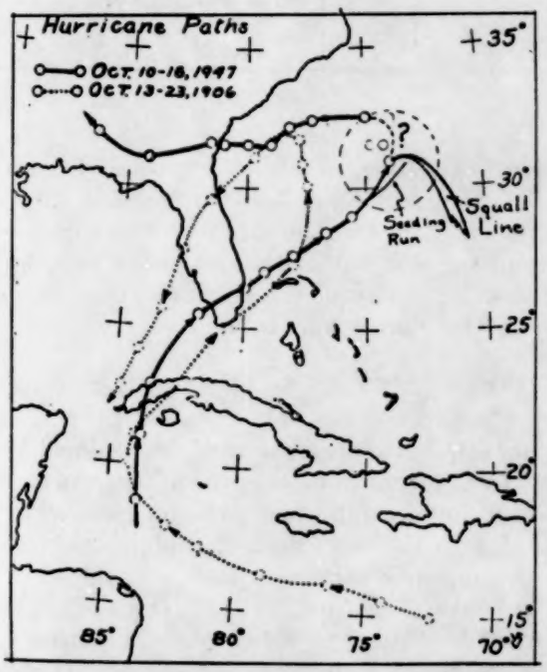

FIGURE 1.—Solid track is the path of the hurricane of October 10–16, 1947, as presented by Langmuir [1]. Note the dashed circle outlining the "approximate area of the clouds of the hurricane" at the time of seeding (1138–1208 EST). (This figure is reproduced, by permission, from the *Proceedings of the American Philosophical Society.*)

2. ADDITIONAL PUBLISHED EVIDENCE OF THE STORM TRACK

Of particular interest is the fact that three of the aircraft which flew in the vicinity of the storm on October 13, 1947, were a part of a cloud seeding expedition. The

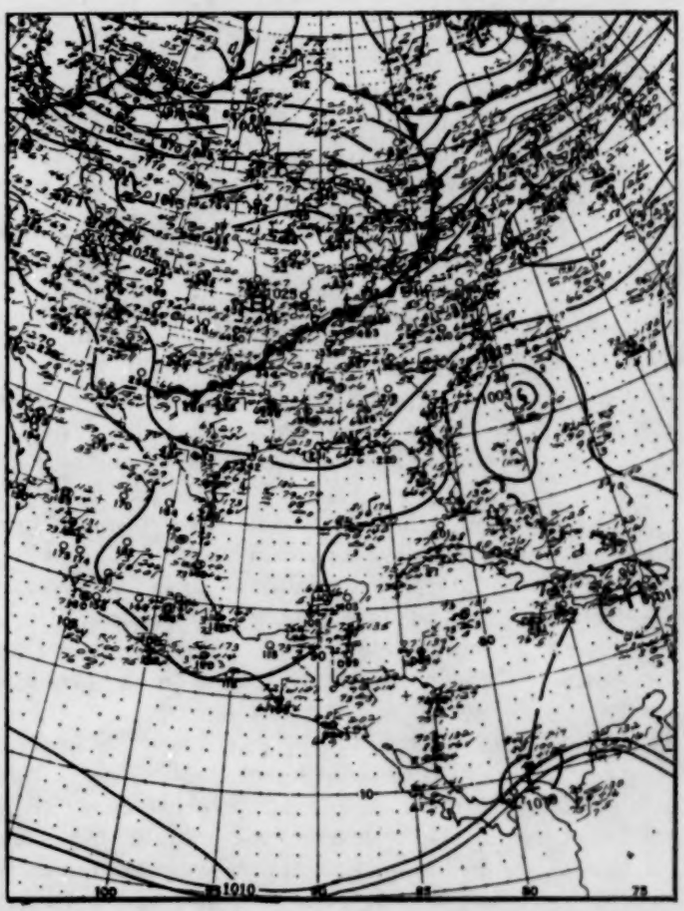

FIGURE 2.—Sea level chart showing the position of the hurricane at 1230 GMT October 13, 1947. (From *Northern Hemisphere Historical Weather Maps.*)

TABLE I

SS. " LISIEUX " - Voyage GALVESTON/LE HAVRE.-

I - POSITIONS :

- Le 11 Octobre à 12h.00 : (L = 25°58' N.)G = 79°50' W.
- Le 11 -"- à 20h.00 : (L = 27°27' N.) G= 79°39' W.
- Le 12 -"- à 14h.00 : (L = 28°39' N.)G = 76°52' W.
- Le 12 -"- à 19h.00 : (L = 29°30' N.)G = 76°15' W.
- Le 13 -"- à 08h.00 : (L = 30°30' N.)G = 74°27' W.
- Le 13 -"- à 09h.00 : (L = 30°39' N.)G = 74°27' W.
- Le 13 -"- à 10h.00 : (L = 30°47' N.)G = 74°18' W.
- Le 13 -"- à 12h.00 : (L = 31°06' N.)G = 74°18' W.
- Le 13 -"- à 24h.00 : (L = 31°45' N.)G = 73°24' W.
- Le 14 -"- à 07h.00 : (L = 32°15' N.)G = 72°00' W.
- Le 14 -"- à 12h.00 : (L = 32°33' N.)G = 70°54' W.

II - RENSEIGNEMENTS DIVERS :

Date	Heure	Vent	(Ind.) Baromètre	Etat de la mer	Observations
12/10	0100	E/9	29,93	Houle	
"	0300	E/9	29,98	"	Coups de vent et grains
"	0500	ENE/8	29,82	"	Pluie continuelle
"	0700	ENE/8	29,92	"	Très mauvaise visibilité
"	1100	ENE/7	29,92	"	
"	1300	ESE/8	29,89	"	
"	1500	ESE/7	29,90	"	
"	1900	E/6	29,90	"	Pluie - vent en rafales
"	2300	SE/8	29,85	"	
13/10	0100	E/6	29,89	"	
"	0300	E/7-8	29,87	"	
"	0500	E/5-6	29,80	"	
"	0700	ESE/7-8	29,74	"	
"	1100	SSE/9	29,69	"	Vent soufflant en tempête
"	1300	SSE/9	29,65	Grosse	Direction instable
"	1500	SSE/9	29,65	Houle	
"	1900	S/9	29,71	"	
"	2100	SSE/7	29,71	"	
"	2300	SSE/7-8	29,73	"	
14/10	0100	SE/8	29,73	"	Bonne visibilité
"	0300	E/8	29,73	"	Eclairs sur tout l'horizon
"	0500	E/8	29,72	"	
"	0700	E/7	29,72	"	
"	1100	ESE/5-6	29,86		Beau temps - clair - Bonne visibilité
"	1300	ESE/5	29,87		
"	1500	ESE/5	29,86		
"	1900	ESE/5	29,96		
"	2300	ESE/3	29,97		Temps humide, ciel se couvrant. Bonne visibilité.

report of this expedition, as published by Langmuir [2], places the storm at the time of seeding (1638–1708 GMT of October 13) at the position shown in figure 1. This position is identical to that shown on the map for 1230 GMT of that date as published in the Northern Hemisphere Sea Level Synoptic series (fig. 2).

The implication, which one could draw from this, is that at the time of seeding the storm had stopped moving, which might be interpreted further as an indication that the storm was about to make a change in its course. However, as one examines this picture further, he finds that the location of the hurricane, as shown on the synoptic chart for 1230 GMT of October 13, hinges almost entirely on a report received by radio from a vessel SS *Lisieux*. No other reports were listed as having been received from this vessel. Therefore, before any conclusion could be reached regarding the accuracy of the 1230 GMT hurricane position, it was decided to attempt to verify the report as received by radio. The National Weather Records Center at Asheville, N. C., has no record of the report, but finally through the cooperation of the French Line, which owned the vessel at the time, the report was tracked down. The log, which they furnished, is shown in table 1. This log shows that at 1230 GMT the ship had been experiencing a wind from the east, rather than from the west, and that the 1230 GMT position of the hurricane, as shown on the Northern Hemisphere map, is in error.

3. COLLECTION OF ADDITIONAL DATA

Further searches of the archives of the National Weather Records Center verified most of the other reports received at the time, but several, which were not received by radio, were added to the collection. In addition, in order to make as complete a survey as possible of the track of the storm in question, the New York City Office of the Weather Bureau made inquiry to many other shipowners which had vessels in the vicinity of the storm. Through the courtesy of various companies thus contacted, several logs were made available to the Weather Bureau which contained weather information not otherwise entered on Weather Bureau forms, especially information entered

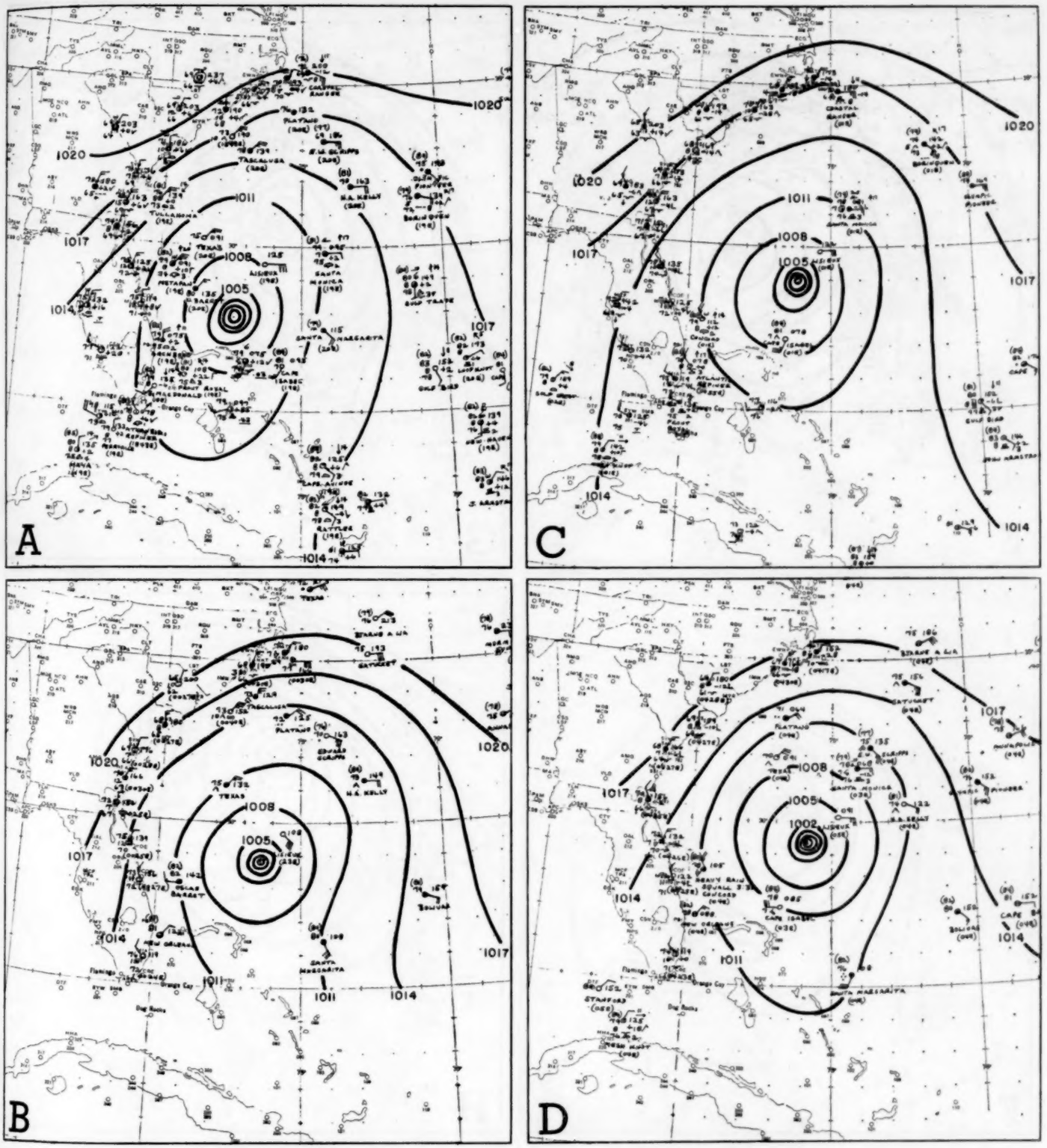

FIGURE 3.—Synoptic sea level charts, based on all data procured from all available sources, showing the history of the hurricane on October 13 and 14, 1947. (A) 0030 GMT, October 13, (B) 0500 GMT, October 13, (C) 0630 GMT, October 13, (D) 0900 GMT, October 13.

each four hours in the logs at times other than the regular time of collection of synoptic weather reports. This made possible the construction of synoptic charts for midnight and noon of the days in question, as well as charts for 4 a. m. and 4 p. m. (75th meridian time).

437310—57——2

4. ANALYSIS OF DATA

These reports, along with coastal reports for the same time, have been plotted with those for the regular synoptic periods on the charts shown in figure 3. After setting aside the data for noon of October 13 for later study, the

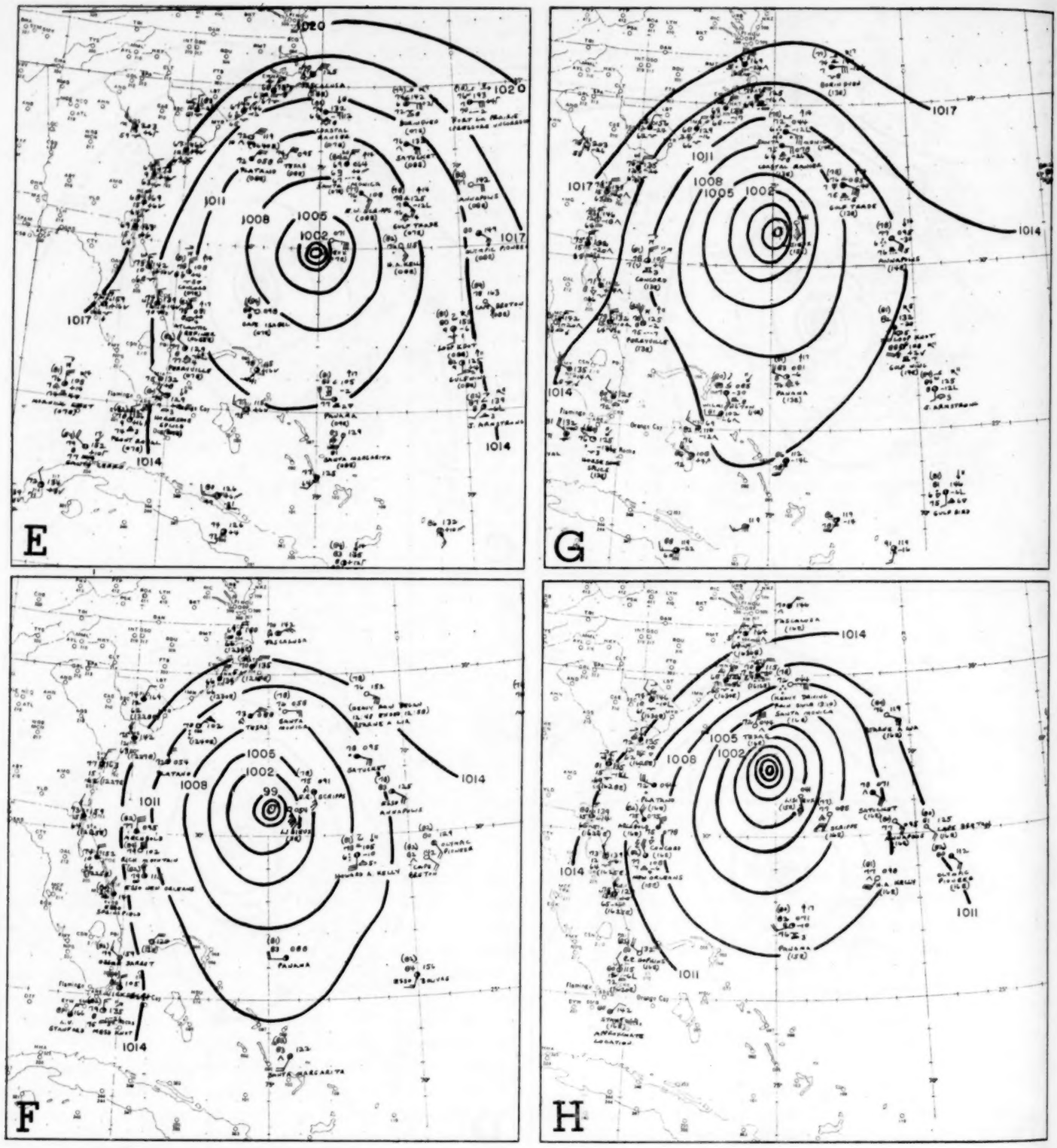

FIGURE 3.—Continued. (E) 1230 GMT, October 13, (F) 1700 GMT, October 13, (G) 1830 GMT, October 13, (H) 2100 GMT, October 13.

charts were analyzed, with an attempt being made to determine any consistent errors in the barometric pressures reported by the various ships. By a process of trial and error, a set of average corrections was developed as shown in table 2. From this came the consistent and symmetrical picture of the storm circulation shown in the maps.

Following this, in order to make the best possible estimate of the position and intensity of the storm at the time of seeding, the same corrections were applied to the reports contained in the ship logs for noon of the 13th. As a result of the corrections, the hurricane position was found to be somewhat to the west of the position where it

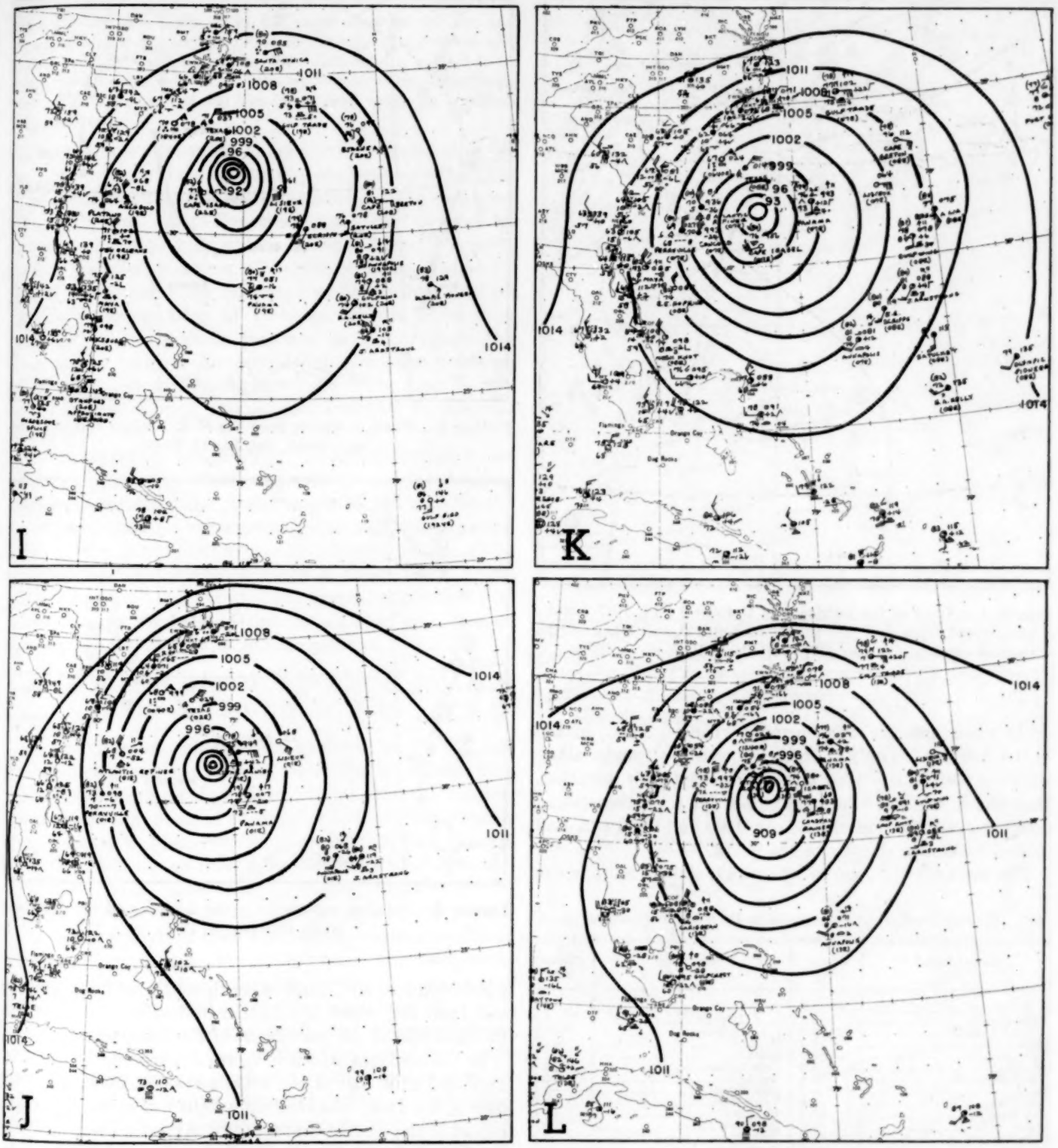

FIGURE 3.—Continued. (I) 0030 GMT, October 14, (J) 0630 GMT, October 14, (K) 1230 GMT, October 14, (L) 1830 GMT, October 14.

was originally believed to have been located (fig. 1), which means that some change in course of the storm was then in progress. Figure 4 shows the track of the storm thus analyzed.

A further detailed analysis was then made of the wind and pressure variations shown by the two ships closest to the storm at that time, the *E. R. Scripps* and the *Lisieux*. Their data are plotted in figures 5 and 6 and in a manner which shows the track of the vessels as well as that of the hurricane as determined above.

In figure 5 it can be seen that from 0400 to 0800 EST the pressure fell 2.7 mb. on the *Scripps* at a time in the diurnal

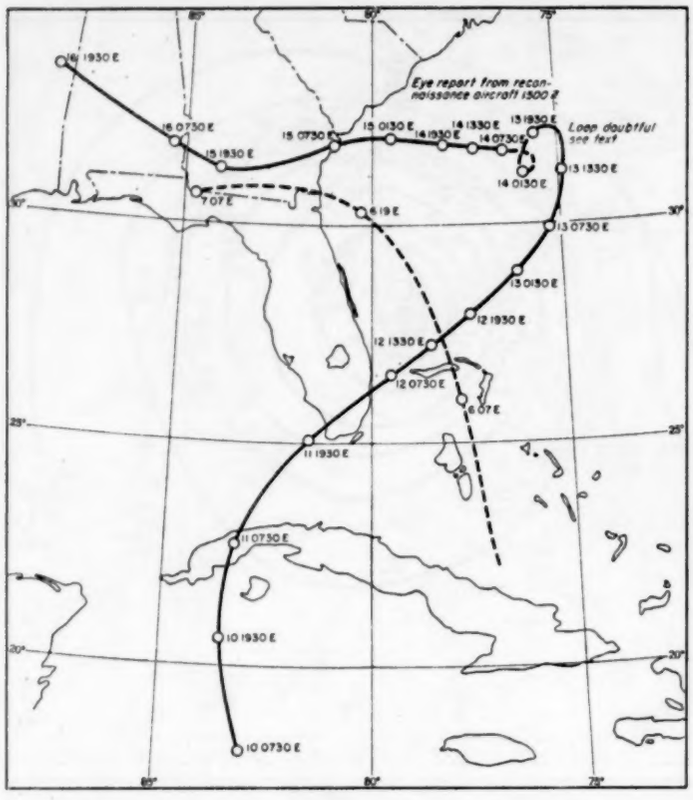

FIGURE 4.—Track of the hurricane of October 12–14, 1947 (solid), as deduced from analyses shown in figure 3, and track of the tropical storm of October 5–7, 1947 (dashed).

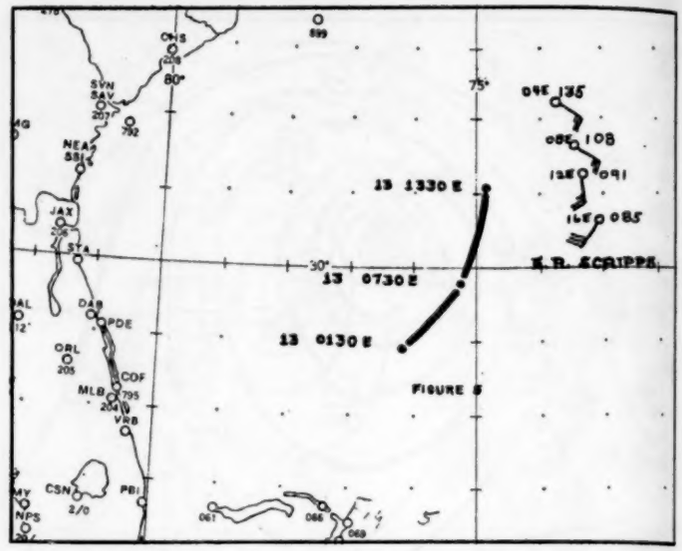

FIGURE 5.—Weather reports from the *E. R. Scripps* and the hurricane track, October 13, 1947.

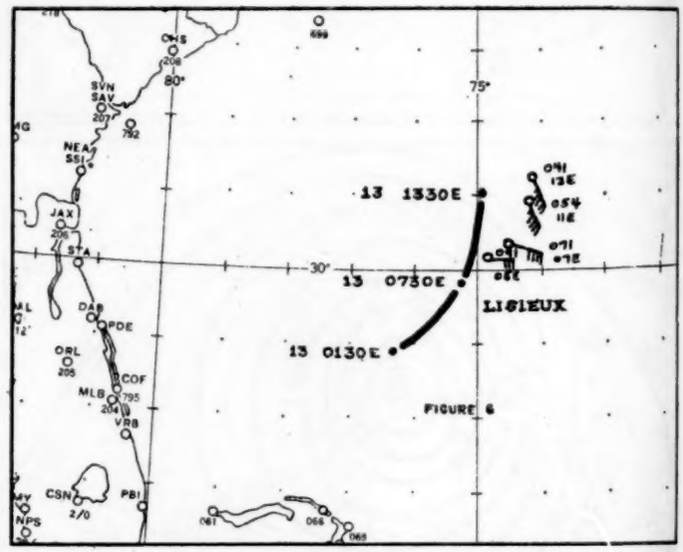

FIGURE 6.—Weather reports from the *Lisieux* and the hurricane track, October 13, 1947.

cycle when pressure was normally rising. Then, in the next 4 hours it fell only 1.7 mb., suggesting strongly, along with the shift of the wind into a more southerly direction, that the hurricane, which had been on a northeastward course toward the vessel between 0400 and 0800 EST, had shifted its course slightly to the north.

The data for the *Lisieux* in figure 6 show a shift in the wind from east-southeast to south-southeast between 0700 and 1100 EST, which is a further indication of a change in the direction of the movement of the hurricane.

In the analyses shown in figure 3, particularly those for 1830 and 2100 GMT of the 13th, and 0030, 0630, and 1230 GMT of the 14th, considerable weight was given to a flight report of the United States Navy, Atlantic Fleet on October 13, 1947, after the seeding operation. Pilot Lt. Cdr. N. H. Rudd and Aerologist Lt. E. H. Ryner made the following observations from a position (verified by Loran) at 32.1° N. and 75.1° W:

At 2000Z the eye was attained. Precipitation and turbulence ceased instantaneously and visibility increased to 5 miles. Radar showed the eye to be elliptical with a major axis orientated north northwest–south southeast and 16 miles long. The minor axis was 12 miles in length. Clouds were scattered fracto-stratus at 400

TABLE 2.—*Corrections applied to the ships' barometers*

Name of ship*	Correction	Name of ship*	Correction
E. R. Scripps	**−3.0	Telde	0.0
Santa Monica	**+2.6	R. E. Hopkins	−2.5
Howard A. Kelly	**−2.0	J. L. Sullivan	**+6.0
Platano	**+4.5	Metapan	+1.0
Borinquen	+2.0	Santa Sofia	−1.5
Satucket	0.0	Cape Avinoe	0.0
ESSO Annapolis	**0.0	Rattler	−2.0
Texas	**+.5	New Haven	−1.0
Gulf Trade	0.0	Front Royal	−1.0
Gulf Wing	+1.5	Liberator	0.0
Bjarne A. Lia	**−1.0	Horseshoe Splice	0.0
Cape Breton	**−1.2	Tullahoma	0.0
Panama	**0.0	Seven Pines	−1.0
Loop Knot	−1.5	J. Armstrong	0.0
Olympic Pioneer	**0.0	W. Ellery	0.0
ESSO Bolivas	**−2.0	African Moon	0.0
Coastal Ranger	0.0	Coastal Liberator	0.0
Santa Margarita	**0.0	Santa Cecelia	−3.0
Lisieux	**−4.3	Mormac Sun	**0.0
Cape Isabel	−.8	Archbold	**0.0
Oscar Barret	**−5.0	Rich Mountain	**+1.0
Concord	0.0	ESSO New Orleans	**0.0
Atlantic Refiner	+3.0	ESSO Springfield	**0.0
Tascalusa	**+3.0		

*Some of these ship reports do not appear on the sea level maps because of space limitations.

**Corrections to ships' barometers used to analyze the 1700 GMT map, October 13, 1947.

to 600 feet and a solid deck of thick alto-stratus estimated at 12,000 feet. The sea was confused in the outer edges of the eye and calmed to almost a glassy condition in the very center of the eye. Lowest pressure was found to be 982 millibars at a point 6 miles before reaching the eye. This pressure was obtained by reducing pressure at flight level of 500 feet to sea level, using the standard lapse rate.

The analyses were made under the assumption that the position and time given by the pilot are both correct. The subsequent small loop is based largely upon the east wind reported by the *Coastal Ranger* at 0630 GMT of October 14. Loops of this kind may not be unusual during hurricane turns. Detailed analyses of hurricane Ione of 1955 [3] and of the Cedar Keys hurricane of September 1950 [4] provide documentation of their occurrence. The data available in the present instance to demonstrate the phenomenon cannot be considered adequate evidence when compared with radar coverage. The loop is presented as one solution to the data available for analysis in this case.

In the report by Langmuir [2], reference is made to an extensive squall line which was seen by radar extending southeastward from the storm center at the time of the seeding operation. A reconnaissance aircraft, which passed south of the storm center on the forenoon of the 13th, reported that he passed through a "cold front". No attempt has been made during the present analysis of this storm to show these and other squall lines and lines of convergence which may have been present.

5. REMARKS CONCERNING THE SYNOPTIC SITUATION ASSOCIATED WITH THE TURN

An examination of tropical cyclone tracks [1], [5] indicated that another tropical storm (fig. 4), though not of full hurricane intensity, made a similar turn on a track shown as having occurred on October 6, 1947. This storm moved northward over the Bahama Islands, then curved westward and moved inland in the vicinity of Jacksonville, Fla. This raises the interesting question as to whether a persistence in the broadscale weather regime could have resulted in such a similar recurrence within a week in approximately the same area. A phenomenon similar to this in connection with hurricanes Connie and Diane of 1955 was noted by Namias and Dunn [6].

Namias [7] had shown previously that abnormal circulations established over the southern portions of the North Atlantic Ocean show a marked month-to-month persistence. That a persistently abnormal pattern in the United States North Atlantic area was operating during the month of October 1947 has been shown by Ballenzweig [8]. Ballenzweig also showed that the pattern which then existed favored the movement of existing hurricanes into the southeastern United States.

The 500-mb. constant pressure chart for 0400 GMT of October 13, 1947, is shown in figure 7a, and the 24-hour, 500-mb. height change field is shown in figure 8a. These

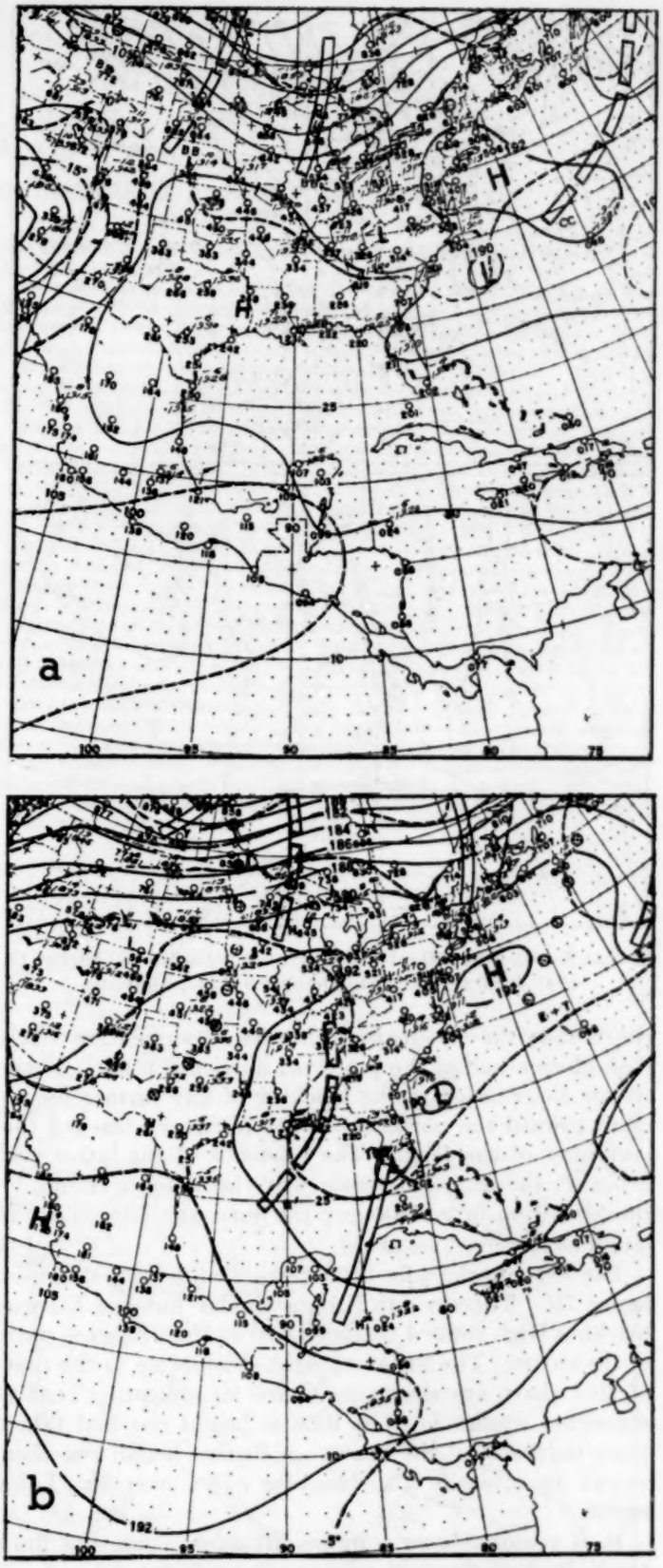

FIGURE 7.—Portions of 500-mb. charts from *Northern Hemisphere Historical Weather Maps* for (a) October 13, 1947, 0400 GMT, and (b) October 6, 1947, 0400 GMT.

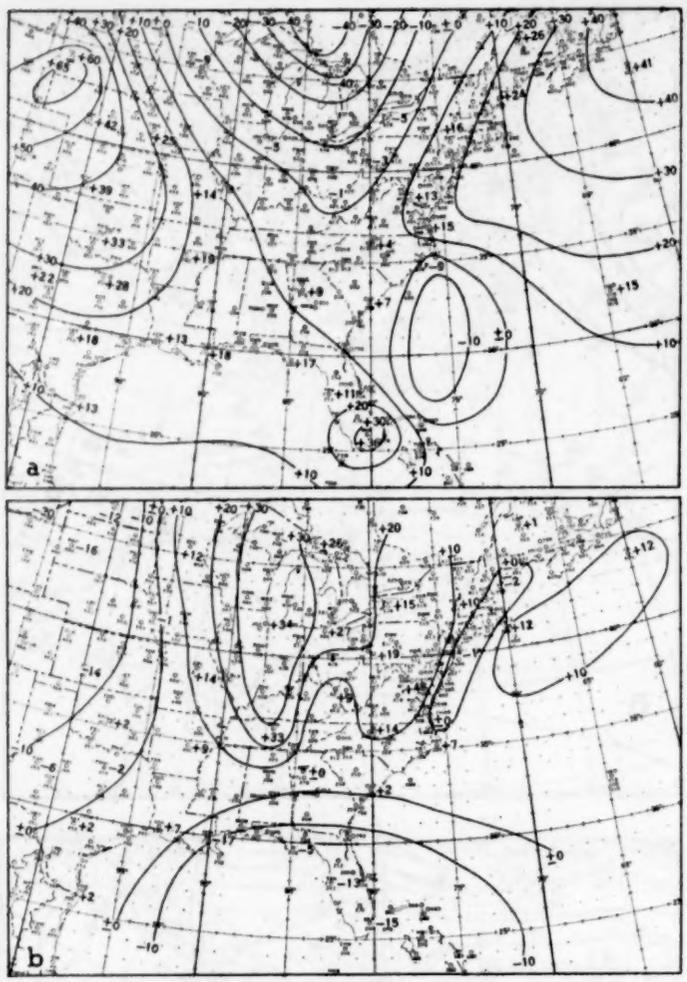

FIGURE 8.—24-hour 500-mb. height change fields for (a) October 13, 1947, 0400 GMT, and (b) October 6, 1947, 0400 GMT.

charts show the changes in the large-scale circulation which took place ahead of the projected hurricane track. These effects contributed to the blocking of any further movement toward the northeast as the hurricane reached the periphery of the High. The existence of the latter was probably the principal reason why the 500-mb. trough in the Mid-West failed to sweep the hurricane into its circulation as it moved eastward.

The 500-mb. chart for 0400 GMT of October 6 is shown in figure 7b. Therein one finds a similar but less intense blocking High toward the northeast in the projected path of the storm. The 24-hour height changes up to the time of this chart are shown as figure 8b indicating that a somewhat similar but less intense height rise had taken place northeast of the storm. A further height rise then served to intensify the blocking effect over the Lake region.

It is reasonable to suppose, therefore, that the final tracks of both storms were the normal outcome of accompanying anomalies in the general circulation and their reflection in the circulation patterns making up the environmental steering pattern over eastern North America and the adjacent portion of the North Atlantic Ocean.

ACKNOWLEDGMENTS

The authors are indebted to several individuals and agencies who assisted in the collection of reports for us in the analysis of this Atlantic hurricane. We wish first of all to express our appreciation to the officials of the French Line, with headquarters in Paris, France, for their untiring efforts in locating weather data as logged by the cargo-passenger steamer, SS *Lisieux*, during a voyage from the United States to France. The French Line officials were most helpful in securing this information for us from the present owners of the ship.

Officials of the New York City Weather Bureau office devoted many extra hours to the process of visiting various shipping lines in New York Harbor to obtain data which might furnish clues to the storm movement. We wish especially to thank Mr. C. J. McGregor and Mr. L. E. Truitt.

Also, we wish to thank Mr. William Haggard of the Office of Climatology and the officials of the National Weather Records Center, Asheville, N. C., for further assistance in supplying data.

Dr. C. L. Jordan and other officials of the National Hurricane Research Project were especially helpful in reviewing the manuscript. It was Dr. Jordan who directed our attention to interesting aspects of the storm track which revealed themselves after the data from the SS *E. R. Scripps* and SS *Lisieux* were plotted, as shown in figures 5 and 6.

REFERENCES

1. I. R. Tannehill, *Hurricanes*, Ninth Edition, Princeton University Press, 1956, 308 pp.
2. I. Langmuir, "The Growth of Particles in Smoke and Clouds and the Production of Snow from Supercooled Clouds", *Proceedings of the American Philosophical Society*, vol. 92, No. 3, 1948, pp. 167–185.
3. H. M. Jordan and D. J. Stowell, "Some Small-Scale Features of the Track of Hurricane Ione", *Monthly Weather Review*, vol. 83, No. 9, Sept. 1955, pp. 210–215.
4. R. C. Gentry, "Forecasting the Formation and Movement of the Cedar Keys Hurricane, September 1–7, 1950", *Monthly Weather Review*, vol. 79, No. 6, June 1951, pp. 107–115.
5. U. S. Weather Bureau, Office of Climatology, Unpublished Manuscript, July 1957.
6. J. Namias and C. R. Dunn, "The Weather and Circulation of August 1955—Including the Climatological Background for Hurricanes Connie and Diane," *Monthly Weather Review*, vol. 83, No. 8, Aug. 1955, pp. 163–170.
7. J. Namias, "Further Aspects of Month-to-Month Persistence in the Mid-Troposphere," *Bulletin of the American Meteorological Society*, vol. 35, No. 3, March 1954, pp. 112–117.
8. E. M. Ballenzweig, "Seasonal Variations in the Frequency of North Atlantic Tropical Cyclones Related to the General Circulation", paper presented at 150th National Meeting of the American Meteorological Society, at New York, N. Y., January 29, 1957. *National Hurricane Research Project Report* No. 9, July 1957.

WEATHER NOTES

ANALYSIS OF THE SQUALLY WAVE IN THE ATLANTIC, JULY 18–19, 1957

A large area of squalls associated with an easterly wave developed in the Atlantic Ocean early on July 17, 1957. The easterly wave had been analyzed and charted several days earlier moving westward at about 20 m. p. h. At 1200 GMT on July 17 the zone of squally weather was localized about 700 miles east of Trinidad, British West Indies, near latitude 10°-12° N., longitude 46°–48° W.

For several days previous to July 17 the Intertropical Convergence Zone had shifted northward from its normal position near the Guianas coastal area to a position about latitude 8.5° N., where it was intersected by the easterly wave mentioned above. Vessel reports in the vicinity during the 16th and 17th of July indicated evidence of a slight circulation. Vessels to the south of the area were reporting southeast to southwest winds 12 to 20 kt., while other ships to the north and west reported northeast winds 20 to 25 kt. Almost all vessels reported rain and heavy showers during this period.

It was decided that the situation warranted further investigation and in view of the proximity of the system to the Windward Islands, low-level reconnaissance was requested. The disturbed area was beyond the range of U. S. Navy aircraft in Puerto Rico, but the Miami Hurricane Center was successful in diverting the Gull-Papa flight to search the area that afternoon. The Gull-Papa search flight, which was conducted at the 700-mb. level, reported unusually strong winds of 45 to 60 kt. from the southeast at flight level in the vicinity of latitude 11°–15° N., longitude 49°–51° W. At the same time, surface winds were of the order of 20 kt. from the northeast indicating the presence of the low level perturbation to the east. A dropsonde released at 1900 GMT near 9.8° N., 50.4° W. indicated a surface pressure of 1006 mb., which is lower than normal for that area. The information reported by the reconnaissance aircraft, although not conclusive, revealed the presence of a suspicious situation and arrangements for low-level reconnaissance the following morning, July 18, were completed. In addition, a request for special ship observations at 3-hourly intervals, beginning at 1200 GMT July 18, in the area 10°–20° N. and 45°–60° W. was sent out.

The normal concern for the safety of interests in the Windward Islands was increased by the presence of a cruiser section of the U. S. Atlantic Fleet on a visit at Trinidad. The narrow confines of the Gulf of Paria are too small for maneuvering safely in case of hurricane development.

The analysis at the 700-mb. level at 1200 GMT, July 17, indicated a trough in the mid-Atlantic near 42° W., associated with a cold Low in the central Atlantic farther to the north, and a weaker, almost stationary, trough oriented north-south near the Lesser Antilles, but some distance to the west of the low-level perturbation. The subtropical high pressure cell was located far to the east near the Cape Verde Islands. This general situation persisted at the 700-mb. level through the period until 0000 GMT, July 19. At the 500-mb. level the trough in the central Atlantic associated with the cold Low to the north was clearly indicated, but farther west the situation was somewhat different. An anticyclonic cell was centered over the Lesser Antilles and extended about 600 miles east and west from this central position. The flow at the 200-mb. level, which gives perhaps the best clue for the failure of the perturbation to intensify, is illustrated in figures 1 and 2. On July 19, 1200 GMT (fig. 1) the analysis indicated a cyclonic cell over eastern Cuba, with troughs extending to the west, south, and southeast across the Caribbean Sea. This cyclonic situation over the Greater Antilles had persisted for some time. Air flow over the Windward Islands during this period showed an interesting sequence of events. Since July 17 the presence of a northerly flow at Trinidad indicated the presence of a trough or cyclonic cell in the area to the east. The contour analysis over the region also pointed to a low pressure area in that zone; but, as is usually the case, the exact nature and position of the center was unknown. The situation persisted during July 18, but on July 19, 1200 GMT, a change in the winds at Trinidad and also at St. Lucia indicated that the cyclonic center was approaching and would pass Trinidad to the south. At this time a closed Low was located just southeast of the station. Continued veering of the winds at Trinidad on July 20, 0000 GMT (fig. 2), confirmed the westward motion of the low center. This series of events gave the first exact picture of the flow in the area. It was then possible to trace the motion of the cyclone backward and make some inferences in regard to the flow prevalent over the surface perturbation during July 18.

In the meantime the surface chart at 1200 GMT on July 18, illustrated in figure 3,

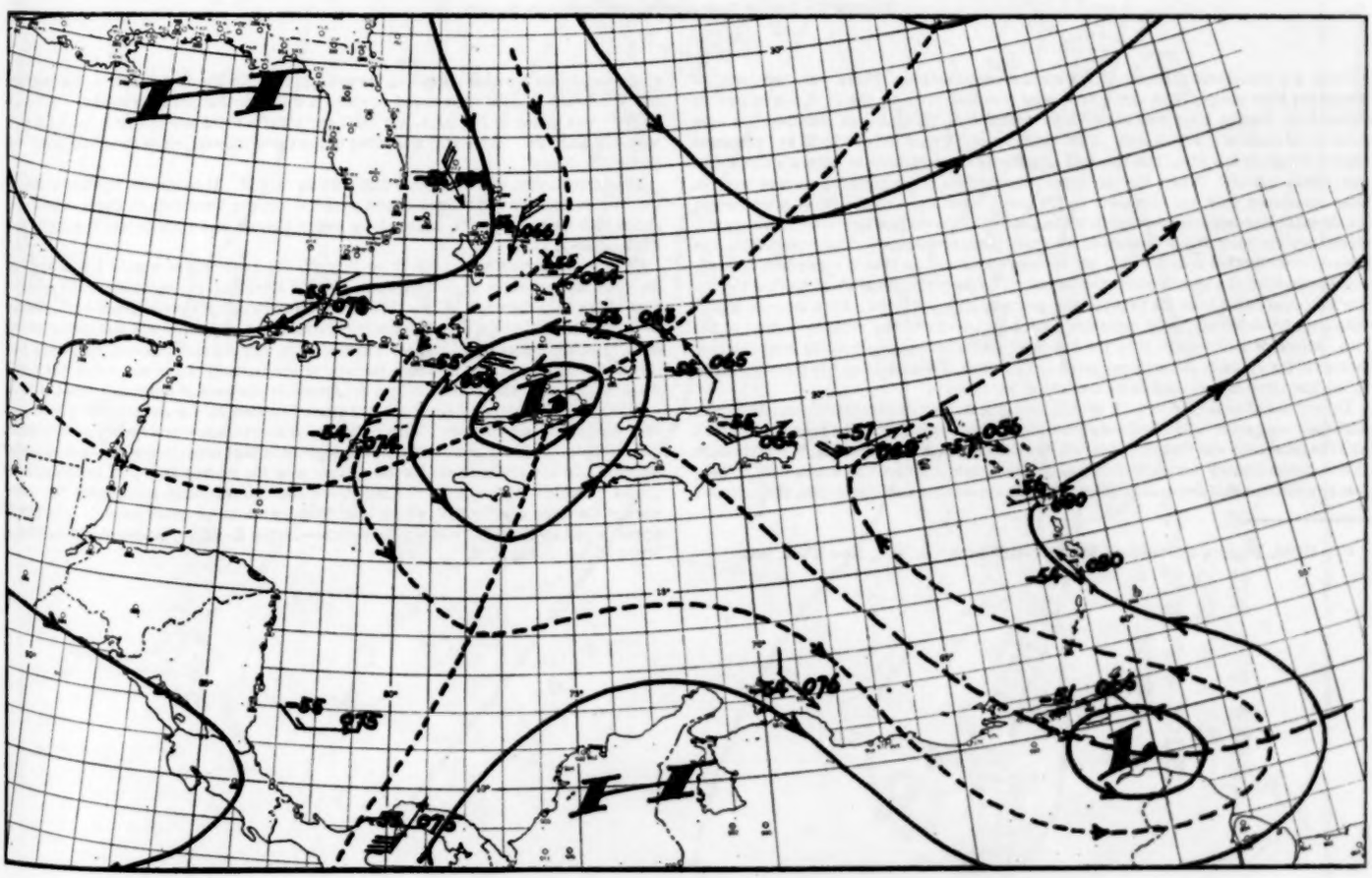

FIGURE 1.—200-mb. flow pattern, 1200 GMT July 19, 1957.

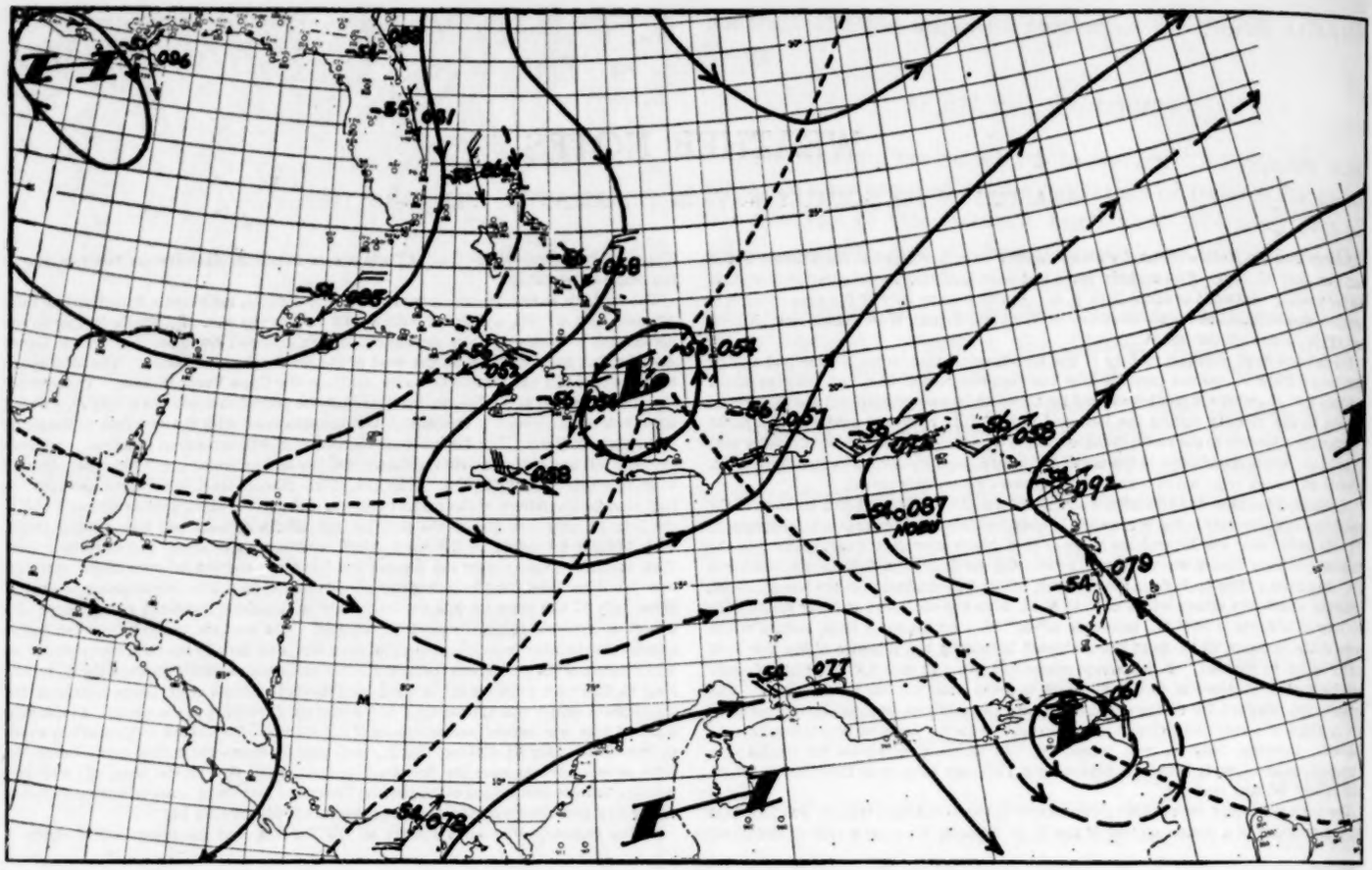

FIGURE 2.—200-mb. flow pattern, 0000 GMT July 20, 1957.

showed the continued presence of the surface perturbation. There was, however, no deepening from the previous day. Low-level reconnaissance by the U. S. Navy aircraft flying from Puerto Rico was successfully completed. The aircraft searched the area from an altitude of 500–1,000 feet. The winds reported were only of 20–25 kt.; pressures reported were rather high, but this was apparently due to failure to calibrate the altimeter before takeoff. When the correction was applied the reported pressures were in close agreement with vessel reports in the area. Significant radar echoes organized in bands extending east-west just north of the position of the surface Low were also reported. Vessel reports from the area showed also considerable weather. The report from the vessel *Nerita* located near 9.0° N., 55° W. was significant in that it confirmed the continued presence of a closed wind circulation. The perturbation showed motion toward the west-southwest from its position the previous day. In view of the changes in circulation at the 200-mb. level described above and study of the relative motion of the two centers, it is apparent that the low-level perturbation was moving into the rear section of the cyclonic cell at upper levels. This type of combination has been described in the literature as unfavorable for deepening (cf. Riehl [1]).

During the afternoon of July 18, at 1900 GMT (3 p. m. AST), a formal bulletin was issued. Although the perturbation had not shown significant deepening in the previous 24 hours and the consensus was that the situation was not favorable for deepening, it was thought that a precautionary notice to interests in the Lesser Antilles was warranted. There was also considerable demand for information in the eastern Caribbean area, since rumors about suspicious weather situations spread rapidly. In the first bulletin the people in the Windward Islands were urged to stand a watch for further information. A second bulletin was issued at 7:00 p. m. AST (2300 GMT) and a third one at 6:00 a. m. (1000 GMT) next day, July 19. The watch was lifted in the third bulletin, since the situation offered no further danger.

The perturbation weakened after 2100 GMT on July 18. It continued its motion toward the west-southwest and moved inland over the eastern Venezuela-Guianas coastal area about 0900 GMT on July 19 attended by heavy shower and thunderstorm activity and winds of 20–25 kt.

During the period from July 17 to July 19, the system was watched and analyzed carefully for any signs of development. While attention was focused on the southern part of the easterly wave, where it joined the Intertropical Convergence Zone, possible development farther north in the upper portion of the wave axis was also under surveillance. Such types of situations are watched with considerable concern, since any hurricane developing in the northern portion of the easterly wave can affect the Lesser Antilles in a very short time, as was evidenced in the case of hurricane Janet of 1955.

Climatological statistics show that 13 storms formed in the eastern Atlantic area in July during the last 70 years. This indicates, of course, a low probability of formations, but on the other hand, shows that developments in that area during July are altogether possible. In the present case the conditions near the surface appeared to be similar to others in which storms have developed. Water temperatures throughout the period were of the order of 81°–83° F. which is sufficiently warm for development. The flow at upper levels apparently, was not favorable.—*Ralph L. Higgs, Meteorologist in Charge, WBAS, San Juan, P. R.*

[1] H. Riehl, *Tropical Meteorology*, McGraw-Hill Book Co., Inc., New York, 1954.

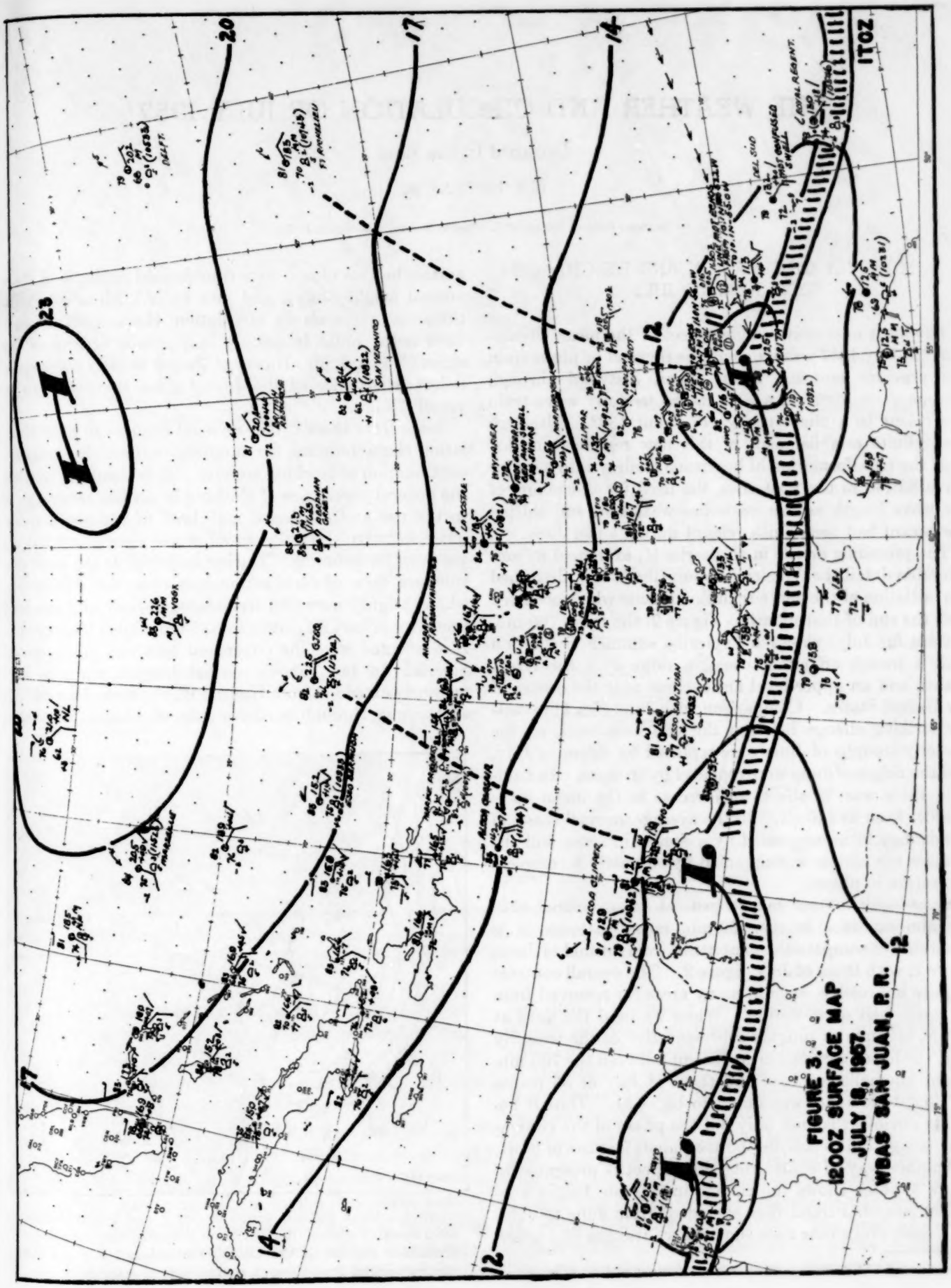

FIGURE 3.—Surface chart 1200 GMT July 18, 1957.

437310—57——3

THE WEATHER AND CIRCULATION OF JULY 1957[1]

Drought in the East

H. F. HAWKINS, JR.

Extended Forecast Section, U. S. Weather Bureau, Washington, D. C.

1. MONTHLY CIRCULATION AND ITS CHANGE FROM JUNE TO JULY

The most impressive single aspect of the mean circulation for July 1957 was its complete reversal in phase from the previous month. From Japan eastward through Europe there occurred a shift in the westerly wave train equivalent to a phase change of about 180°. Although the definite establishment of this new regime coincided with the transformation of hurricane Audrey into a major perturbation in the westerlies, the need for shortening of the wave length as the westerlies weakened and shifted northward had been quite evident during latter June.

The preceding article in this series [1] examined in considerable detail the June circulation (fig. 1) and described the initiation of the new circulation regime which occurred near the end of that month. Figure 2, the mean 700-mb. pattern for July, shows a typically summer circulation with a trough off either coast, a ridge over the Great Plains, and an upper level anticyclone near the center of the United States. Comparison with June (fig. 1) reveals the striking change between the two months; i. e., the westerly troughs of June were replaced by ridges in July, and the ridges of June were replaced by troughs. In addition, there was, in effect, an increase in the mean wave number from five to six. In the average, normal seasonal trends may be accompanied by a similar increase, but the changes are seldom accompanied by so nearly a complete opposition in phase.

Since local weather can, in general, be associated with the abnormalities in the 700-mb. mean patterns, it is profitable to compare the departures from normal in June, figure 1, with those of July, figure 2. The overall contrast is quite impressive, even in many areas far removed from the main belt of westerlies. When we used the data at 50° N. latitude as roughly representative of the westerly belt, the linear correlation coefficient between the 700-mb. height anomalies of June and those of July at 36 points 10° longitude apart was found to be −.61. Thus it becomes obvious that not only did the phase of the circulation change, but so also did the anomalous features or flows.

Another way of illustrating this aspect is presented in figure 3 which shows the change in 700-mb. height *anomalies* (seasonal trend thus excluded) from June to July. In almost every case rises show where troughs and below normal heights (June) were transformed to ridges of above normal height (July), and vice versa. Monthly oscillations—or reversals in circulation characteristics—have been noted quite frequently in previous articles of this series [2, 3, 4, 5, 6]. However, July is usually more apt to reflect persistence of the June regime than a sharp reversal [7].

Aside from these rather unusual changes in local circulation characteristics, the monthly pattern also reflects a continuation of blocking activity. It is tempting to relate the general prevalence of blocking in the last several years to the rise and continued high level of sunspot activity, but conclusive statistical proof of the association has not yet been forthcoming. During July (fig. 2) the most conspicuous area of such action was over the Bering Sea, where heights were 340 feet above normal and sea level pressures (Chart XI, inset) some 7 mb. higher than normal. Also affected were the Greenland area and north central Siberia. In fact, above normal heights and sea level pressures extended from Hudson Bay eastward (at 65° N.) all the way through northern Asia to Alaska—an almost

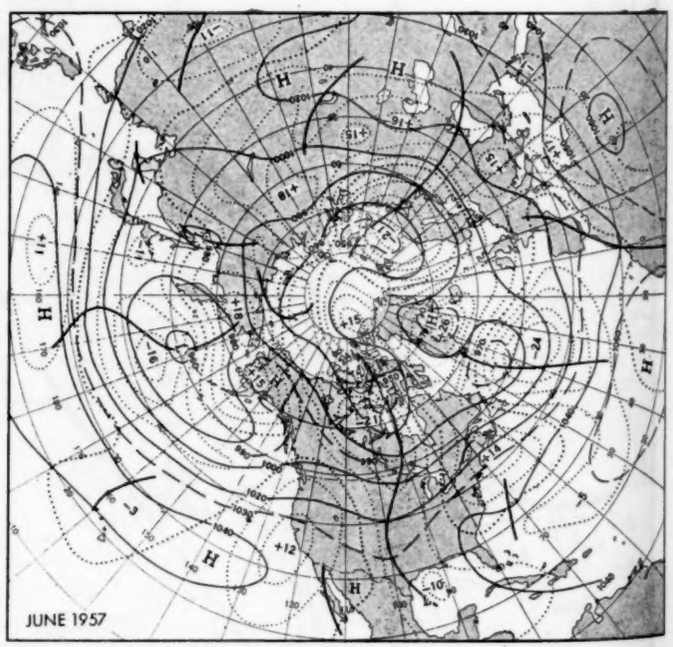

FIGURE 1.—Mean 700-mb. contours (solid) and height departures from monthly normal (dotted) (both in tens of feet) for June 1957. Dominant feature in the United States was the mean trough (heavy vertical line) through central part of country.

[1] See Charts I–XVII following p. 268 for analyzed climatological data for the month.

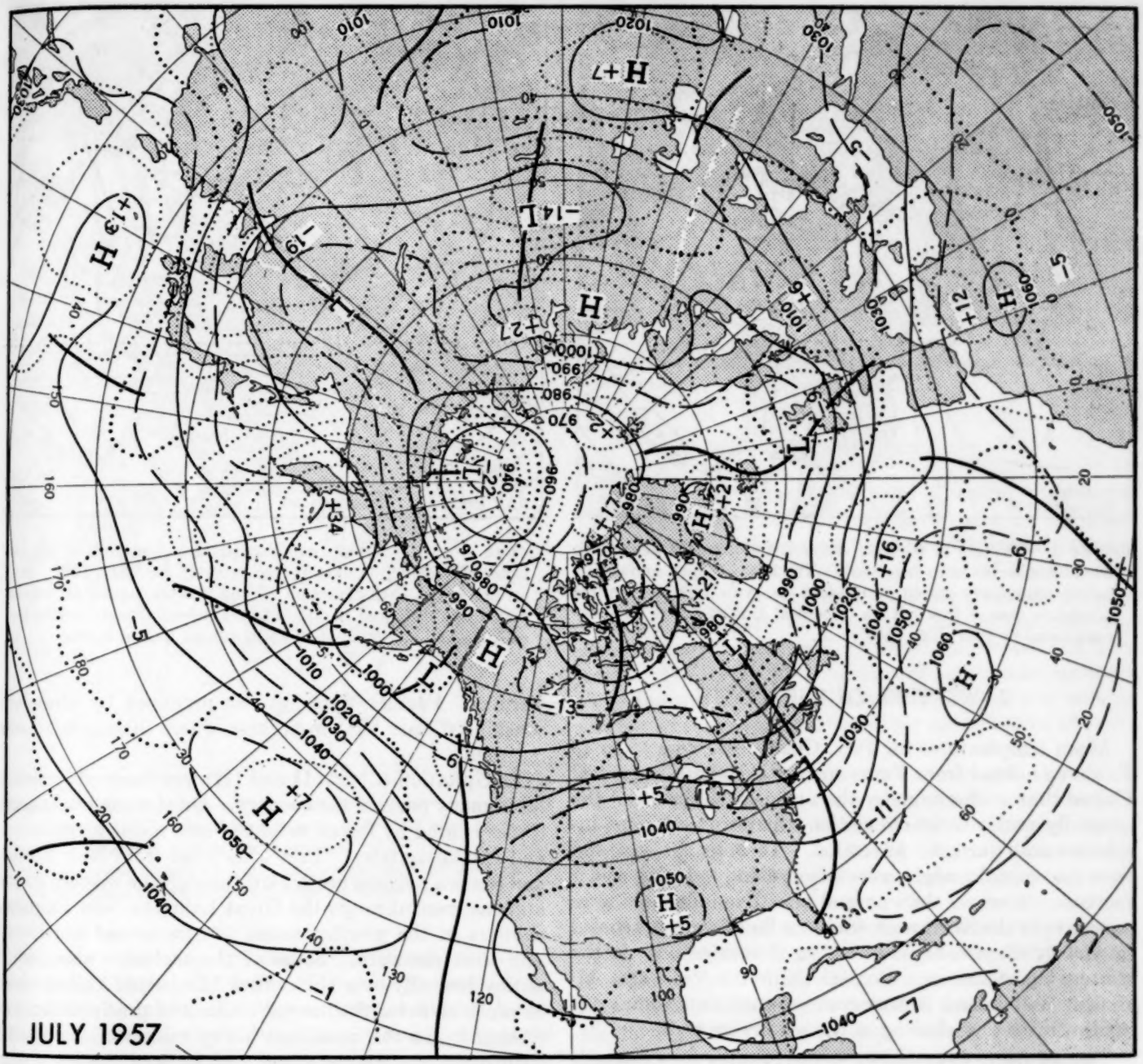

FIGURE 2.—Mean 700-mb. contours (solid) and height departures from monthly normal (dotted) (both in tens of feet) for July 1957, with troughs indicated by heavy vertical lines. Note complete change in phase from June (fig. 1).

complete circumpolar ring. The only other conspicuous high latitude feature was the strong, persistent, closed polar Low around 75° N. latitude and 160° E. longitude. The Icelandic Low (or Lows), although still present, was considerably weakened by the blocking.

An aspect of no little importance was the stability of the major westerly wave train. This was most noteworthy in the United States where successive 5-day mean maps reveal only minor shifts in the long wave pattern throughout the month. Variations in depth of the coastal troughs, minor fluctuations in their position, and changes in the upper level anticyclone over central United States constituted the major 5-day circulation features. More sizable alterations were noted in Canada where the direct effects of blocking surges were stronger and more apparent.

The 200-mb. circulation features, figure 4, were essentially similar to the 700-mb. pattern except for the disappearance of the Greenland anticyclone at higher levels. As usual, the summer maritime troughs were better defined aloft, but the westerly waves retained the same relation and identity. Both Arctic and temperate mean jets were present with a clear westerly maximum just about girdling the globe between 40° and 50° N. The mean jet over the United States also demonstrated the phase change from June [1] noted in other circulation features.

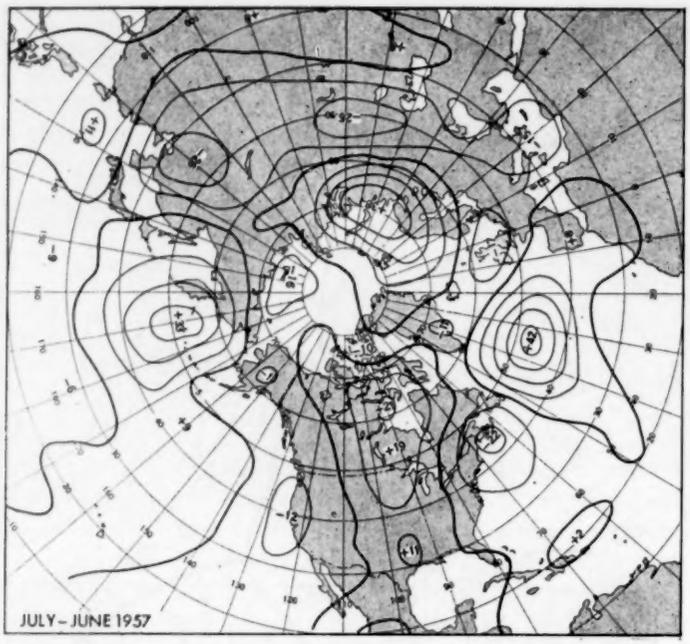

FIGURE 3.—Changes in monthly mean 700-mb. height departures from normal—June to July 1957. The lines of equal anomalous height change are drawn at 100-foot intervals with the centers labeled in tens of feet. Rises in central United States were accompanied by falls along each coast.

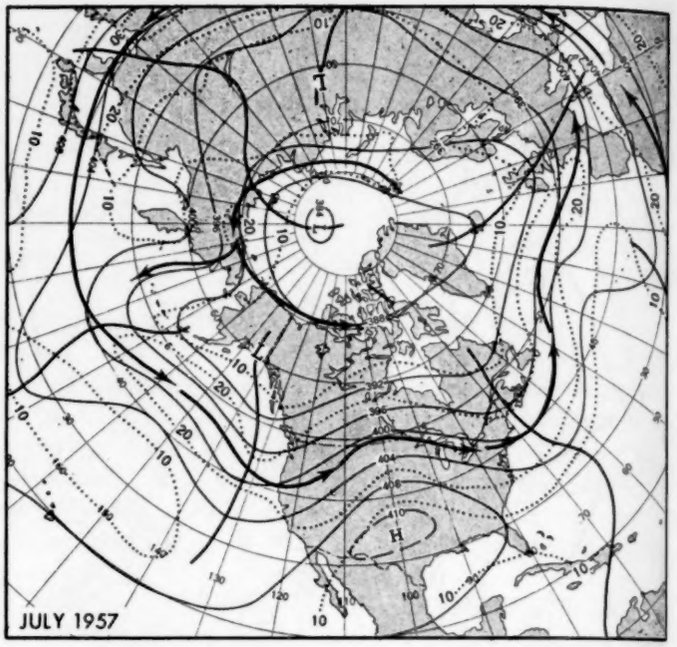

FIGURE 4.—Mean 200-mb. contours (solid, in hundreds of feet) and isotachs (dotted, in meters per second) for July 1957. Solid arrows indicate the position of the 200-mb. mean jet stream, which was displaced northward and curved sharply anticyclonically around strong mean High in central United States.

2. WEATHER OF THE MONTH

Mean temperatures for July, Chart I–B, were 1° to 4° F. above normal from Texas to North Dakota in central United States where, under the upper-level High and the generally anticyclonic circulation, there was sufficient insolation and warm air advection. To both the east and west the coastal troughs were effective in producing cooler regimes. Stronger than normal maritime influences were operative in the Northwest, while the Southwest was cooled in part by the cloudiness attending shower activity in the western moist tongue. Coastal California was warm, although well inland it was cool—a condition commonly attributed to a weakening of the sea-breeze regime.

Temperatures over eastern United States were interesting in that near to below normal temperatures did occur as usual to the rear of the coastal trough, but a coastal strip from the Outer Banks of North Carolina to New Hampshire remained above normal. Considering the depth of the offshore trough, this warmth appears rather difficult to rationalize, especially since the thicknesses from 1000 to 700 mb. (not shown) were definitely below (mean virtual temperatures cooler than) normal over the entire area. However, temperatures in interior regions of the East averaged only 1° to 2° F. below normal at the surface, and even these departures seemed intimately associated with precipitation (Chart II) and the cloudiness associated with it (Chart VI). Thus, for the most part, air only slightly cooler than normal at lower levels was advected over the coastal strip and, in the descent from the Appalachians, was heated enough to account for the coastal warmth. Further warming was produced by abundant sunshine (Chart VII) in an area where little rainfall was recorded.

Precipitation (Charts II and III) was reasonably plentiful in many parts of the country. On the northwest coast it was caused by forced ascent of cool moist maritime air and frontal activity. In a wide band from New Mexico and eastern Arizona northward through the western Plains and eastward through the Great Lakes to New England, showers in the western moist tongue spread northward and then eastward. Some of the moisture also eddied anticyclonically over the central Mississippi Valley where as much as twice the normal amount of precipitation was recorded. In the Southeast heavy rains were associated with quasi-stationary frontal activity and the instability induced by the attending cyclonic circulation. Less than ½ inch of rain was recorded over a wide belt of the Far West lying between the rains on the southern edge of the westerlies in the extreme Northwest and the continental summer showers in the Southwest and central Rockies. It was also a period of drying-out in Texas and Oklahoma, where little flow of Gulf moisture and no perturbations of consequence were noted. The only other dry area of significance occurred in the East behind the mean trough off the East Coast.

In the preceding discussion of circulation changes the obvious reversal in flow characteristics from June to July was highlighted to some extent. It would seem appropriate therefore also to indicate the accompanying changes in temperature and precipitation. The monthly changes in temperature by class are shown in figure 5A. (For

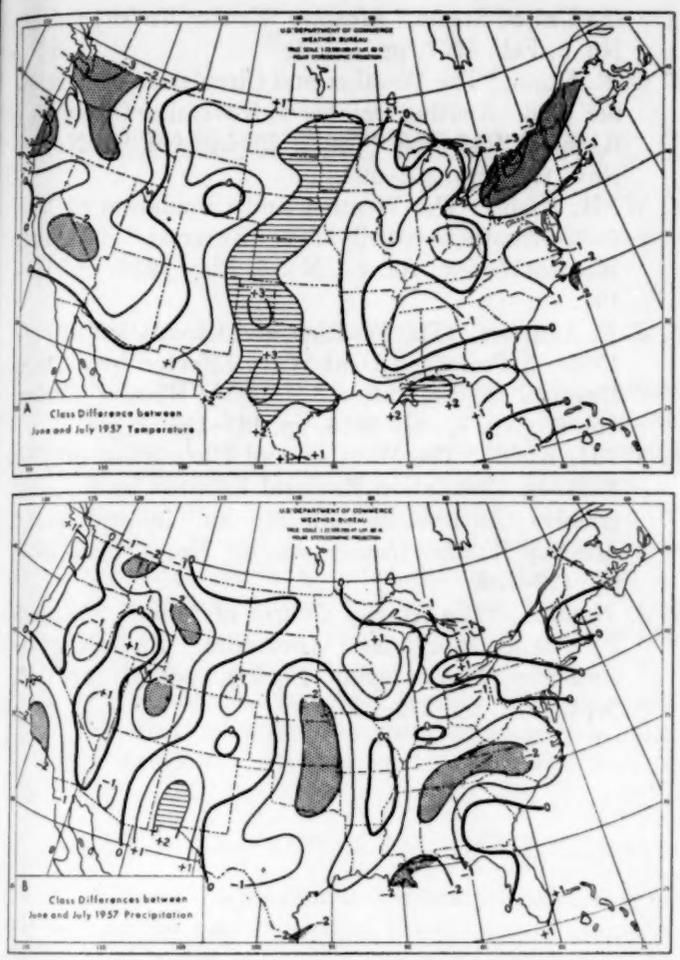
A
Class Difference between June and July 1957 Temperature
B
Class Differences between June and July 1957 Precipitation

FIGURE 5.—Number of classes the anomaly of temperature (A) and precipitation (B) changed from June to July 1957, with increased values considered positive and decreased values negative. Areas with increases of two or more classes are cross-hatched; areas with decreases of two or more classes are dotted.

definition of classes, see reference [7].) Temperatures fell one to three classes in the Far West (except coastal California) due to increased trough activity in the north and cloudiness in the south. Temperatures rose two to three classes from Texas to Minnesota as heights rose and the ridge of July replaced the trough of June. Along the east coast cooling was generally in order as the trough deepened offshore.

Precipitation changes, also by class, are indicated in figure 5B. Drying occurred under the upper-level High in central United States and also over most of the East to the rear of the trough, except the Southeast which remained wet, and the eastern drought area which remained dry. The continental showers of summer produced wetter conditions from New Mexico north-northeastward as well as in eastern Nevada and Idaho. Most of California received no rain at all as the westerlies shifted northward and typically arid summer weather was established. However, in northern California westerly trough activity caused an increase in coastal precipitation

TABLE 1.—*Total precipitation (inches) and its departure from normal in eastern drought area.*[1]

Station	April 8 to August 18 period				
	1957		Record minimum for previous 50 years		
	Total	Dep.	Total	Dep.	Year
Boston, Mass.	7.89	−6.10	6.94	−7.05	1950
Nantucket, Mass.	8.03	−5.54	5.71	−7.86	1949
Providence, R. I.	5.65	−8.17	8.69	−5.13	1914
Bridgeport, Conn.	7.83	−8.47	8.07	−8.23	1911
New York, N. Y.	9.12	−7.30	6.91	−9.51	1939
Philadelphia, Pa.	5.81	−11.23	10.80	−6.23	1923
Harrisburg, Pa.	7.23	−8.07	9.16	−6.14	1939
Baltimore, Md.	6.67	−10.18	7.54	−9.31	1930
Washington, D. C.	6.52	−10.19	8.11	−8.60	1930
Norfolk, Va.	11.89	−7.27	10.44	−8.72	1944
Richmond, Va.	11.68	−6.97	8.62	−10.03	1911

[1] From *Weekly Weather and Crop Bulletin, National Summary*, vol. XLIV, No. 33, U. S. Weather Bureau, Washington, D. C., Aug. 19, 1957.

3. EASTERN DROUGHT

Certainly one of the major items of topical interest was the intense drought which gripped parts of the East. From North Carolina to southern New England the coastal areas received only 25 to 50 percent of normal July precipitation. The lack of rainfall could be directly associated with the offshore trough and the dry northerly and northwesterly components of flow which prevailed at most levels. The upper-level continental anticyclone appeared to be too weak to carry the moisture on the rear side up and across central United States far enough to be effective in the East.

In June, when the circulation was reversed, the central United States trough was apparently too far west for significant precipitation in the East [1]. A similar condition prevailed during April and May. The transition from one regime to the other was sharp and rapid with little opportunity for effective relief. As a result, much of the East, which had enjoyed a satisfactory ground moisture condition in early spring, was suffering a very severe drought. In duration, this could not compare to many quite recent occurrences in the central and southern Plains, but in severity the eastern drought was quite noteworthy. Numerous July minimum precipitation records were set, but of greater significance is table 1 which compares the indicated 19-week precipitation totals with record minima for the previous 50 years at 11 selected eastern drought stations. Thus one sees that at Providence, R. I.; Bridgeport, Conn.; Philadelphia, Pa.; Harrisburg, Pa.; Baltimore, Md.; and Washington, D. C., this has been the driest growing season in 50 years.

The riddle of basic causation as related to a phenomenon such as the eastern drought still lies beyond the scope of present meteorological theory. Although certain aspects of atmospheric behavior are better understood and better explained than ever before, the role of instantaneous interactions within the mean ensemble is just beginning to be appreciated and analytically investigated. As of now, one can only point out that the very stable pattern of July—

strong trough off the east coast and small upper-level anticyclone over central United States—was sufficient to maintain extreme drought along the coastal strip. The cyclonic activity associated with the trough was too far east, and the High was too weak and/or too far west to transport adequate moisture into the East. How much the preceding dryness (April–June) contributes to such a regime may be evaluated in the not far distant future. But, given such knowledge, the essential problem is still only once removed. There remains basically a problem in understanding which will never be satisfied with the old saying: "All signs fail in time of drought."

REFERENCES

1. W. H. Klein, "The Weather and Circulation of June 1957—Including an Analysis of Hurricane Audrey in Relation to the Mean Circulation," *Monthly Weather Review*, vol. 85, No. 6, June 1957, pp. 208–220.
2. C. M. Woffinden, "The Weather and Circulation of February 1957—Another February with a Pronounced Index Cycle and Temperature Reversal over the United States," *Monthly Weather Review*, vol. 85, No. 2, Feb. 1957. pp. 53–61.
3. C. R. Dunn, "The Weather and Circulation of November 1956—Another October to November Circulation Reversal," *Monthly Weather Review*, vol. 84, No. 11, Nov. 1956, pp. 391–400.
4. W. H. Klein, "The Weather and Circulation of May 1956—Another April–May Reversal," *Monthly Weather Review*, vol. 84, No. 5, May 1956, pp. 190–197.
5. J. F. Andrews, "The Weather and Circulation of July 1955—A Prolonged Heat Wave Effected by a Sharp Reversal in Circulation," *Monthly Weather Review*, vol. 83, No. 7, July 1955, pp. 147–153.
6. W. H. Klein, "The Weather and Circulation of May 1954—A Circulation Reversal Effected by a Retrogressive Anticyclone During an Index Cycle," *Monthly Weather Review*, vol. 82, No. 5, May 1954, pp. 123–130.
7. J. Namias, "The Annual Course of Month-to-Month Persistence in Climatic Anomalies," *Bulletin of the American Meteorological Society*, vol. 33, No. 7, Sept. 1952, pp. 279–285.

BREAK IN THE HEAT WAVE ON THE EAST COAST, JULY 1957

ABE ROSENBLOOM AND NORMAN C. THOMAS

National Weather Analysis Center, U. S. Weather Bureau, Washington, D. C.

1. INTRODUCTION

During the latter half of July 1957 a heat wave occurred along the central Atlantic seaboard. The area affected extended from Connecticut southward to Virginia and inland from the coast to the Appalachians. This spell of intense hot weather was of short duration, lasting only two days, July 21 and 22, over most of this area. The maximum temperatures recorded during this period in the large populous centers such as New York, Philadelphia, Baltimore, and Washington, D. C., were sufficiently high to be noteworthy. The heat wave in the affected area ended as fast as it began. The welcomed relief was effected by the opportune passage of a polar cold front previously situated to the north and west of this area.

2. SURFACE TEMPERATURE AND PRECIPITATION

Table 1 shows the maximum temperatures occurring at the peak of the heat wave and the maximum temperatures following the passage of the polar cold front. As shown in the table, these relatively high maximum temperatures occurred most generally during the 21st and 22d. The exceptions were Albany and Providence which experienced high maximum temperatures on the 20th and 21st, and Richmond and Norfolk where warm maximum temperatures prevailed until the 23d. The maximum temperatures for these cities averaged 99° F. during the heat spell, which was 14° F. higher than the average normal maximum of 85° F. for the above-mentioned cities during the month of July. With the passage of the cold front the maximum temperatures dropped markedly. The decrease in maximum temperatures for these cities averaged 20° F.

During the heat wave, temperature records were established at Baltimore, Wilmington, Newark, and Providence. The 103° F. temperature in Baltimore on July 21 was the highest temperature experienced there since July 28, 1941, when the mercury also reached 103° F. In addition, a record maximum was established for the 22d with a temperature of 102° F. In Wilmington, a new maximum temperature record was established for the 22d and the maximum temperature high for the 21st was equalled. Maximum temperature records for the 20th, 21st, and 22d were established in Newark and for the 20th in Providence. Although no new record maxima were established for the other cities listed in table 1, in some instances the temperatures recorded on the 21st and 22d were the highest for the past several years and closely approached the maximum temperatures for these dates. This was evidenced at Trenton where the consecutive 100° F. maxima on the 21st and 22d were the first such occurrence since July 1936, and at New Haven where the 100° F. maximum on the 22d was the highest since the 100° F. temperature that was recorded on August 27, 1948.

Although the passage of the cold front brought welcomed relief from the heat, the accompanying precipitation was rather disappointing in that it failed to bring any substantial relief from the drought that had plagued the Middle Atlantic States since spring. What rainfall did occur was of a spotty nature with some localities receiving little more than a trace while nearby sections received an inch or more. For example, Philadelphia, which suffered through the driest July on record, received

TABLE 1.—*Record of maximum temperatures July 20–24, 1957, normal maxima [1] for July, and precipitation totals July 22–24, 1957 for selected stations.*

Station	Date	Max. temp. (° F.)	Date	Max. temp. (° F.)	July normal max. temp. (° F.)	Precip. (in.)
Albany, N. Y. (Airport)	20	95	23	79	82.5	0.01
	21	95	24	79		
Providence, R. I.	20	97	23	81	82.6	.15
	21	91	24	74		
	22	97				
New Haven, Conn.	21	99	23	81	80.1	.05
	22	100	24	80		
Bridgeport, Conn.	21	99	23	82	81.6	.03
	22	103	24	80		
New York, N. Y. (Central Park)	21	100	23	82	84.7	.04
	22	101	24	84		
Newark, N. J.	21	99	23	83	84.9	.02
	22	101	24	83		
Trenton, N. J.	21	100	23	82	84.6	.25
	22	100	24	82		
Allentown, Pa.	21	100	23	78	85.5	.16
	22	100	24	82		
Harrisburg, Pa.	21	97	23	79	85.6	1.23
	22	97	24	78		
Philadelphia, Pa. (Airport)	21	101	23	81	86.5	.17
	22	100	24	82		
Wilmington, Del.	21	102	23	81	86.7	.43
	22	101	24	83		
Frederick, Md.	21	100	23	78	87.9	.51
	22	100	24	79		
Baltimore, Md. (City Office)	21	103	23	88	86.9	.49
	22	102	24	83		
Washington, D. C. (Airport)	21	101	23	87	87.1	.15
	22	101	24	83		
Richmond, Va. (Airport)	21	98	24	81	87.8	1.20
	22	100				
	23	95				
Norfolk, Va. (Airport)	21	98	24	80	86.0	1.53
	22	99				
	23	98				

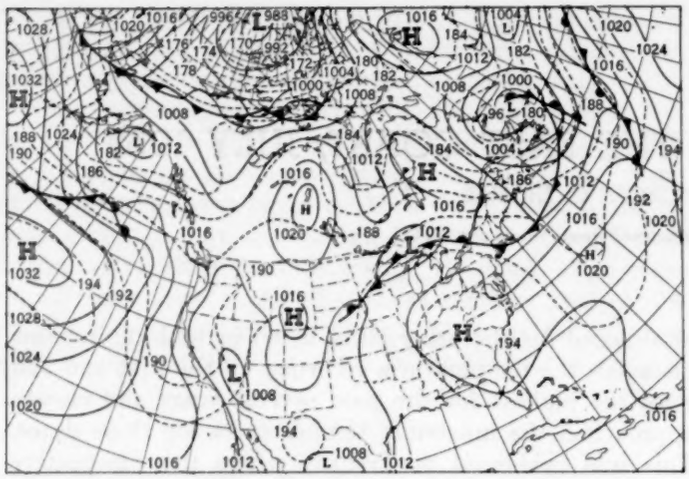

FIGURE 1.—Sea level pressure and 500-mb. chart at 1200 GMT, July 21, 1957. Sea level isobars (solid lines) are at 4-mb. intervals and 500-mb. isohypses (dashed lines labeled in hundreds of geopotential feet) are at 200-ft. intervals. Surface fronts are indicated with conventional symbols.

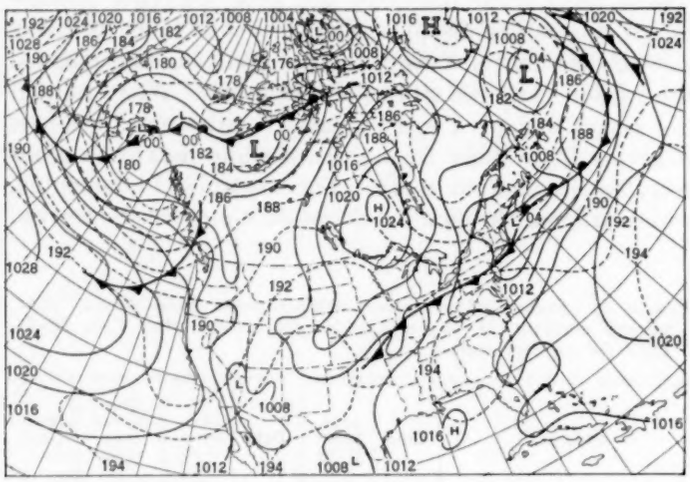

FIGURE 2.—Sea level pressure and 500-mb. chart at 0000 GMT, July 23, 1957. Sea level isobars (solid lines) are at 4-mb. intervals and 500-mb. isohypses (dashed lines labeled in hundreds of geopotential feet) are at 200-ft. intervals. Surface fronts are indicated with conventional symbols.

only 0.17 inch of rainfall while more than one inch fell at nearby Lyndell, Pa. (located 30 miles west of Philadelphia). Providence, recording its longest dry spell on record, received only 0.15 inch which approximated the average for southern New England. Some stations in northern West Virginia and southeastern Virginia (Norfolk area) recorded over two inches in a 24-hour period but only 0.15 inch fell at Washington National Airport, which hadn't experienced a drier July since 1872.

3. SYNOPTIC SITUATION—SURFACE MAPS

As indicated by the surface pattern in figure 1, the central and southern Atlantic seaboard was dominated by a flat amorphous extension of the Bermuda High. The center of this anticyclonic appendage was located

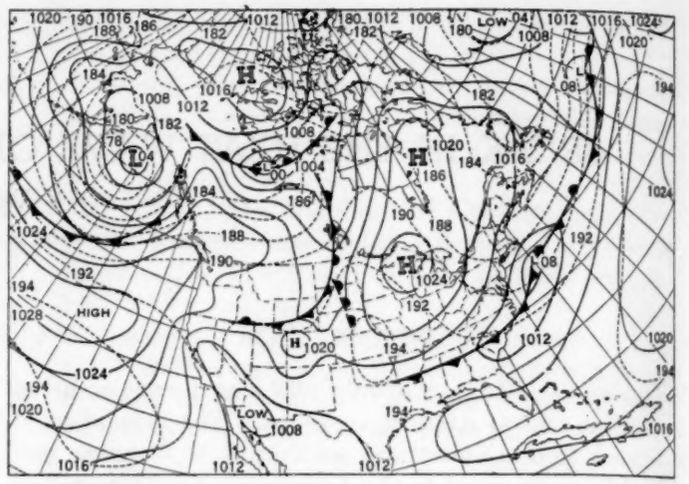

FIGURE 3.—Sea level pressure and 500-mb. chart at 1200 GMT, July 24, 1957. Sea level isobars (solid lines) are at 4-mb. intervals and 500-mb. isohypses (dashed lines labeled in hundreds of geopotential feet) are at 200-ft. intervals. Surface fronts are indicated with conventional symbols.

at 1200 GMT, July 21, 1957, slightly north of Athens, Ga.; the central pressure was 1019 mb. Historically this appendage was the remnant of a more potent High which had travelled eastward across western Canada and then southeastward into the States in the eastern Great Lakes region. A quasi-stationary cold front to the north with a flat wave in the Sault Ste. Marie area separated this feature from two colder Canadian Highs to the north and northwest.

Off the west coast of the United States, a significant feature was the well developed eastern cell of the Pacific High. This cell was surmounted to the north by a cyclonic vortex in the Gulf of Alaska. About midway between these two features stretched a maritime polar front with a wave crested in the vicinity of weather ship Papa (50°N., 145°W.)

Thirty-six hours later at 0000 GMT, July 23 (fig. 2) the quasi-stationary front of figure 1 had taken on more pronounced cold frontal characteristics and was moving down the middle Atlantic seaboard. The Bermuda High extension was melting away and the Canadian polar High which was to replace it was well poised behind the advancing front. In the Far West the center of the eastern cell of the Pacific High had diminished somewhat in intensity and had retrograded noticeably westward. Concurrently a maritime polar front was emerging from the Gulf of Alaska and approaching Tatoosh, Wash.

By 1200 GMT, July 24 (fig. 3) the cold front was well on its way down the Atlantic coast sweeping out the above normal temperatures which had previously prevailed and replacing them with noticeably lower ones. The source of the colder air was the Canadian High shown in figure 3 in the Lake Superior region.

4. SYNOPTIC SITUATION—500-MB. CHARTS

Superimposed on the surface maps in figures 1, 2, and

3 are the 500-mb. charts for the corresponding times. In total, they illustrate a characteristic upper air meteorologicial event, namely the passage of a short-wave trough over the top (to the north) of a stagnating flat ridge or High. Such short-wave troughs after passing the ridge position in more or less small amplitude and subdued forms of development, frequently pick up varying amounts of southward component in their motion and after passing several hundred miles downstream from the ridge line, quite often increase their amplitudes and intensities. Such a portrayal is in substantial agreement with Fultz's [2] suggested life cycle of the minor waves in conjunction with the major waves.

On some occasions, however, the position of redevelopment or intensification of this short-wave trough occurs at very close proximity to the ridge line, in fact, so close, that the High or ridge completely disappears in that area and is replaced by a cyclonic circulation. The emergence of this new (farther westward) large-scale trough position and the concomitant westward shift of the old ridge line represents the phenomenon known as "long-wave retrogression."

A comparison of figures 1, 2, and 3 shows that retrogression has indeed taken place. In figures 1 and 2, two salient features in the East in mid-latitude are the High centered over northern Georgia and the major trough line just east of Bermuda's longitude. In figure 3, the major trough line now lies along the east coast while its accompanying major ridge line to the west is located on the west side of the Mississippi River.

5. MEAN FLOW CHARTS

It has long been noted by many meteorologists that the determination of a long-wave position (trough or ridge) through the inspection of a single synoptic chart was often highly unsatisfactory, if not impossible. In an AROWA publication [3], it is claimed that "in all but the simplest situations, two meteorologists working independently would produce substantially different long-wave analyses." The authors of this publication also conclude that a method which they had previously proposed, using the tracks of 500-mb. height change centers for determining the position of long waves, would also not be completely satisfactory [3], [4]. The use of "time mean" charts for locating the long-wave positions on a current synoptic chart will also have its shortcomings. This has been pointed out by Martin [5] and others [3].

At NAWAC a space–averaged mean chart of the 500-mb. flow has been used for several years as a method for objectively determining the long-wave positions on any current synoptic chart. The grid length used is 12 degrees of latitude (measured at latitude 60° on a polar stereographic projection). The method of preparation, including the grid length used, follows the procedure recommended by Fjørtoft [6] and is similar to the method employed by the Air Weather Service [7].

Figures 4 and 5 are space-averaged mean charts for the

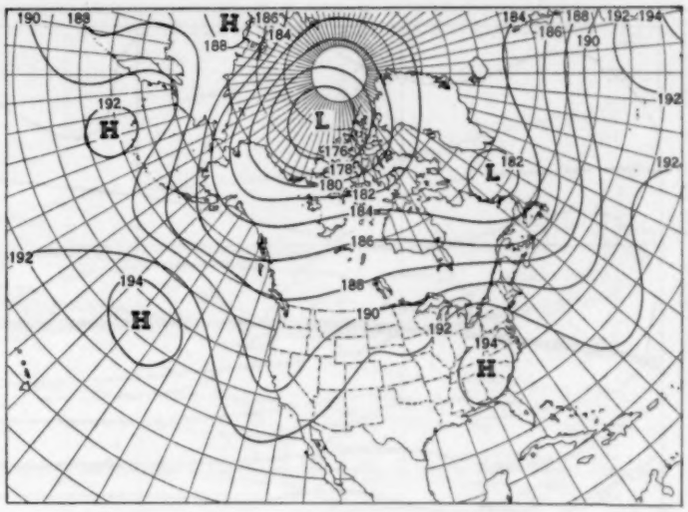

FIGURE 4.—Space-mean chart for 500 mb. at 1200 GMT, July 21, 1957.

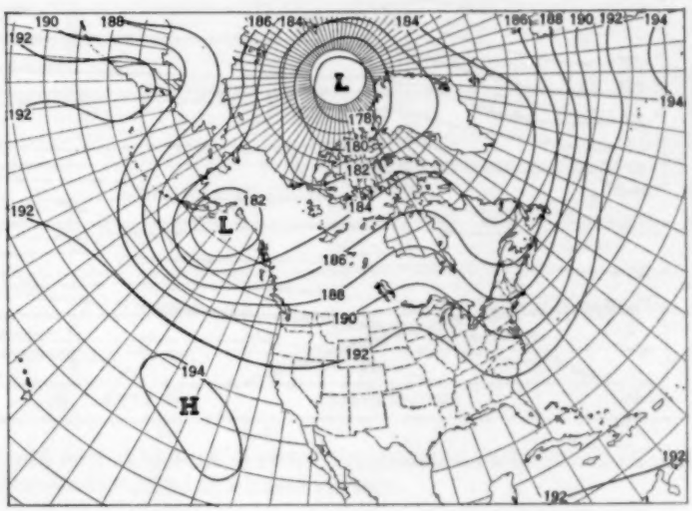

FIGURE 5.—Space-mean chart for 500 mb. at 1200 GMT, July 24, 1957.

indicated times. In figure 4, a long-wave trough position is indicated in the vicinity of a line running from latitude 55° N., longitude 53° W. to latitude 25° N., longitude 62° W. The long-wave ridge position is somewhat more nebulous but in the interval of latitudes 30° N. to 45° N. seems to lie somewhere between longitudes 80° W. and 85° W. Farther west another long-wave trough position is indicated just off the coast of California.

Seventy-two hours later, a drastic change has taken place (fig. 5). The long-wave trough position off the east coast has definitely retrogressed westward. The same is true for the long-wave ridge position in the United States. Off the west coast the long-wave trough position has also undergone a pronounced displacement to the west.

6. CROSS SECTION ANALYSIS

Cross section analyses (figs. 6 and 7) were prepared for 1200 GMT, July 21 (when the ridge pattern at 500-mb.

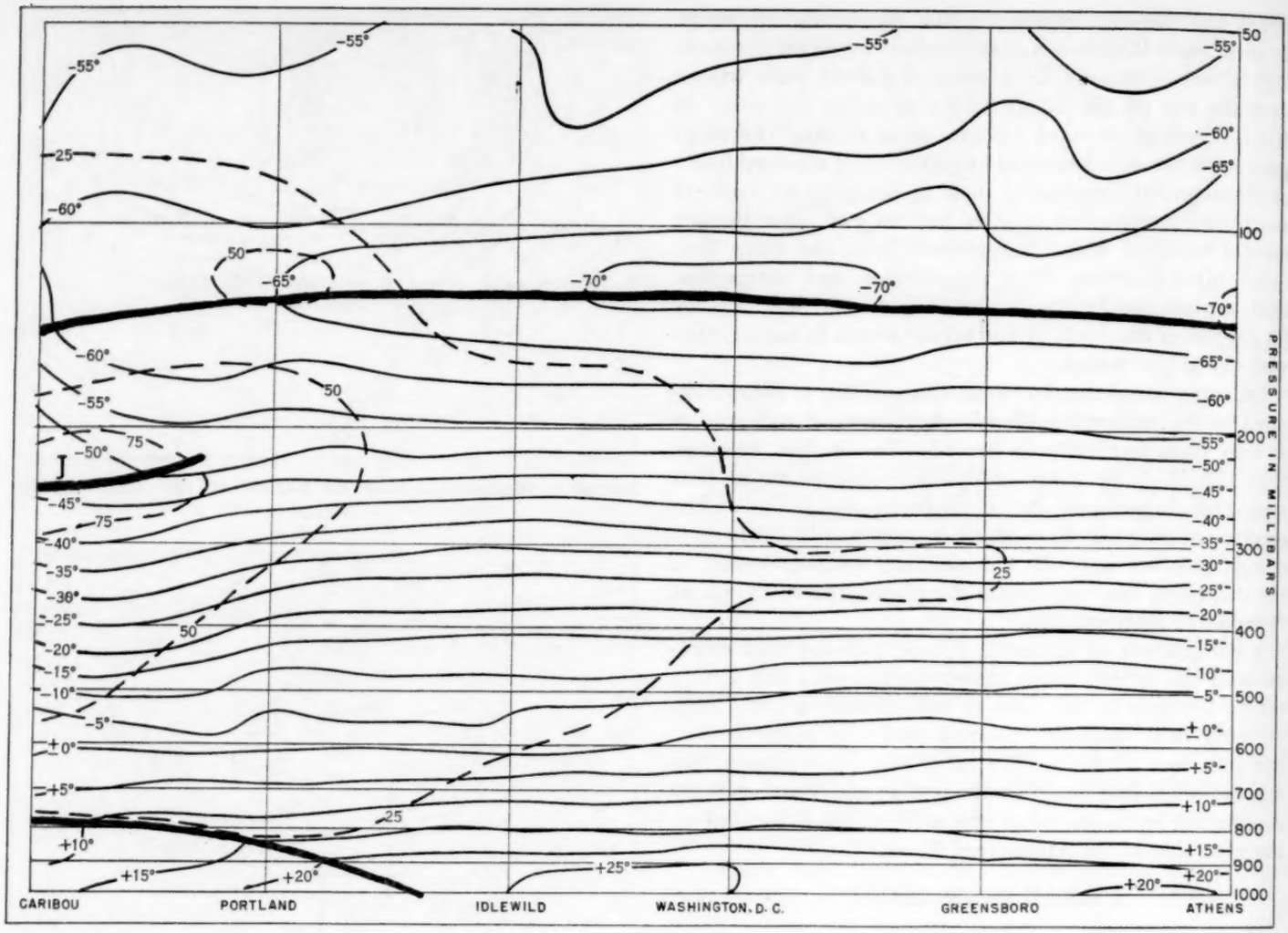

FIGURE 6.—Vertical cross section, Caribou to Athens, at 1200 GMT, July 21, 1957. Thin solid lines are isotherms in degrees C. Dashed lines are isotachs in knots. Heavy solid lines are fronts and tropopause leaves.

prevailed on the east coast) and 1200 GMT, July 24 (when the trough pattern prevailed on the east coast). A cross section which included both New York and Washington, D. C., was considered desirable since both places had experienced high maximum temperatures on the 21st and appreciably lower ones by the 24th. The technical desirability of a section normal to the mid and upper troposphere flow for both synoptic times was also a consideration. Fortunately, all of these desirable qualities could be met with cross sections from Athens, Ga., to Caribou, Maine.

As shown in figure 6, the only notable baroclinic features in the troposphere were in the frontal zone (lower left hand corner of the diagram) and between Portland and Caribou above the 500-mb. level. Two tropopause leaves are shown in the cross section. Along the upper one, the potential temperature varied from 359° at Athens to about 376° at Caribou. The lower leaf with a potential temperature of about 339° at Caribou could not be readily detected in the soundings for Portland or the other stations to the south. The tropopause leaf at Caribou did not quite satisfy the arbitrary definition for a "first tropopause" which has been defined as "the lowest level at which the lapse rate decreases to 2° C./km. or less, and averages 2° C./km. or less for at least 2 km. above. In addition . . . the lowest tropopause must satisfy both of the following conditions: (a) It must occur between the 600 and 30-mb. levels, and (b) its temperature must be colder than −30° C." [8]. The requirements for a "first tropopause" at Caribou were satisfied at about the 150-mb. level. Sufficient stabilization, however, occurred at 250 mb. to indicate the existence of another leaf.

Seventy-two hours later (fig. 7) the troposphere had become considerably more baroclinic as the change from anticyclonic to cyclonic conditions took place and as the polar air displaced the tropical air; the frontal zone now stretched over the entire distance covered by the cross section. The stratospheric picture was more complicated with three tropopause leaves of varying intensities. The jet, which was now of double structure, was located between the two lower leaves; the lowest leaf was a continuation of the low leaf at Caribou in figure 6. Stratospheric

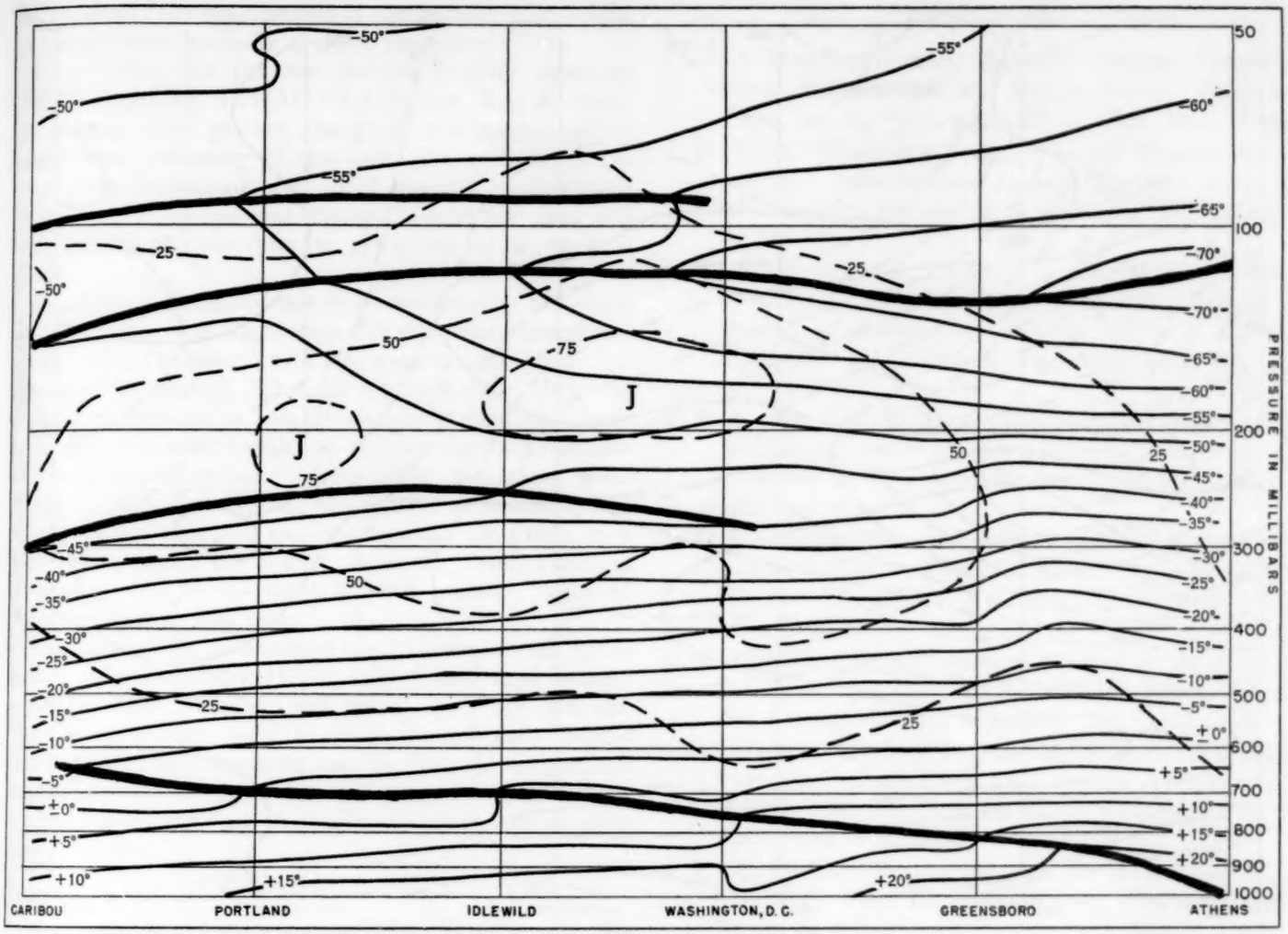

FIGURE 7.—Vertical cross section, Caribou to Athens, at 1200 GMT, July 24, 1957. Thin solid lines are isotherms in degrees C. Dashed lines are isotachs in knots. Heavy solid lines are fronts and tropopause leaves.

warming had occurred to the north of Greensboro. This is more readily indicated by the cross section in figure 6.

The 72-hour change in temperature and isohypses are shown in figure 8. The major axis of the positive isallotherm field was almost horizontal and was found at about 130 mb. The pattern of the isallohypses was more complex, with the most pronounced feature being the nearly horizontal axis near 250 mb. between Portland and Washington. This axis of greatest height change was noticeably out of phase with the axis of greatest temperature change. Between Portland and Caribou the major axis of the height falls was tilted more toward the vertical with a second center of height falls indicated in the vicinity of or somewhere northward of Caribou. The lack of sufficient high level data precluded further interpretation in that area.

7. THE FORECAST PROBLEM

Abnormally high surface temperatures are most often found below upper air (500-mb.) ridge patterns. To terminate the existence of these large positive temperature anomalies it would, therefore, be necessary to replace this upper air pattern with a more cyclonic one. In essence then, to forecast from the 1200 GMT, July 21 map (fig. 1) the termination of the incipient heat wave over the middle Atlantic seaboard, it would be necessary to foresee the development of a good trough aloft over this same area. This major trough would have to be a development, essentially, of the short-wave trough located over Hudson Bay.

Inspection of the situation leads one to conclude that reasoning from jet stream principles would not be fruitful in this case. In the classical case of "digging", the winds to the rear of a deepening trough are significantly stronger than either the winds at the base of the trough or immediately in advance. Such was not the case. The wind field immediately to the rear of the Hudson Bay trough could be seen from the 500-mb. isohypses to be relatively weak. The two main jet streams in the general area were not too favorably located. One jet was located somewhat too far to the north. Its west-east orientation, in addition, was not the most desirable one for anticipating "digging". The other jet appeared to be located too far to the south

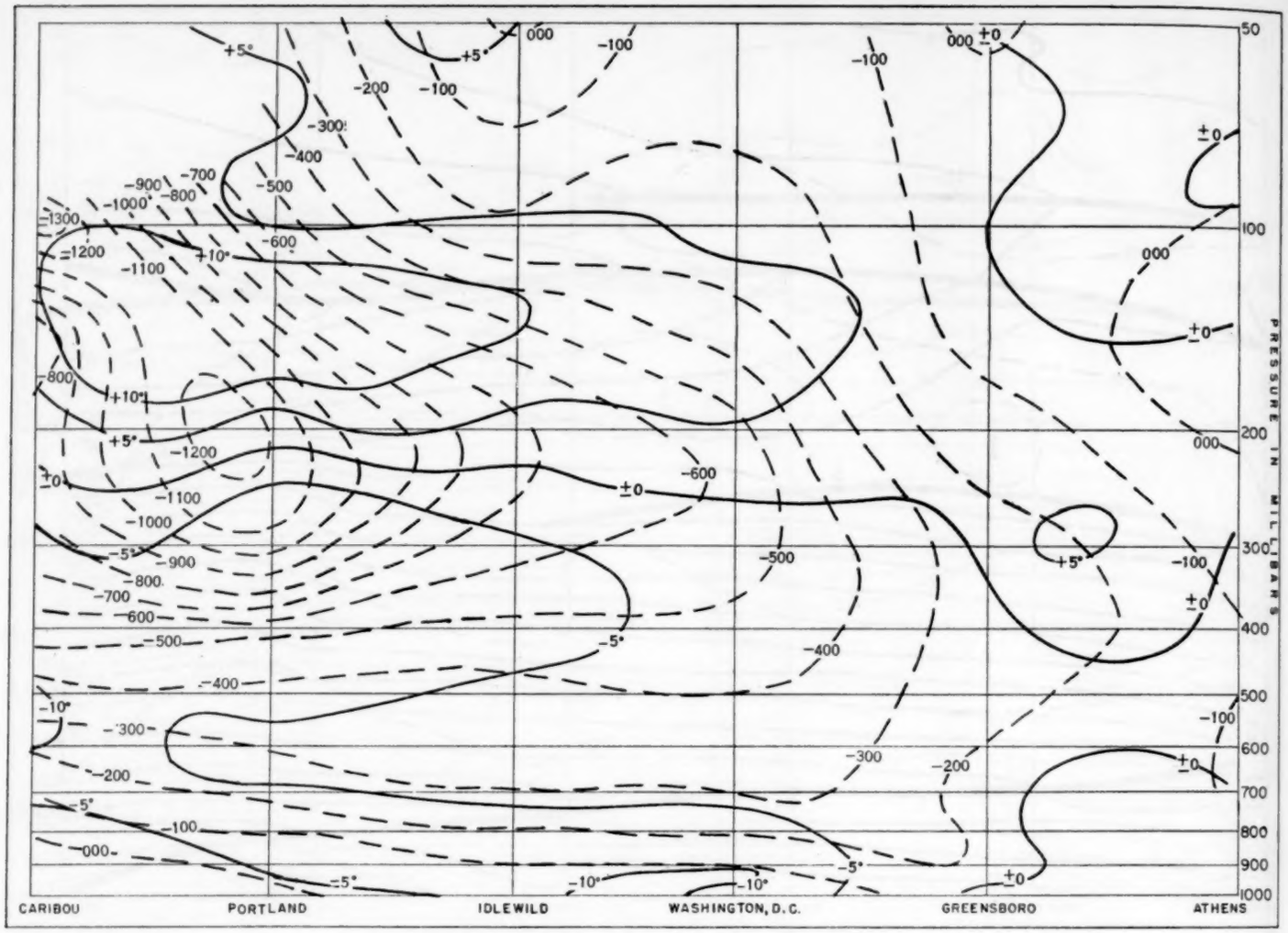

FIGURE 8.—Vertical cross section, Caribou to Athens, with 72-hour changes from 1200 GMT, July 21, 1957, to 1200 GMT, July 24, 1957. Isallohypses (dashed lines) are labeled in hundreds of geopotential feet per 72 hours. Isallotherms (solid lines) are labeled in degrees C. per 72 hours.

to be of much influence. Inferring a development primarily or solely from jet reasoning would thus appear to be unwarranted in this case.

A principle often used for predicting intensification states that deepening of a trough will continue as long as the winds in the cold air moving into the trough continue from north to northwest [9]. In this case there was no cold air advection of any consequence from the direction north to northwest for this rule to be of any avail.

Application of the upstream influence effect was not deemed apropos. This would attribute downstream deepening of the Hudson Bay trough as a consequence of upstream ridge building. Unfortunately there was no discernible building of the upstream ridge as of 1200 GMT, July 21, although 12 hours later building of the upstream ridge was definitely taking place.

One apparently fruitful attack on the problem involved a tie-in with events occurring in the Gulf of Alaska. In that region significant falls had been occurring by 1200 GMT, July 21 both at the surface and aloft. The mean flow chart for that time (fig. 4) also indicated advection of cyclonic vorticity into that same area. This combination of events, experience has shown, would tend to favor the movement inland of any trough immediately off the west coast of the United States with the resultant establishment of the intensifying trough in the Gulf of Alaska as the new off shore major trough. In essence, the new long-wave trough position off the west coast would be located farther west than previously. The establishment of this new long-wave trough position off the west coast, unless accompanied by a "sympathetic" retrogression of the long-wave trough position off the east coast, would result in a wavelength of much too large a value to be in accord with either the theoretical requirement of the Rossby long wave formula or the empirical knowledge of the experienced forecaster. It would therefore be logical to conclude that retrogression of some consequence would have to take place in the East. This would of necessity require a westward shift of the ridge from the Atlantic

seaboard and the replacement of the pattern in this area by one of more decidedly cyclonic character.

In actuality the pressure pattern outlook summary (FSUS) issued by NAWAC for 1200 GMT, July 21 called for a broad scale pattern change of this general nature based upon reasoning of this sort. In addition, a 24-hour previous outlook warned of possible readjustment of the long-wave positions during the next few days as a consequence of developments appearing in the Gulf of Alaska.

In addition, there appears to be some reason to believe that development of the Hudson Bay short-wave trough was helped by a "phasing" with the weak trough which had appeared in central Nebraska by 1200 GMT, July 21. Some contribution to this development must also have come from "phasing" with the cyclonic vorticity remnant of the southern portion of an older east coast polar trough. After shearing off, this older trough was steered clockwise around the east coast upper-air High to a favorable position for merging with the weak trough in Nebraska, and ultimately this joint product "phased" with the Hudson Bay trough.

It is interesting to note that the 72-hour 500-mb. prognostic chart issued by JNWP Unit (using their current quasi-barotropic model) and based upon the 500-mb. chart of 1200 GMT, July 21 as the initial map, showed definite east coast retrogression. In fact, the main defect in the portion of the numerical prognostic for eastern United States was that, ironically, too much retrogression was predicted.

ACKNOWLEDGMENTS

Appreciation is hereby expressed by the authors to the staff members of NAWAC for their helpful comments and to the members of the Daily Map Unit of the Weather Bureau who drafted the figures.

REFERENCES

1. U. S. Weather Bureau, "Monthly Normal Temperatures, Precipitation, and Degree Days," *Technical Paper* No. 31, Washington, D. C., Nov. 1956, 39 pp.
2. D. Fultz, "Upper-Air Trajectories and Weather Forecasting," *Miscellaneous Reports*, No. 19, Dept. of Meteorology, University of Chicago, 1945, 123 pp. (p. 56).
3. F. A. Berry, W. H. Haggard, and P. M. Wolff, "Description of Contour Patterns at 500 Millibars," Bureau of Aeronautics Project AROWA (TED–UNL–MA–501), Norfolk, Va., April 1954, 108 pp. (pp. 11–16).
4. F. A. Berry, W. H. Haggard, and P. M. Wolff, "500-Millibar Studies at Project AROWA," *Bulletin of the American Meteorological Society*, vol. 34, No. 10, Dec. 1953, pp. 444–453.
5. D. E. Martin, "Forecasting Rules and Techniques Used in Tokyo Weather Central," *Special Study* 105–2, 1st Weather Wing, U. S. Air Force, Tokyo, Aug. 1956, 141 pp. (p. 19).
6. R. Fjørtoft, "On a Numerical Method of Integrating the Barotropic Vorticity Equation," *Tellus*, vol. 4, No. 3, Aug. 1952, pp. 179–194.
7. Air Weather Service, "Forecasting Upper-Level Winds; Part One, Forecasting by Vorticity Techniques," *AWSM* 105–50/1, U. S. Air Force, Washington, D C., June 1954, 50 pp. (p. 7).
8. U. S. Weather Bureau, *Manual for Radiosonde Code (WBAN)*, First Ed., Washington, February 1956, 55 pp. (p. 24).
9. E. A. Aime and E. C. Johnson, *Methods for the Preparation of Six-Day Forecasts*, U. S. Weather Bureau, Washington, Nov. 1943, 26 pp. (p. 18).

Suggestions for Authors

Articles are accepted for the *Monthly Weather Review* with the understanding that they have not been published or accepted for publication elsewhere.

Two copies of the *manuscript* should be submitted. All copy, including footnotes, references, tables, and legends for figures should be double spaced with margins of at least 1 inch on sides, top, and bottom. Some inked corrections are acceptable but pages with major changes should be retyped. The style of capitalization, abbreviation, etc., used in the *Review* is governed by the rules set down in the Government Printing Office Style Manual.

Tables should be typed each on a separate page, with a title provided. They should be numbered consecutively in arabic numerals.

In *equations* conventional symbols in accordance with the American Standards Association Letter Symbols for Meteorology should be used. If equations are written into the manuscript in longhand, dubious-looking symbols should be identified with a penciled note.

References should be listed on a separate sheet and numbered in the order in which they occur in the text; or, if there are more than 10, in alphabetical order according to author. The listing should include author, title, source (if a magazine the volume, number, month, year, and complete page numbers; if a book the publisher, place of publication, date, and page numbers). If reference is made to a self-contained publication, the author, title, publisher, place of publication, and date should be given. Within the text references should be indicated by arabic numbers in brackets to correspond to the numbered list.

Footnotes should be numbered consecutively in arabic numerals and indicated in the text by superscripts. Each should be typed at the bottom of the page on which the footnote reference occurs.

Illustrations. A list of legends for the illustrations should be typed (double spaced) on a separate sheet. Each illustration should be numbered in the margin or on the back outside the image area. To fit into the *Review* page, illustrations must take a reduction not to exceed 3½″ x 9″ (column size) or 7½″ x 9″ (page size). Map bases should show only political and continental boundaries and latitude and longitude lines, unless data are to be plotted, when station circles will also be needed. Usually the less unnecessary detail in the background the better will be the result from the standpoint of clear reproduction. Line drawings and graphs should also be uncluttered with fine background grids unless the graph demands very close reading. It is not necessary to submit finished drawings, as drafting work can be done at the time the paper is prepared for publication.

Photographs should be sharp and clear, with a glossy surface. Bear in mind that marks from paper clips or writing across the back will show up in the reproduction. Drawings and photographs should be protected with cardboard in mailing.

Publication of Weather Notes

Many years ago the *Monthly Weather Review* published detailed eye-witness accounts of exceptional storms. These accounts both enrich the meteorologist's knowledge of storms and provide him with particular details that cannot be found elsewhere. Because such information bears directly upon questions the meteorologist must attempt to answer about weather phenomena (for example, the identification of storms as tornadoes), and because the information has potential value in both the research and service programs of the Weather Bureau, publication of eye-witness accounts and brief analyses of exceptional storms and other meteorological phenomena was resumed in the April 1955 issue. They appear from time to time under the heading "Weather Notes."

Contributions to these "Notes" are invited from readers of the *Review*. There is no limitation placed on length of description but it is expected that most will be short accounts. Any weather pecularities, whether storms or other phenomena, are acceptable subject matter. Material should be addressed to Editor, Monthly Weather Review, U. S. Weather Bureau, Washington 25, D. C.

Change in Climatological Charts

Beginning on June 1, 1957, a change was made in surface observation times. This has had the following effect on the charts listed below. Charts not listed are not affected.

Chart V–B. Snow depth is now measured at 7 a. m. EST instead of 7:30.

Charts IX and X. Circle indicates cyclone and anticyclone positions at 7 a. m. EST instead of 7:30.

Chart XI. Average sea-level pressure is computed from the 7 a. m. and p. m. EST readings instead of 7:30 a. m. and p. m.

Charts XII–XVII. All the upper-air charts are now for 1200 GMT instead of 0300 GMT. All winds are based on rawinsonde observations. Use of pibal data has been discontinued in these charts.

Description of Charts

CHART I. *A. Average Temperature (°F.) at Surface. B. Departure of Average Temperature from Normal.*—The average monthly temperature presented in Chart I–A is computed from the average daily maximum and the average daily minimum which in turn are computed from the daily maximum and minimum temperatures reported by some 225 first-order Weather Bureau stations and 700 cooperative stations. The departures from normal are presented in Chart I–B. They are based on the 30-year normals (1921–50) for the first-order Weather Bureau stations and on means of 25 years or more (mostly 1931–55) for the cooperative stations.

CHART II. *Total Precipitation.*—

CHART III. *A. Departure of Precipitation from Normal (inches). B. Percentage of Normal Precipitation.*—Chart II is based on daily precipitation records at about 800 Weather Bureau and cooperative stations. In Chart III the anomaly in the month's precipitation is shown as a departure from the normal total and as a percentage of the normal total. These anomalies show the deviations from the 30-year normals (1921–50) for about 225 first-order Weather Bureau stations in Charts III A and B, supplemented in Chart III–A by the deviation from means of 25 years or more (mostly 1931–55) for about 700 cooperative stations.

CHART IV. *Total Snowfall.*—

CHART V. *A. Percentage of Normal Snowfall. B. Depth of Snow on Ground.*—Chart IV gives the total depth in inches of unmelted snowfall as reported during the month by Weather Bureau and cooperative stations. This is converted in Chart V–A into a percentage of the normal total amount computed for each Weather Bureau station having at least 10 years of record. The depth of snow on ground is that reported by both Weather Bureau and cooperative stations as of 7:00 a. m. Eastern Standard Time on the last Monday of the month. This is reported only for the months December through April. The snowfall charts are presented each month November through April.

CHART VI. *A. Percentage of Sky Cover Between Sunrise and Sunset. B. Percentage of Normal Sky Cover Between Sunrise and Sunset.*—These charts are based on visual observations made hourly at Weather Bureau stations and averaged for the month. Sky cover includes, in addition to cloudiness, obscuration of the sky by fog, smoke, etc. Normal amount of sky cover is computed for stations having at least 10 years of record.

CHART VII. *A. Percentage of Possible Sunshine. B. Percentage of Normal Sunshine.*—Chart VII–A shows the amount of sunshine received in terms of percentage of the total hours of sunshine possible during the month. In Chart VII–B this is shown as a percentage of the normal number of hours of sunshine received. Normals are computed for Weather Bureau stations having at least 10 years of record.

CHART VIII. *Average Daily Values of Solar Radiation, Direct and Diffuse.*—Plotted on the chart are the monthly means of daily total solar radiation, both direct and diffuse, in langleys (gm. cal. $cm.^{-2}$) for all Weather Bureau stations which record this element. Supplementary data for which limits of accuracy are wider than for those data shown are drawn upon in making the analysis. The inset shows the percentages of the mean based on the period 1951–55.

CHART IX. *Tracks of Centers of Anticyclones at Sea Level.*—

CHART X. *Tracks of Centers of Cyclones at Sea Level.*—Centers which can be identified for 24 hours or more are tracked in these charts. Semi-permanent features such as the Great Basin and Pacific Highs and Colorado and Mexico Lows are not shown. The 7:00 a. m. EST positions are shown by open circles, with the intermediate positions at 6-hour intervals shown by solid dots. The date is given above the circle and the central pressure to whole millibars below. A dashed track indicates a regeneration rather than actual movement to the next position. Solid squares indicate position of stationary center for period shown beside it.

CHART XI. *Average Sea Level Pressure (mb.) and Surface Windroses.*—The average monthly sea level pressure is obtained from the averages of the 7:00 a. m. and 7:00 p. m. EST pressures reported at Weather Bureau stations. Windroses are based on the hourly wind directions (to 16 points of the compass) reported by Weather Bureau stations, each circle or arc indicating 5 percent of the time. The inset shows the departure of the average pressure from the normal average computed for each station having at least 10 years of record and for each 10° intersection in a diamond grid over the oceans from interpolated values read from the Historical Weather Maps for the 20 years of best coverage prior to 1940.

CHARTS XII–XVII. *Average Height, Temperature, and Resultant Winds, 850, 700, 500, 300, 200, and 100 mb.*—Height is given in geopotential meters and temperature in degrees Celsius. These are the averages of the 1200 GMT radiosonde reports. Wind speeds are given in knots; flag represents 50 knots, full feather 10 knots, and half feather 5 knots. Directions are shown to 360° of the compass. Winds are based on rawins at the indicated pressure surface and at 1200 GMT.

Tabulations of exact values of most of these charted elements for Weather Bureau stations are printed each month in Tables 2, 20, or 33 in *Climatological Data, National Summary*, and annual averages are presented in the CDNS Annual Issue each year.

U. S. GOVERNMENT PRINTING OFFICE: 1957

Chart I. A. Average Temperature (°F.) at Surface, July 1957.

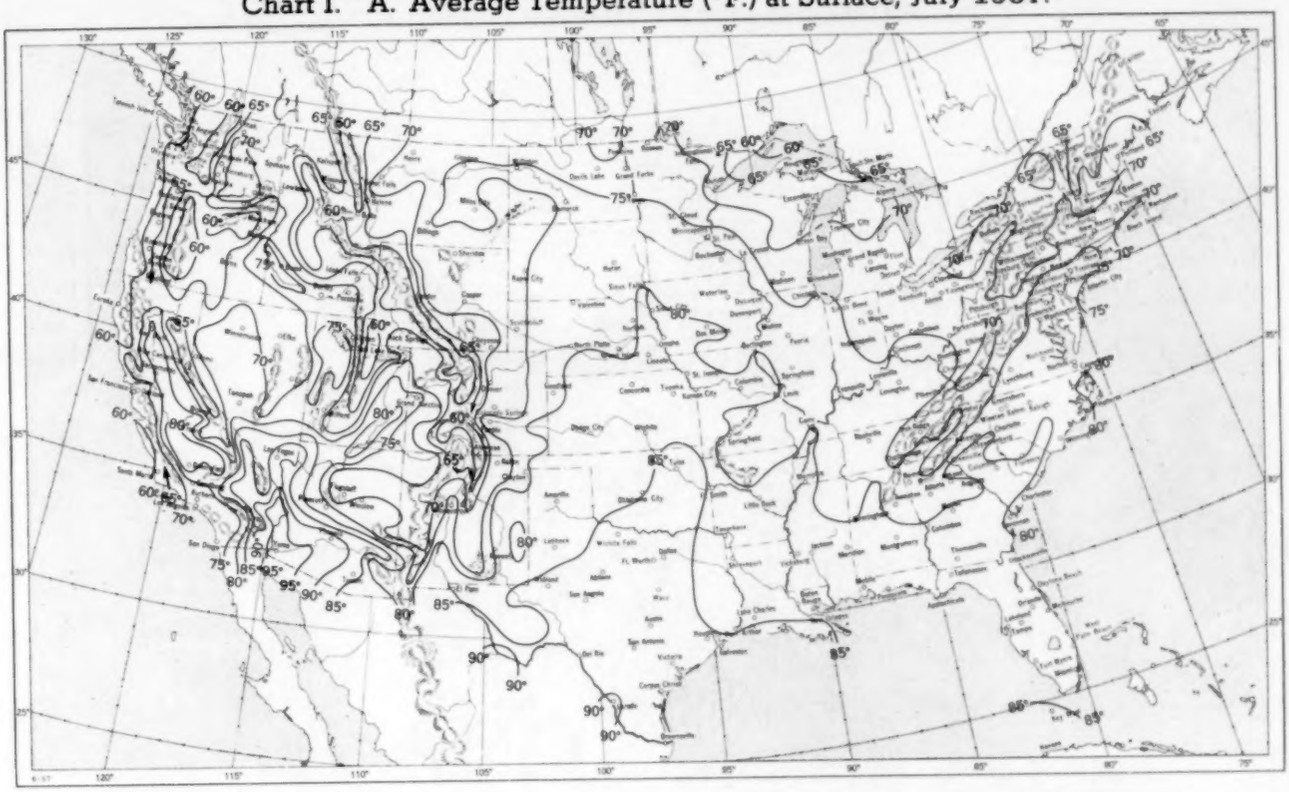

B. Departure of Average Temperature from Normal (°F.), July 1957.

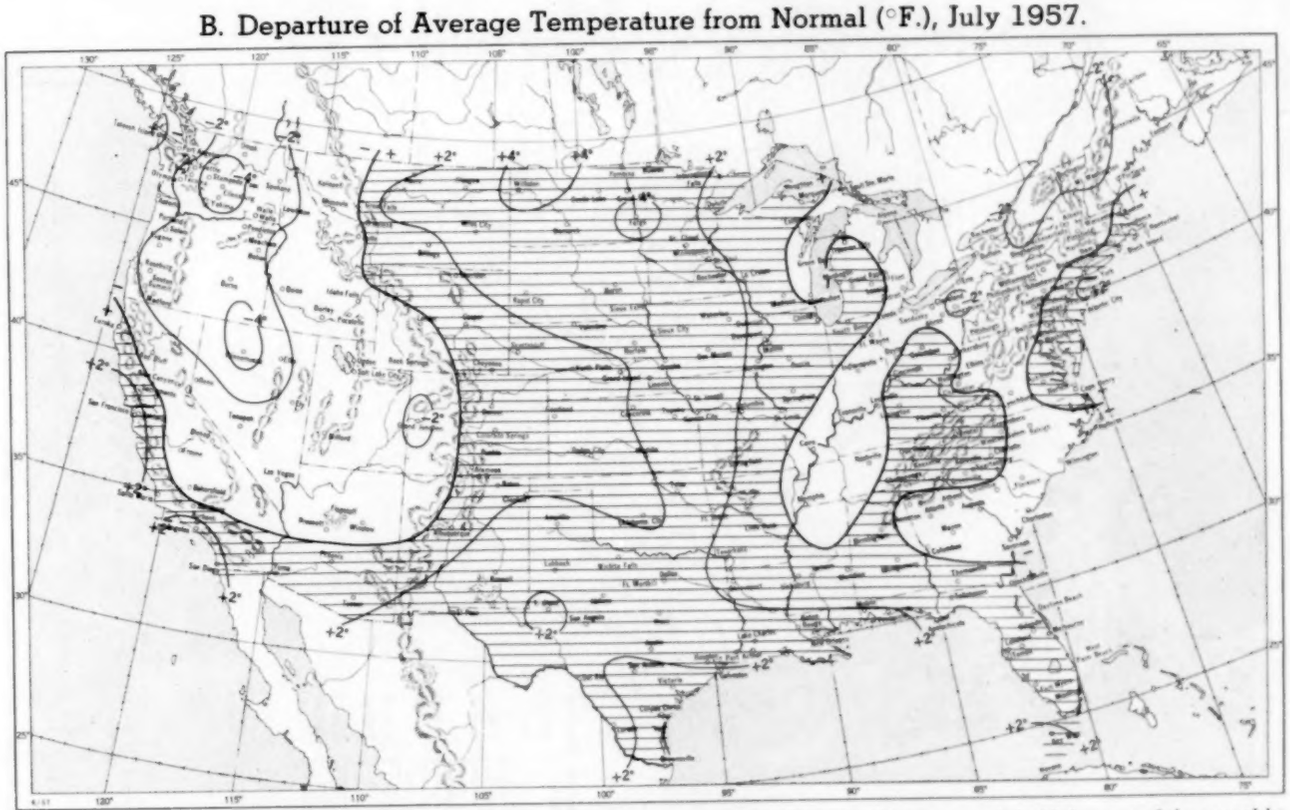

A. Based on reports from over 900 Weather Bureau and cooperative stations. The monthly average is half the sum of the monthly average maximum and monthly average minimum, which are the average of the daily maxima and daily minima, respectively.

B. Departures from normal are based on the 30-yr. normals (1921-50) for Weather Bureau stations and on means of 25 years or more (mostly 1931-55) for cooperative stations.

Chart II. Total Precipitation (Inches), July 1957.

Scale of Shades
0 to 1 inch
1 to 2 inches
2 to 4 inches
4 to 6 inches
Over 6 inches
SCALE OF MILES
LAMBERT CONFORMAL PROJECTION TRUE AT 30° AND 60°

Based on daily precipitation records at about 800 Weather Bureau and cooperative stations.

Chart III. A. Departure of Precipitation from Normal (Inches), July 1957.

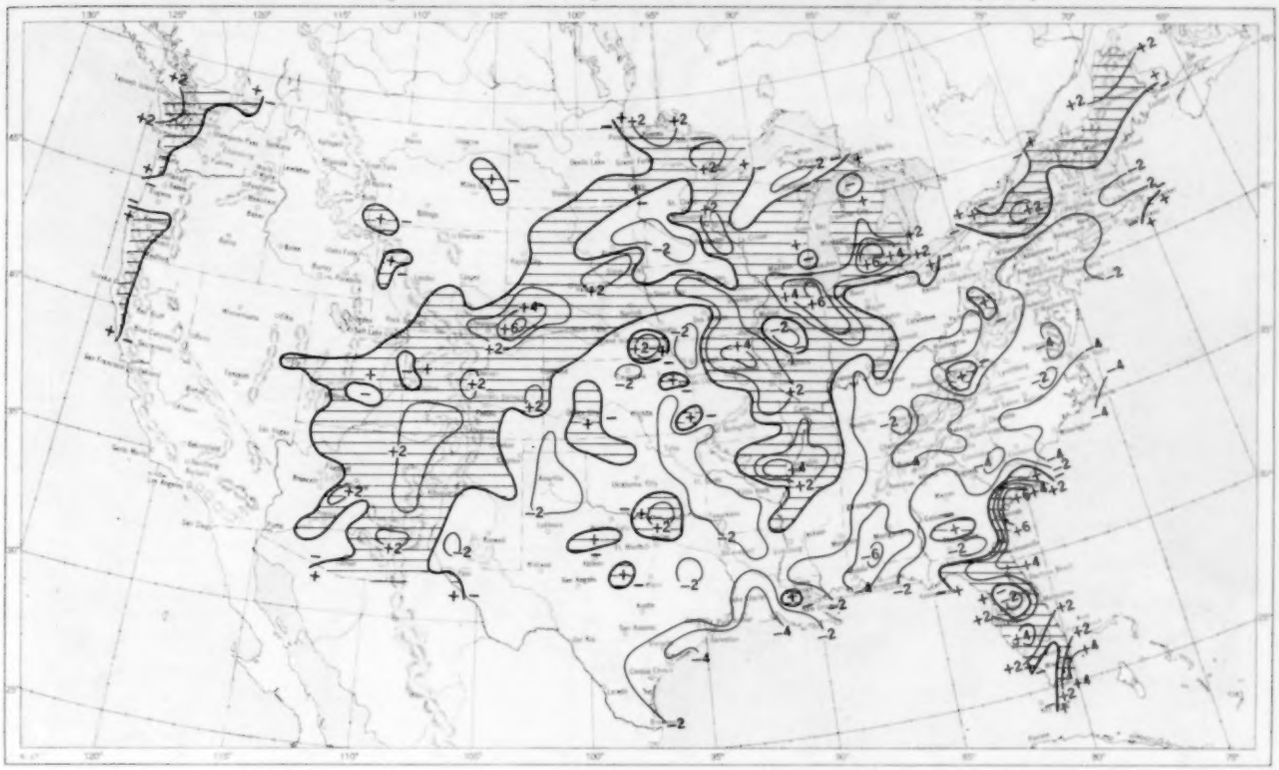

B. Percentage of Normal Precipitation, July 1957.

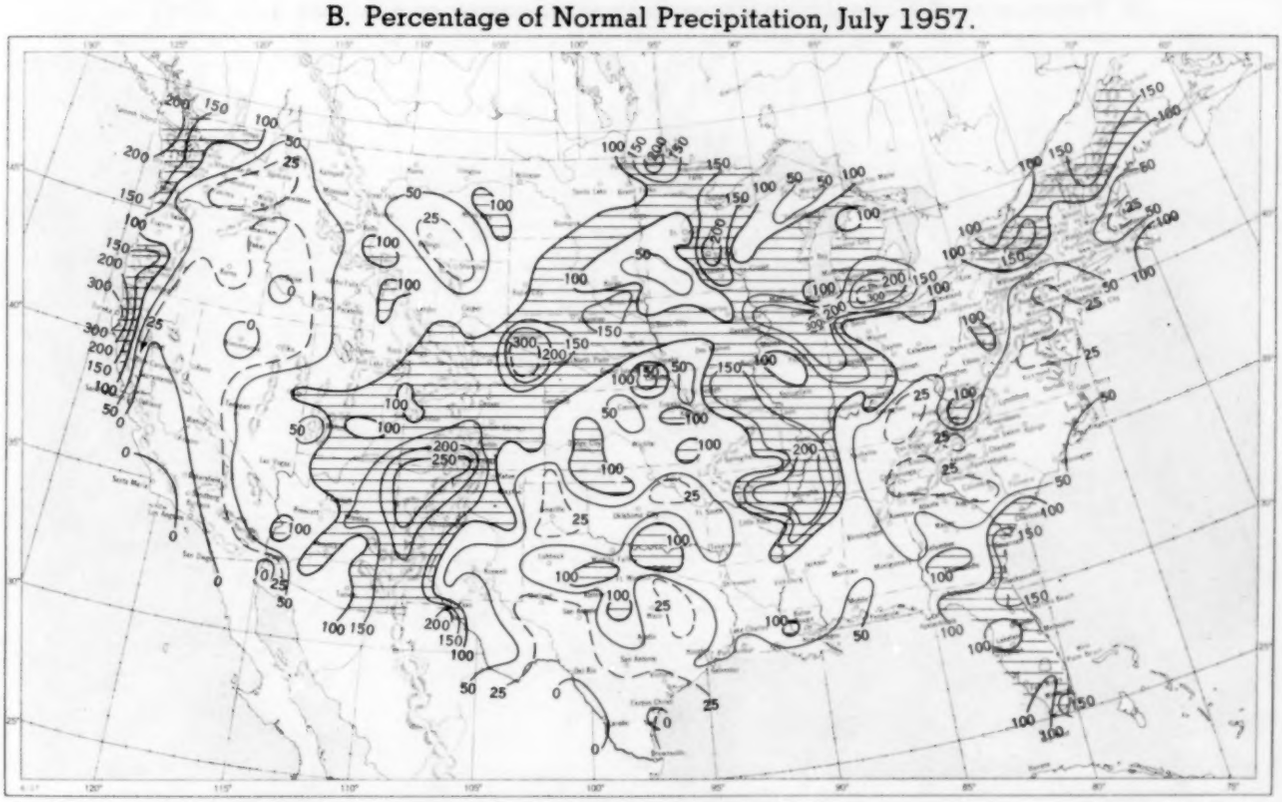

Normal monthly precipitation amounts are computed from the records for 1921-50 for Weather Bureau stations and from records of 25 years or more (mostly 1931-55) for cooperative stations.

Chart VI. A. Percentage of Sky Cover Between Sunrise and Sunset, July 1957.

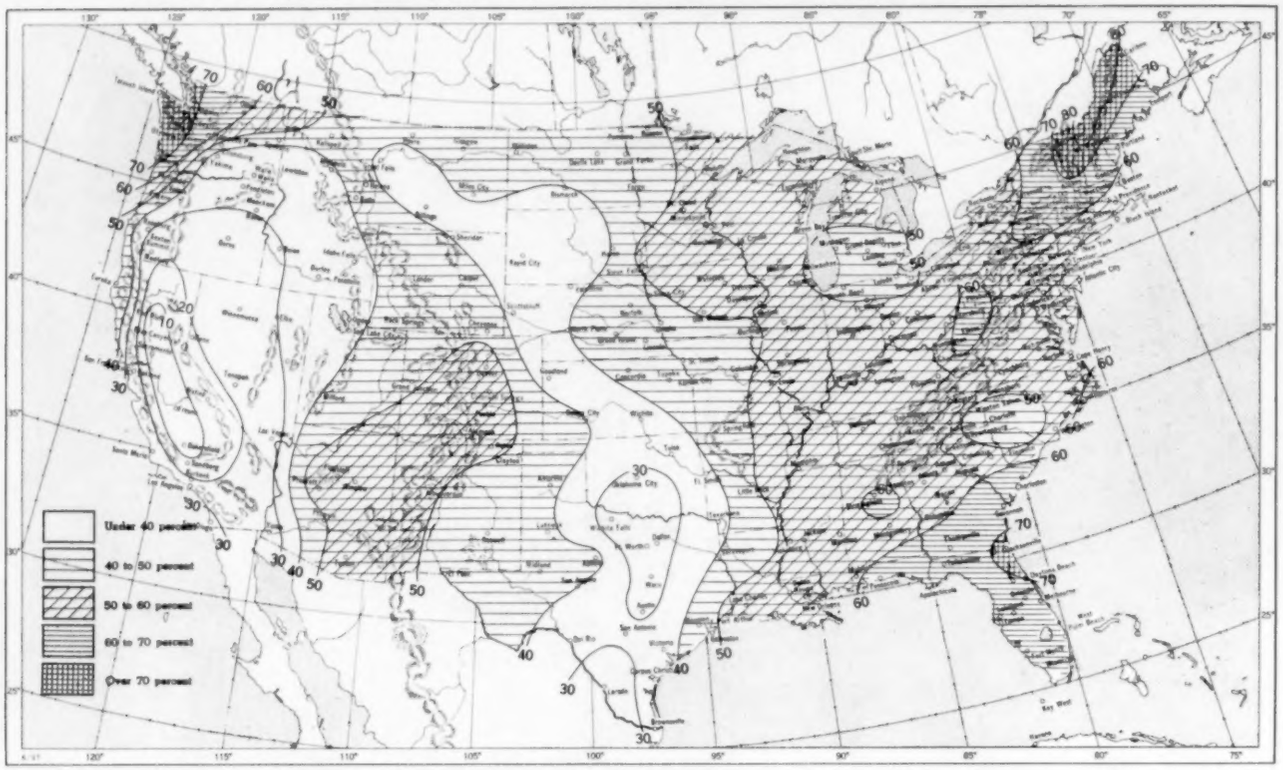

B. Percentage of Normal Sky Cover Between Sunrise and Sunset, July 1957.

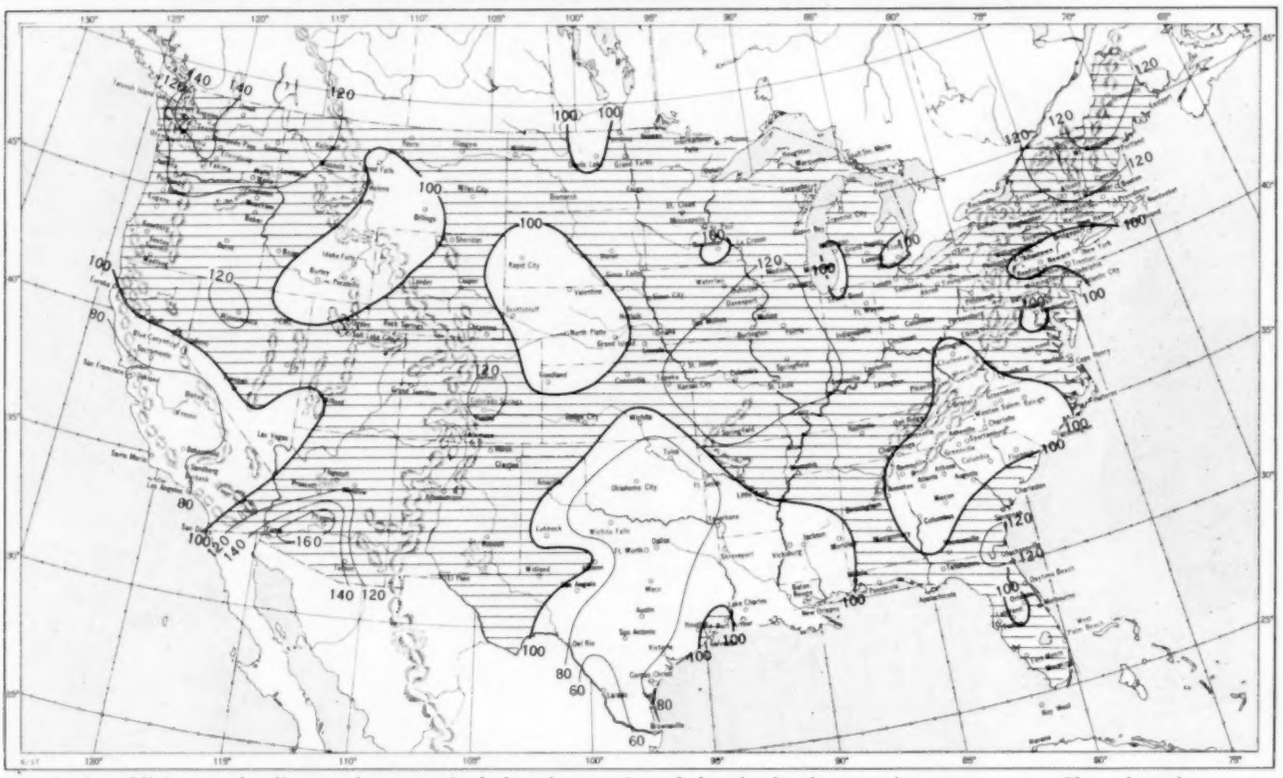

A. In addition to cloudiness, sky cover includes obscuration of the sky by fog, smoke, snow, etc. Chart based on visual observations made hourly at Weather Bureau stations and averaged over the month. B. Computations of normal amount of sky cover are made for stations having at least 10 years of record.

Chart VII. A. Percentage of Possible Sunshine, July 1957.

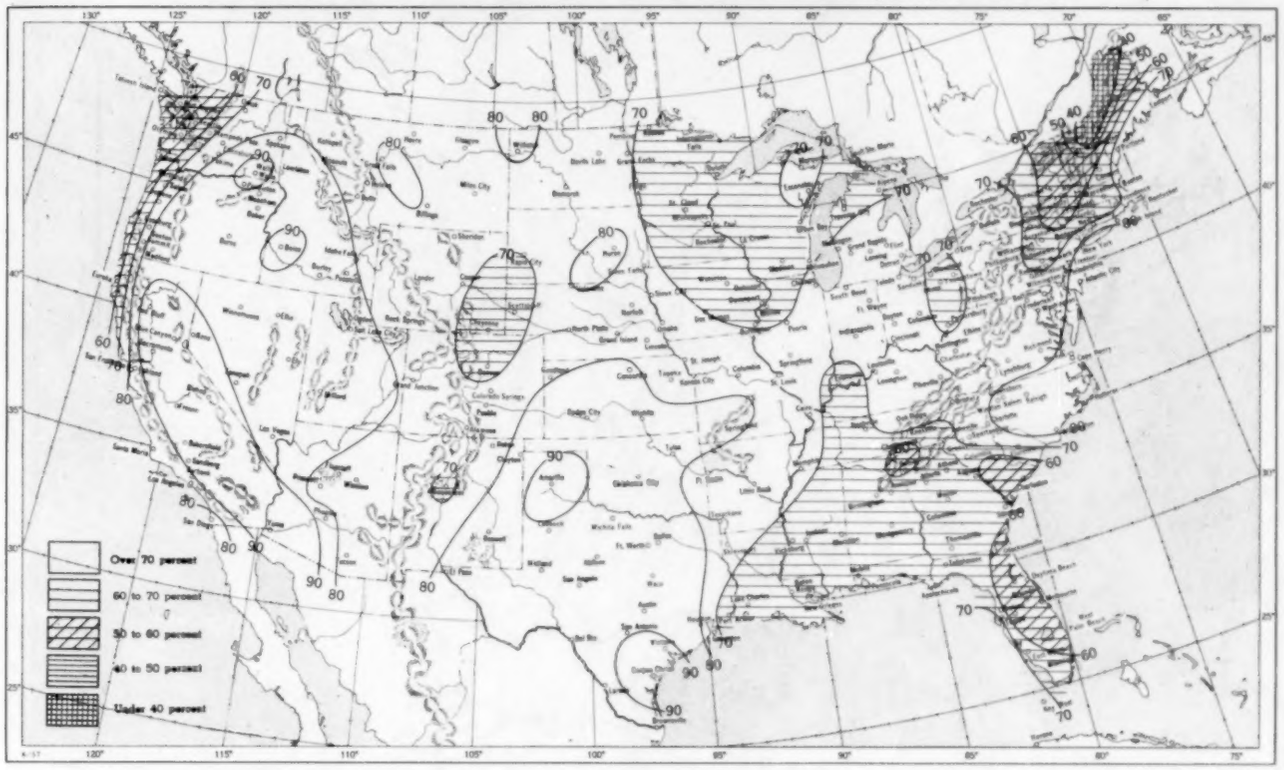

B. Percentage of Normal Sunshine, July 1957.

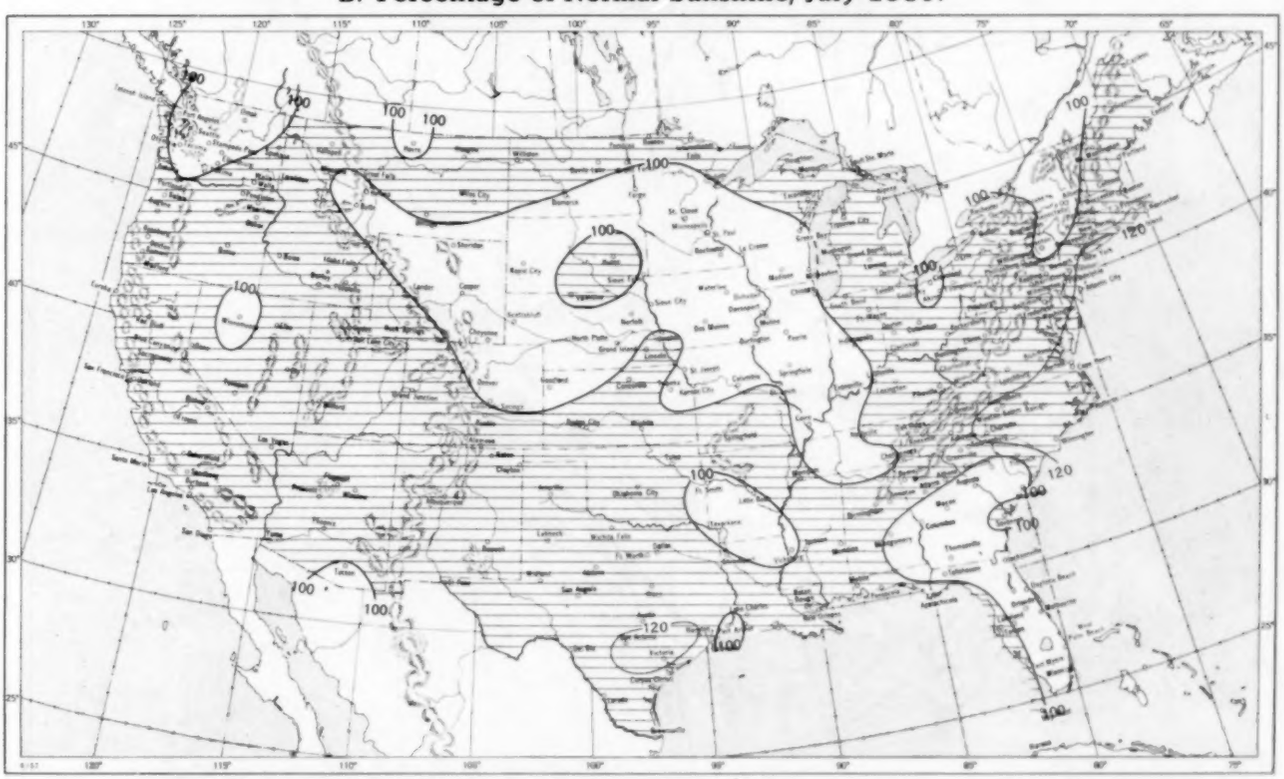

A. Computed from total number of hours of observed sunshine in relation to total number of possible hours of sunshine during month. B. Normals are computed for stations having at least 10 years of record.

Chart VIII. Average Daily Values of Solar Radiation, Direct + Diffuse, July 1957. Inset: Percentage of Mean Daily Solar Radiation, July 1957. (Mean based on period 1951-55.)

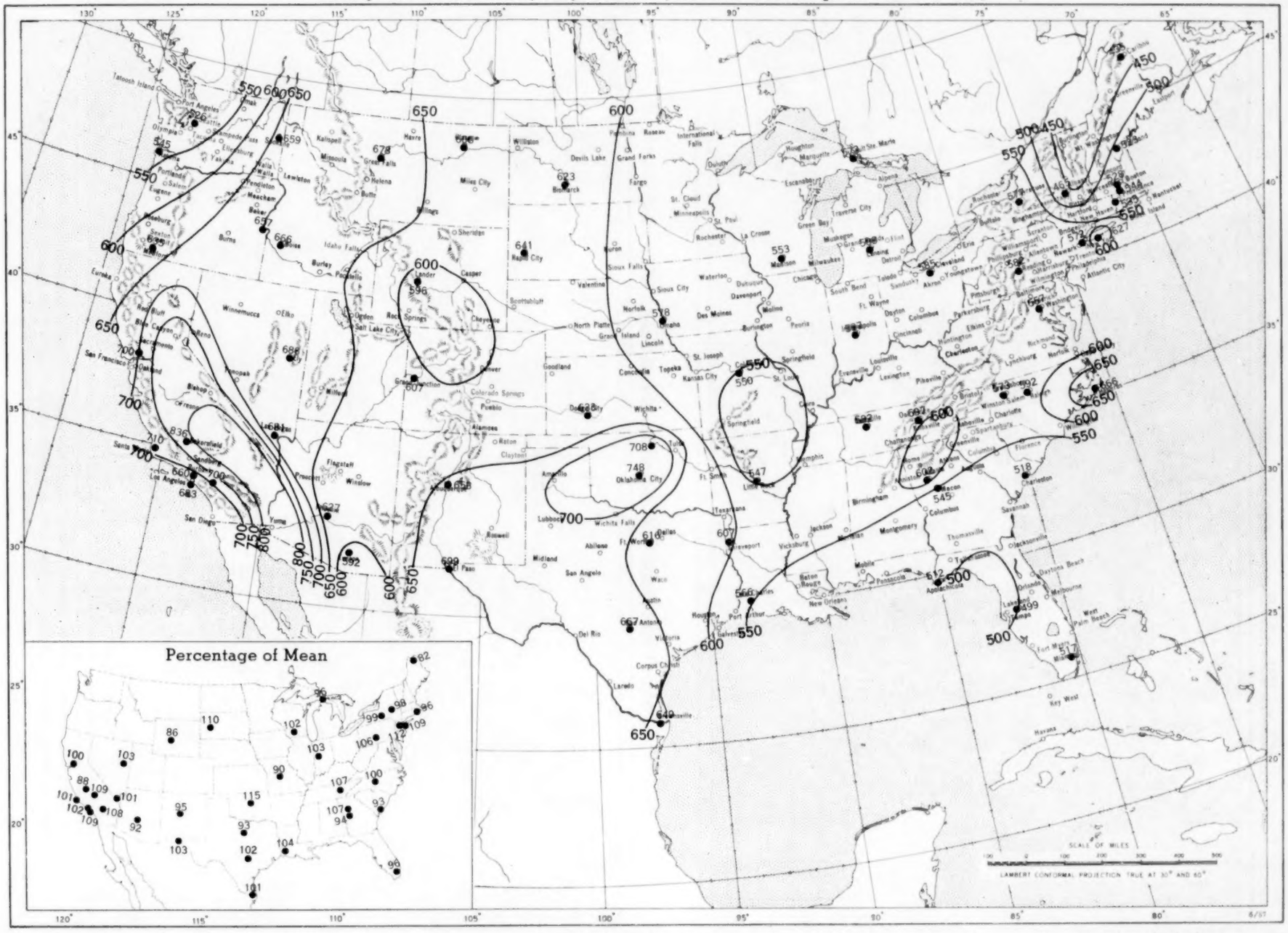

Chart shows mean daily solar radiation, direct + diffuse, received on a horizontal surface in langleys (1 langley = 1 gm. cal. cm. $^{-2}$). Basic data for isolines are shown on chart. Further estimates are obtained from supplementary data for which limits of accuracy are wider than for those data shown. The inset shows the percentage of the mean based on the period 1951-55.

Chart IX. Tracks of Centers of Anticyclones at Sea Level, July 1957.

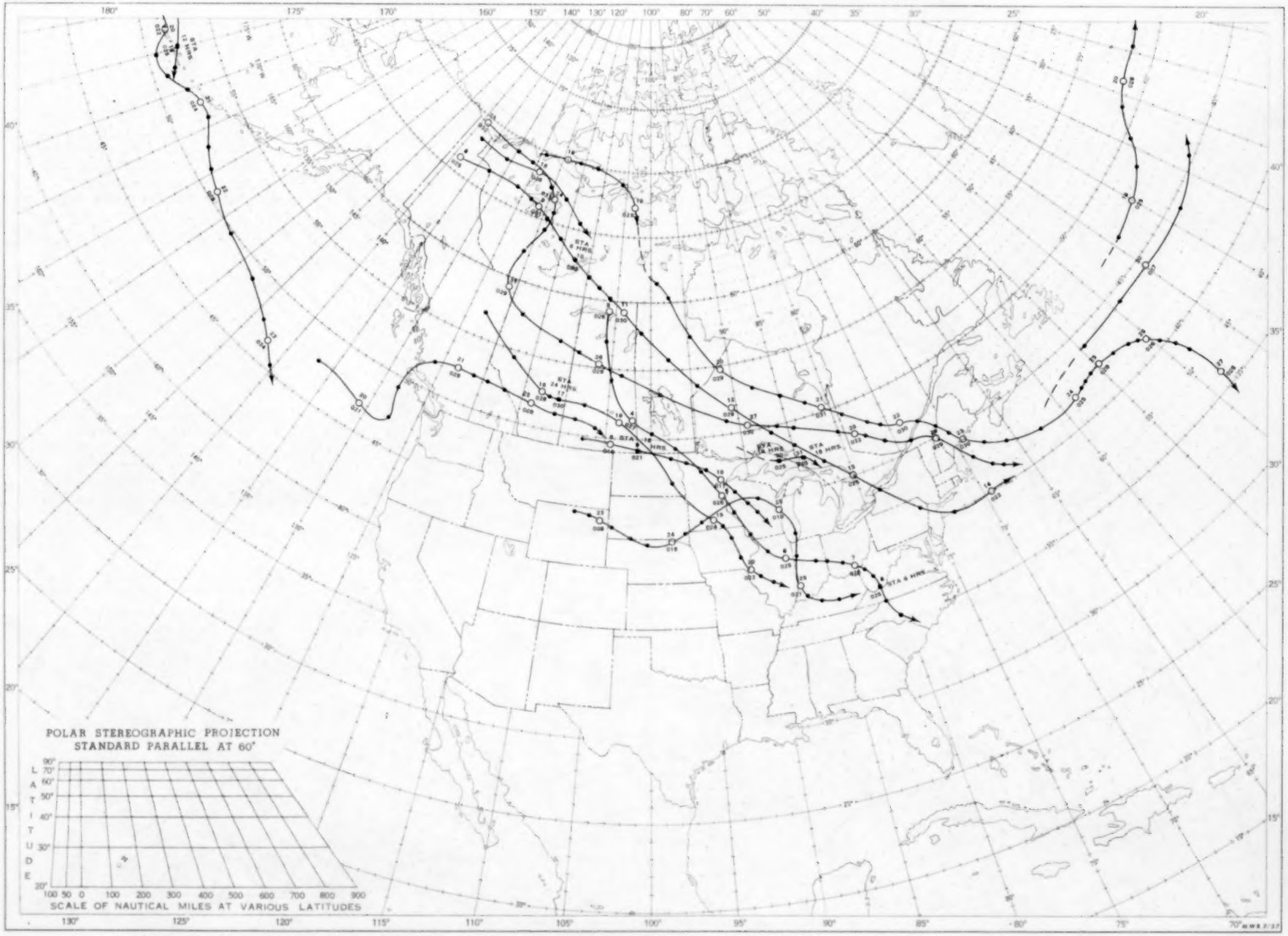

Circle indicates position of center at 7:00 a. m. E. S. T. Figure above circle indicates date, figure below, pressure to nearest millibar. Dots indicate intervening 6-hourly positions. Squares indicate position of stationary center for period shown. Dashed line in track indicates reformation at new position. Only those centers which could be identified for 24 hours or more are included.

Chart X. Tracks of Centers of Cyclones at Sea Level, July 1957.

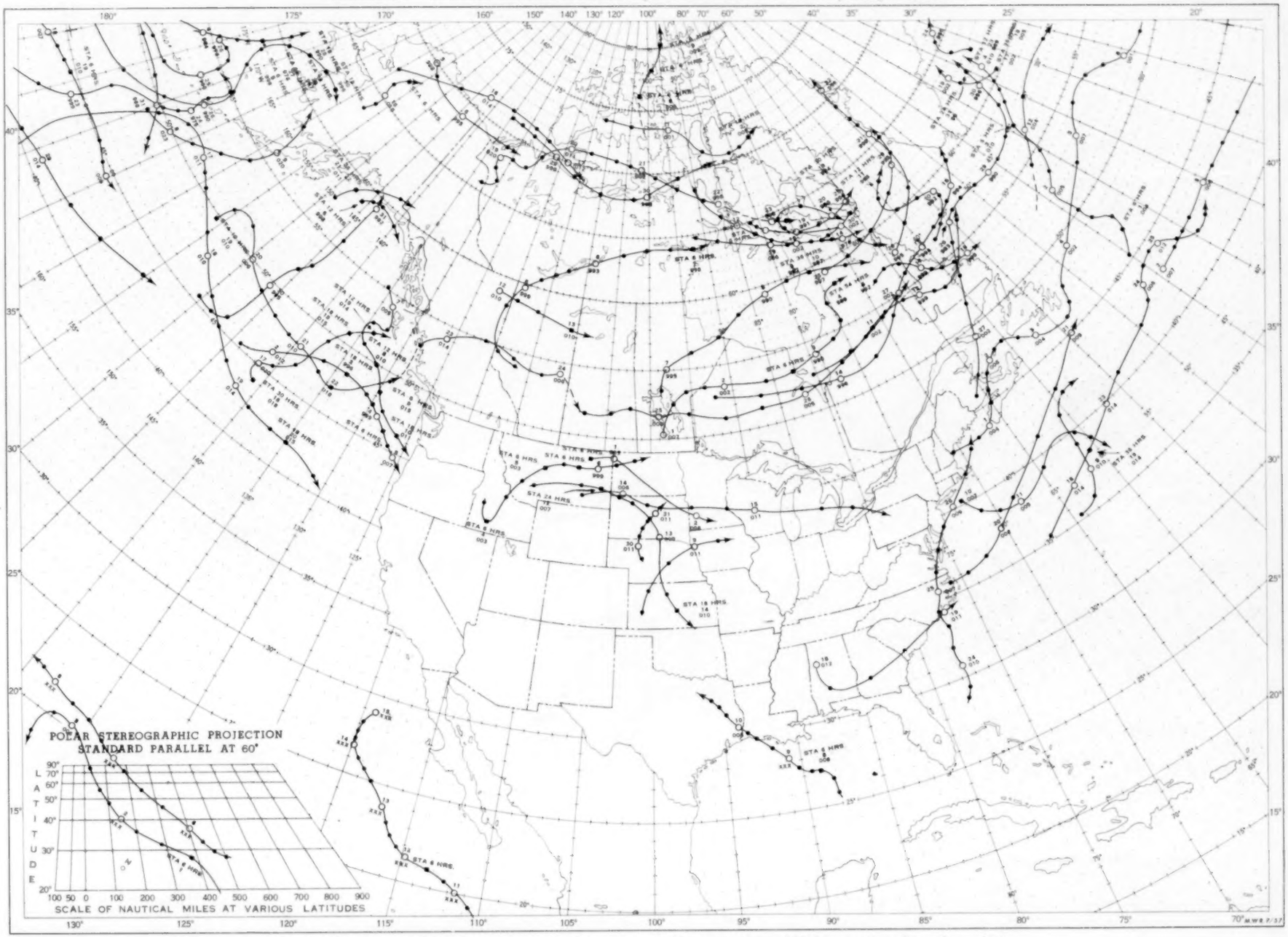

Circle indicates position of center at 7:00 a. m. E. S. T. See Chart IX for explanation of symbols.

Chart XI. Average Sea Level Pressure (mb.) and Surface Windroses, July 1957. Inset: Departure of Average Pressure (mb.) from Normal, July 1957.

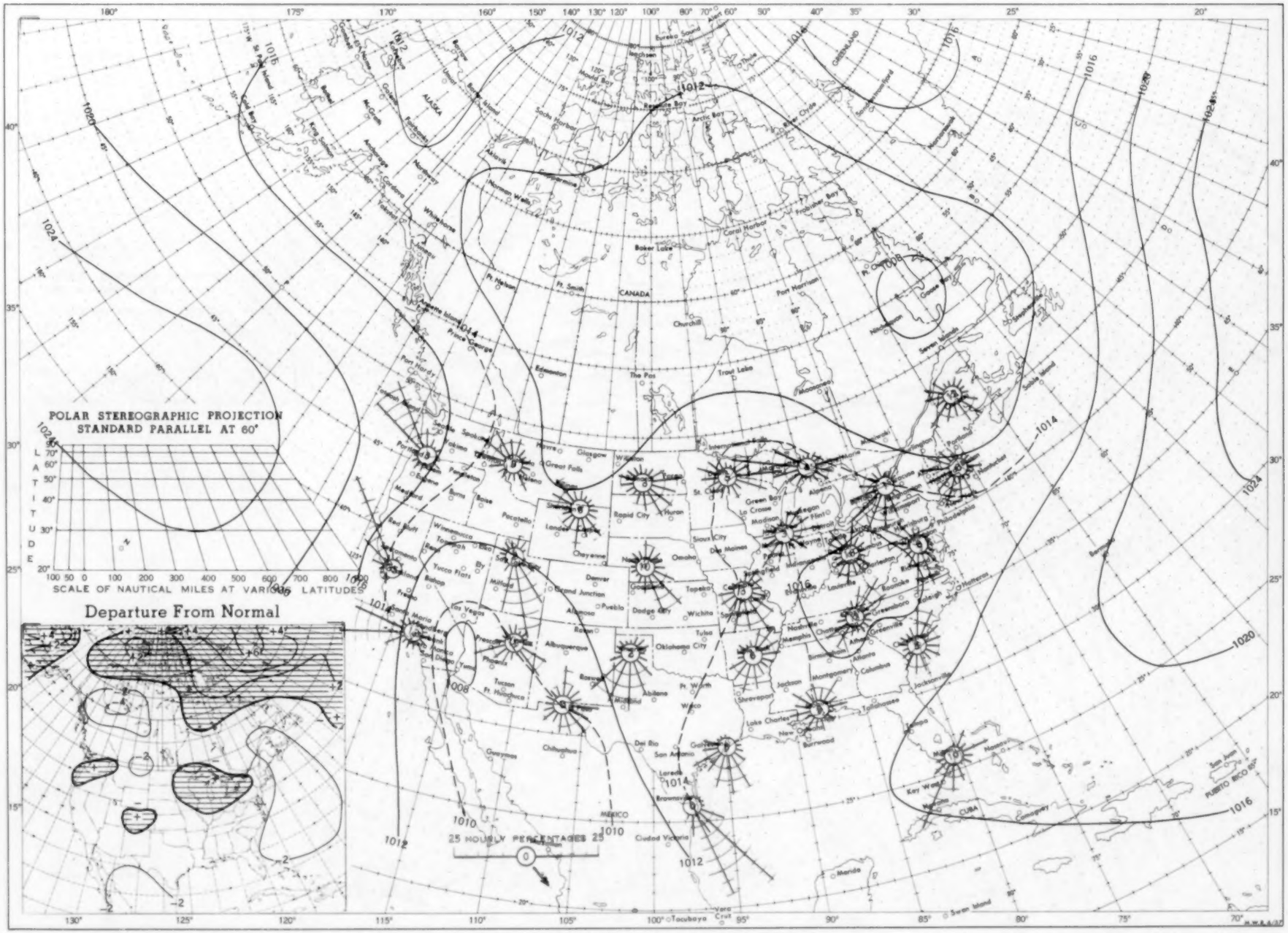

Average sea level pressures are obtained from the averages of the 7:00 a. m. and 7:00 p. m. E. S. T. readings. Windroses show percentage of time wind blew from 16 compass points or was calm during the month. Pressure normals are computed for stations having at least 10 years of record and for 10° intersections in a diamond grid based on readings from the Historical Weather Maps (1899-1939) for the 20 years of most complete data coverage prior to 1940.

Chart XII. 850-mb. Surface, 1200 GMT, July 1957. Average Height and Temperature, and Resultant Winds.

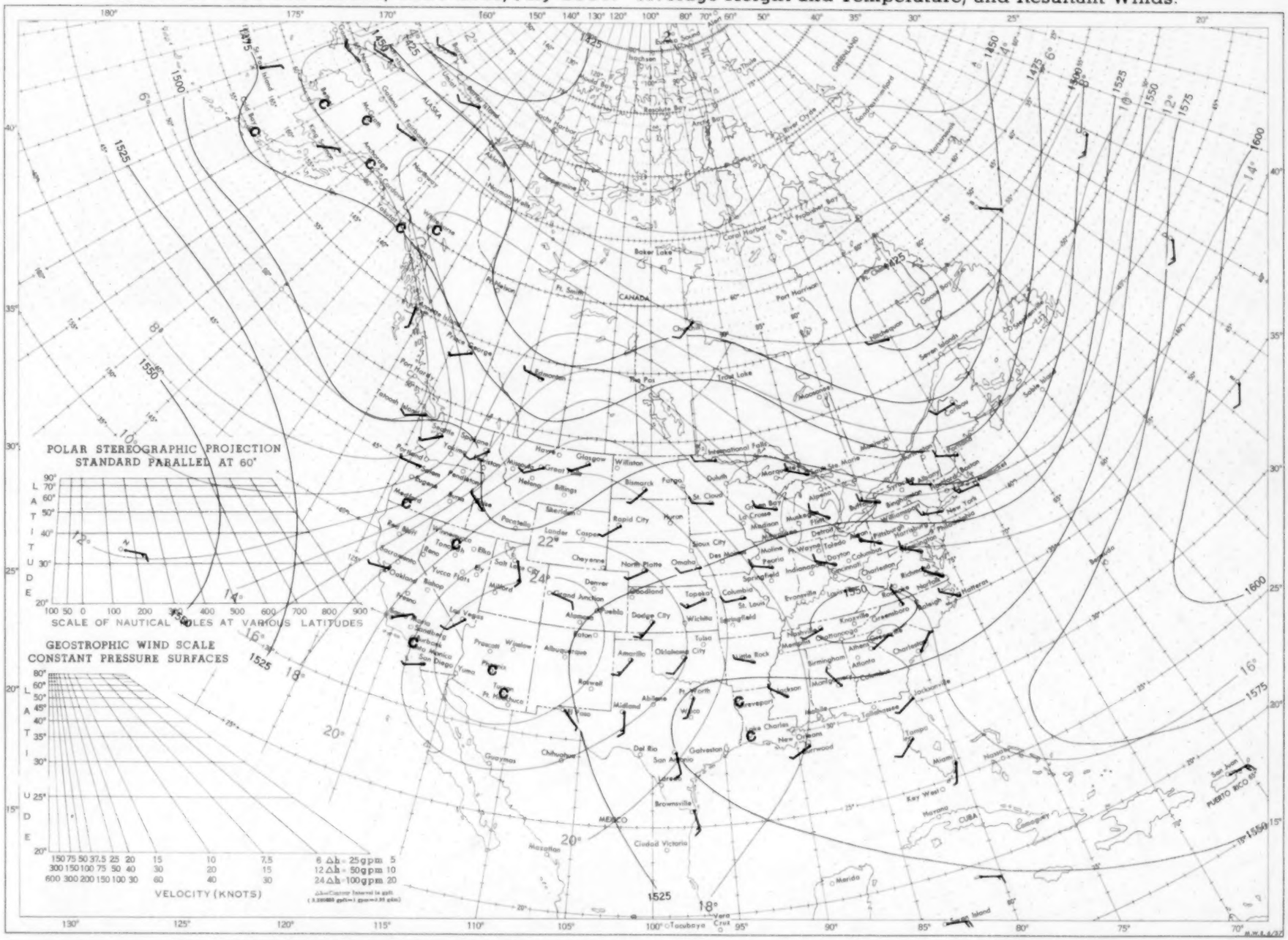

Height in geopotential meters (1 g.p.m. = 0.98 dynamic meters). Temperature in °C. Wind speed in knots; flag represents 50 knots, full feather 10 knots, and half feather 5 knots. All wind data are based on rawin observations.

Chart XIII. 700-mb. Surface, 1200 GMT, July 1957. Average Height and Temperature, and Resultant Winds.

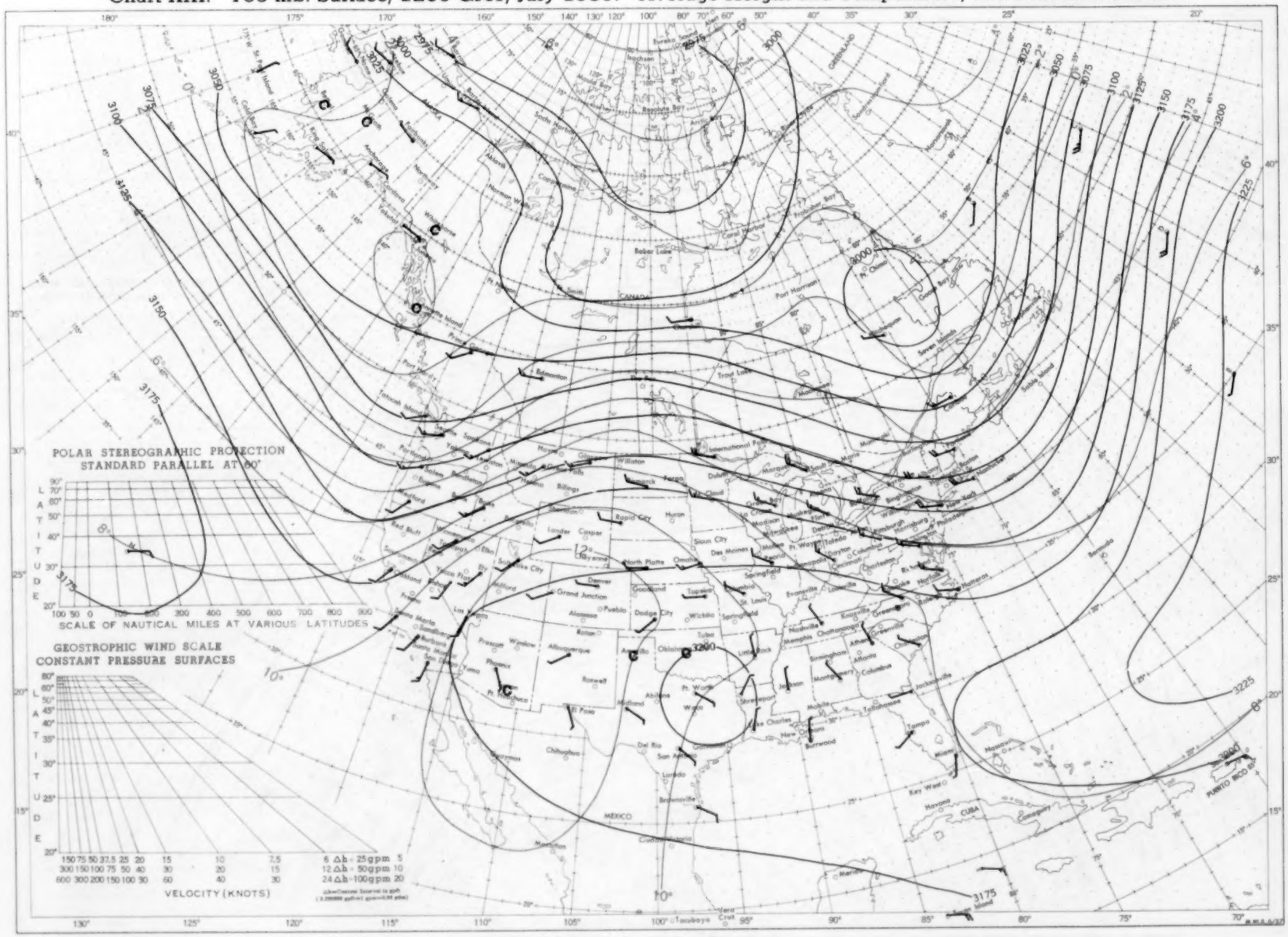

See Chart XII for explanation of map.

Chart XIV. 500-mb. Surface, 1200 GMT, July 1957. Average Height and Temperature, and Resultant Winds.

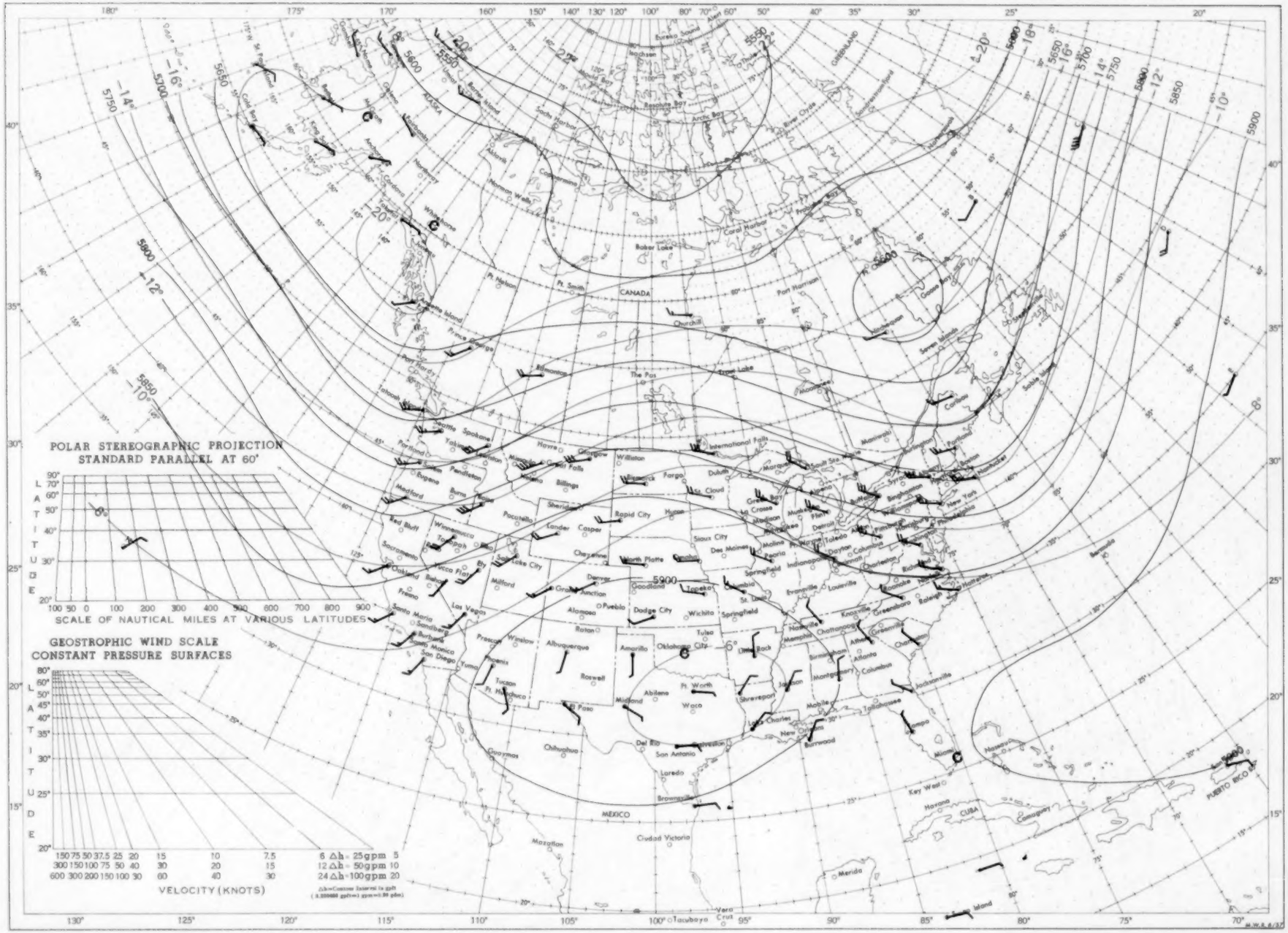

See Chart XII for explanation of map.

Chart XV. 300-mb. Surface, 1200 GMT, July 1957. Average Height and Temperature, and Resultant Winds.

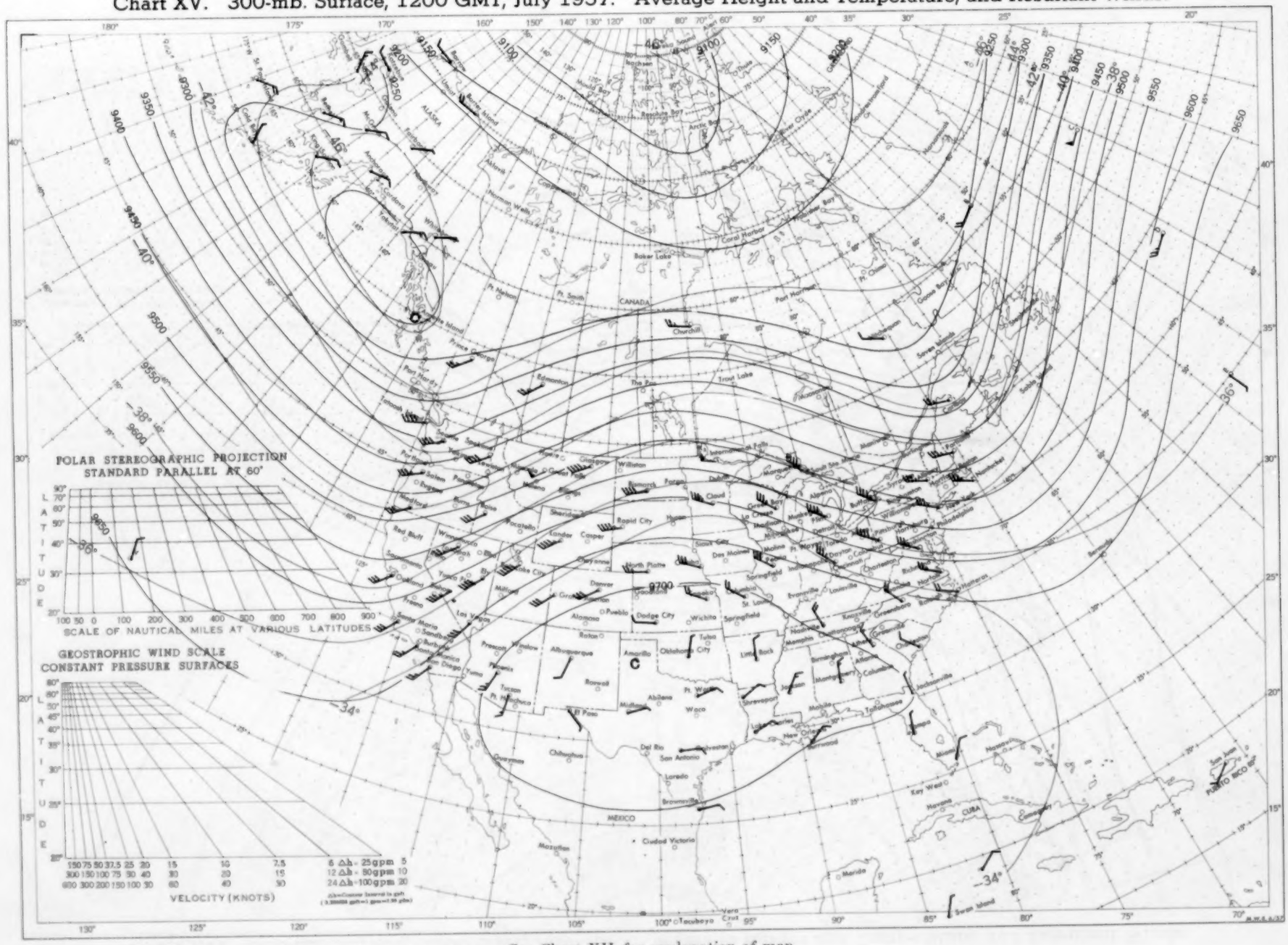

See Chart XII for explanation of map.

Chart XVI. 200-mb. Surface, 1200 GMT, July 1957. Average Height and Temperature, and Resultant Winds.

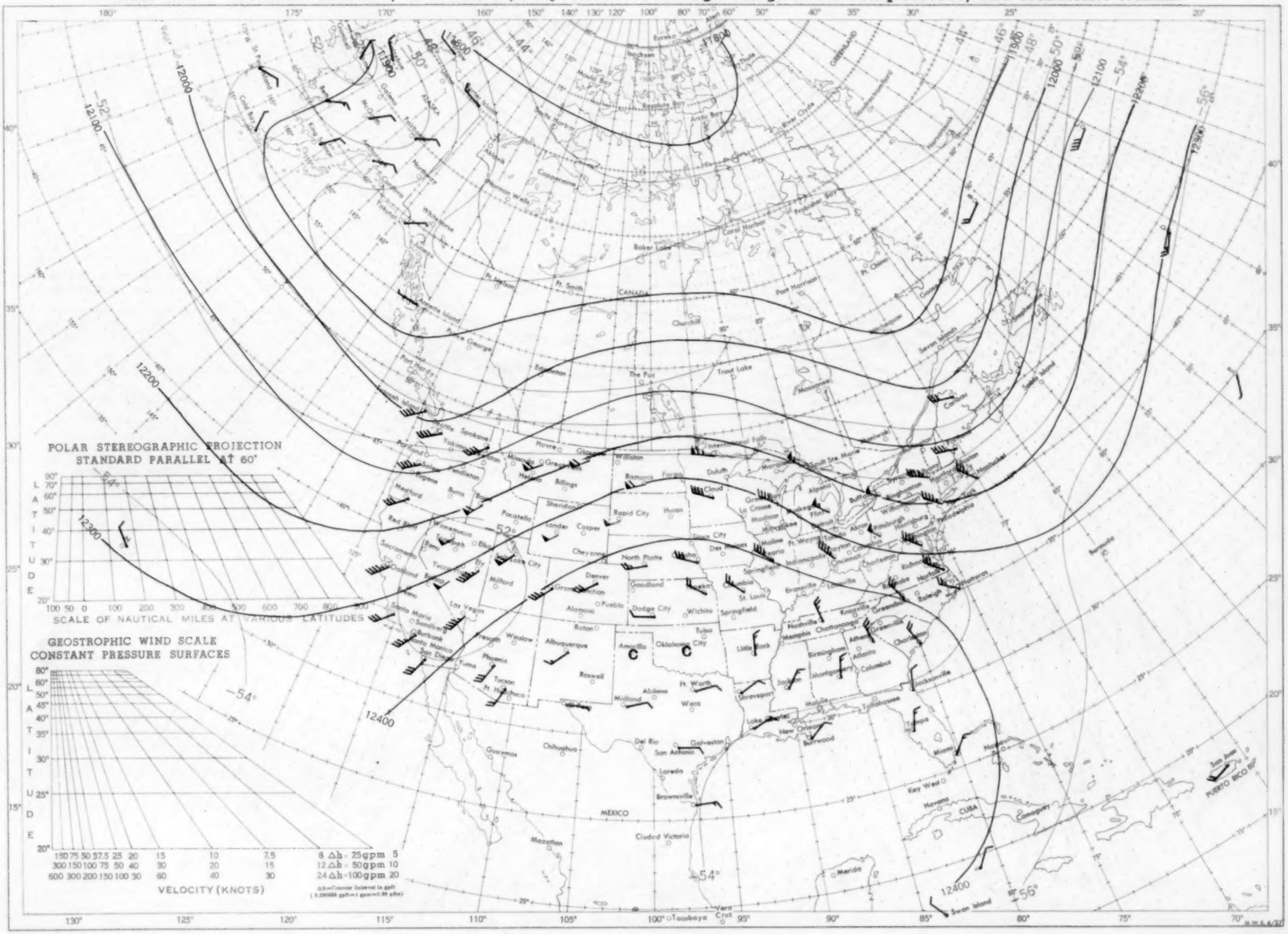

See Chart XII for explanation of map.

Chart XVII. 100-mb. Surface, 1200 GMT, July 1957. Average Height and Temperature, and Resultant Winds.

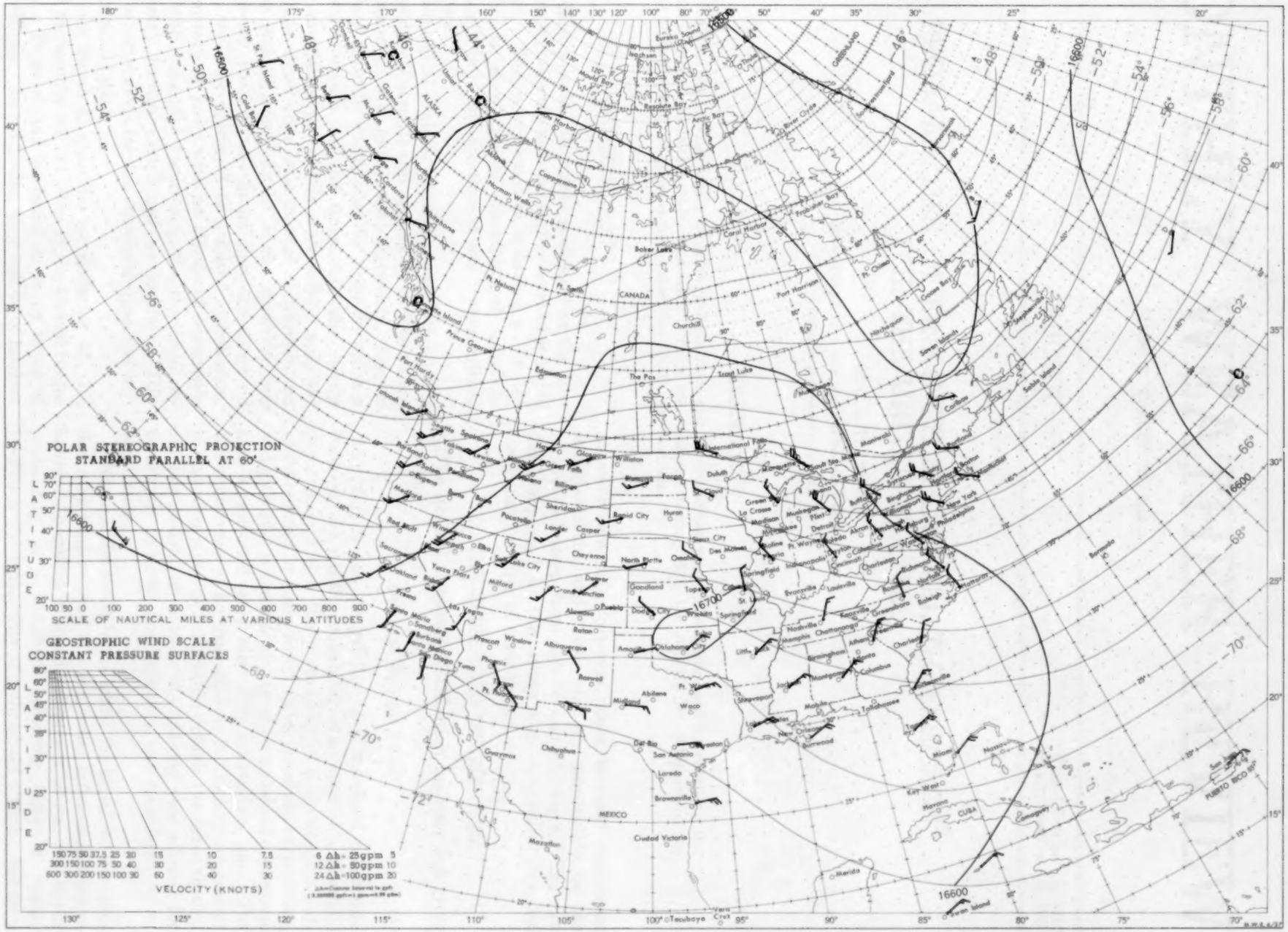

See Chart XII for explanation of map.